REMOVAL OF HEAVY METALS BY ACTIVATED CARBONS PREPARED FROM HYDROTHERMALLY TREATED BIOMASS WITH PHOSPHORIC ACID TREATMENT

GANIYU ABIMBOLA ADEBISI

INSTITUTE OF GRADUATE STUDIES
UNIVERSITY OF MALAYA
KUALA LUMPUR

2017

REMOVAL OF HEAVY METALS BY ACTIVATED CARBONS PREPARED FROM HYDROTHERMALLY TREATED BIOMASS WITH PHOSPHORIC ACID TREATMENT

GANIYU ABIMBOLA ADEBISI

THESIS SUBMITTED IN FULFILMENT OF THE REQUIREMENTS FOR THE DEGREE OF DOCTOR OF PHILOSOPHY

INSTITUTE OF GRADUATE STUDIES UNIVERSITY OF MALAYA
KUALA LUMPUR

2017

UNIVERSITY OF MALAYA

ORIGINAL LITERARY WORK DECLARATION

Name of Candidate: Ganiyu Abimbola Adebisi

Matric No: HHC130002

Name of Degree: Doctor of Philosophy

Title of Project Paper/Research Report/Dissertation/Thesis ("this Work"): **Removal of Heavy Metals by Activated Carbons Prepared from Hydrothermally Treated Biomass with Phosphoric Acid Treatment.**

Field of Study: Chemistry (Nanotechnology)

I do solemnly and sincerely declare that:

(1) I am the sole author/writer of this Work;
(2) This Work is original;
(3) Any use of any work in which copyright exists was done by way of fair dealing and for permitted purposes and any excerpt or extract from, or reference to or reproduction of any copyright work has been disclosed expressly and sufficiently and the title of the Work and its authorship have been acknowledged in this Work;
(4) I do not have any actual knowledge nor do I ought reasonably to know that the making of this work constitutes an infringement of any copyright work;
(5) I hereby assign all and every rights in the copyright to this Work to the University of Malaya ("UM"), who henceforth shall be owner of the copyright in this Work and that any reproduction or use in any form or by any means whatsoever is prohibited without the written consent of UM having been first had and obtained;
(6) I am fully aware that if in the course of making this Work I have infringed any copyright whether intentionally or otherwise, I may be subject to legal action or any other action as may be determined by UM.

Candidate's Signature Date:

Subscribed and solemnly declared before,

Witness's Signature Date:

Name: Dr. Zaira Zaman Chowdhury

Designation: Supervisor

ABSTRACT

The production of adsorbents for heavy metal adsorption from agricultural by-products (waste), is a research area of high interest that deals with solving problems associated with waste disposal as well as producing value added products that can be applied in a number of ways environmentally. In fulfilment of this esteemed objective, this research aimed at developing novel powdered adsorbents (PAC) from banana empty fruit bunch (BEFB), rattan sawdust (RS) and granular activated adsorbent (GAC) from longan fruit shell (LFS). To enhance the adsorption capacities of the activated carbons, the precursors were pre-treated through hydrothermal method followed by chemical activation with phosphoric acid (H_3PO_4). The results demonstrated that the optimum condition to obtain highest removal percentage and yield were dependent on the characteristics of the raw materials and the adsorbate under investigation. The results of characterization showed significant improvement in the surface area and pore size distribution characteristics of the hydro-char after activation process. BET surface area of BEFBAC and RSAC are 762.05 m2/g and 1151.23 m2/g respectively. The results further reveal maximum adsorption capacity of 82.86%, 61.03% [Pb(II), Zn(II)] and 86.71%, 64.26% [Pb (II), Zn (II)] for BEFBAC and RSAC respectively at the equilibrium conditions (time = 210min, pH = 5.5, temperature = 30^{o}C and initial adsorbate concentration of 350mg/L). This indicated a promising potential in the use of these biomass as precursors for preparing adsorbents for removing heavy metals from wastewaters. Furthermore, the adsorption isotherms and kinetics reveal that the process fitted perfectly into Langmuir isotherm and pseudo-second-order reaction model. The thermodynamics study showed that the adsorption process is endothermic, spontaneous and feasible under the investigated temperatures. The result for longan fruit shell granular activated carbon (LFSAC) indicated that the adsorption capacities for the single solute systems were higher than

those obtained for the binary mixture for the two metals. The maximum adsorption capacity for the single solute at different initial concentrations of the adsorbates for Pb(II) and Zn(II) are 80.4% and 59.3% respectively. The adsorption processes were best fitted into the Langmuir isotherm model for both metals. The results were further subjected to pseudo-first-order, pseudo-second-order, intra-particle diffusion and elovich kinetic models. The result showed that the single solute adsorption data best fitted into pseudo-second-order kinetic model. The adsorption capacity of Pb(II) is higher than that obtained for Zn(II) for the binary system. The percentage removal of the metals in the binary system decreases with increase in the initial concentration of the other metal ion.

.

ABSTRAK

Pengeluaran adsorben untuk penjerapan logam berat daripada produk pertanian (sisa) adalah kawasan penyelidikan faedah yang tinggi yang berkaitan dengan menyelesaikan masalah yang berkaitan dengan pembuangan sampah serta menghasilkan nilai tambah produk yang boleh digunakan dalam beberapa cara alam. Sebagai memenuhi objektif ini, kajian ini bertujuan untuk membangunkan adsorben serbuk novel (PAC) dari sekumpulan buah pisang kosong (BEFB), habuk rotan papan (RS) dan penyerap aktif berbutir (GAC) dari kulit buah longan (PTB). Untuk meningkatkan keupayaan penyerapan karbon aktif, prekursor adalah pra-irawat melalui kaedah hidroterma untuk menghasilkan hidro char diikuti oleh pengaktifan kimia dengan asid fosforik (H_3PO_4). Keputusan menunjukkan bahawa keadaan optimum untuk mendapatkan peratusan penyingkiran tertinggi dan hasil adalah bergantung kepada ciri-ciri bahan-bahan mentah dan bahan penyerap di bawah invetigasi. Keputusan pencirian menunjukkan peningkatan yang ketara di kawasan permukaan dan sifat taburan saiz liang hidro char selepas proses pengaktifan. kawasan permukaan BET BEFBAC dan RSAC adalah 762,05 m^2/g dan 1151,23 m^2/g. Keputusan lanjut menunjukkan kapasiti penyerapan maksimum adalah 82.86%, 61.03% [Pb (II), Zn (II)] dan 86,71%, 64,26% [Pb (II), Zn (II)] untuk BEFBAC dan RSAC keadaan keseimbangan (masa = 210min, pH = 5.5, suhu = 30^oC dan kepekatan bahan serap awal 350mg / L). Ini menunjukkan potensi yang menjanjikan dalam penggunaan biomass ini sebagai pelopor untuk menyediakan adsorben bagi mengeluarkan logam berat daripada air buangan. Tambahan lagi, isoterma penyerapan dan kinetik menunjukkan bahawa proses menepati Langmuir isoterma dan model tindak balas pseudo-tertib kedua. Kajian termodinamik menunjukkan bahawa proses penyerapan adalah endotermik, spontan dan sesual dilaksanakan di bawah suhu yang ditetapkan. Hasil kulit buah longan berbutir karbon aktif (LFSAC) menunjukkan bahawa kapasiti penyerapan untuk sistem bahan larut tunggal adalah lebih tinggi daripada yang diperolehi bagi campuran binari untuk

kedua-dua logam. Kapasiti penyerapan maksimum untuk bahan larut tunggal pada kepekatan awal yang berbeza daripada penyerap untuk Pb (II) dan Zn (II) iaitu 80.4% dan 59.3%. Proses penyerapan telah menepati model isoterma Langmuir untuk kedua-dua logam. Keputusan itu juga menepati pseudo-tertib pertama, pseudo-kedua untuk, penyebaran antara zarah dan model kinetik elovich. Hasilnya menunjukkan bahawa data bahan larut penyerapan tunggal memenuhi model kinetic pseudo-kedua. Kapasiti penyerapan Pb (II) adalah lebih tinggi daripada yang diperolehi untuk Zn(II) untuk sistem binari. Penyingkiran peratusan logam dalam sistem binari berkurangan dengan peningkatan dalam kepekatan awal ion logam lain.

ACKNOWLEDGEMENTS

I wish to acknowledge Almighty Allah for His mercies, favour and grace in granting me the opportunity, understanding and knowledge to go through this programme. To Him alone be the glory and adoration.

My eternal gratitude goes to my supervisor, Prof. Dr. Sharifah Bee Abd Hamid, for her dynamism, constructive criticism as well as critical assessment of my work which no doubt assisted me immensely through the research. I am mostly grateful to her for the opportunity granted to use part of her grants to undertake the study. May Allah be pleased with her. I also appreciate the contributions of my co-supervisor, Dr. Md. Eaqub Ali. I will be an ingrate if I fail to appreciate the contributions of my co-supervisor and mentor, Dr. Zaira Zaman Chowdhury, for her mentoring, immense contributions, encouragement and understanding throughout the period of the research.

The brotherly encouragement and special support I enjoyed in the hand of the Rector, Osun state Polytechnic, Iree, Nigeria, Dr. J.O. Agboola, is hereby noticed. To all other members of the management of the institution, for encouraging, supporting and recommending me for the programme, I say thank you. I am high indebted to TETFUND, Nigeria, for providing the fund to undertake the programme.

My special gratitude goes to my family (my wife and children). My wife, Iyabo Olusola, for your unflinching support, love, care and prayer which saw me through this far, I am grateful. For taking adequate care of the home while I was away, I say thank you.

To others too numerous to mention, for your support, prayers and encouragement which I enjoyed throughout and still enjoying, I am most grateful.

May Almighty Allah continue to be with you all. Ameen.

TABLE OF CONTENTS

LIST OF FIGURES

LIST OF TABLES

LIST OF SYMBOLS AND ABBREVIATIONS

A	:	Initial sorption rate for Elovich equation (mg/g h)
AC	:	Activated carbon
ACF	:	Activated Carbon Fibres
ANOVA	:	Analysis of variance
A_T	:	Constant for Temkin isotherm (L/g)
B	:	Constant for Elovich equation (g/mg)
B	:	Constant for Temkin isotherm (mg/g h)
BBD	:	Box Behnken Design
BCSIR	:	Bangladesh Scientific Institute of research
BEFB	:	Banana Empty Fruit Bunch
BEFBAC	:	Banana Empty Fruit Bunch Activated Carbon
BEFBC	:	Banana Empty Fruit Bunch Char
BET	:	Brunauer-Emmett-Teller
C	:	Solute concentration (mg/L)
C_T	:	Concentration of adsorbate at time, t (mg/L)
C	:	Concentration of adsorbate at equilibrium (mg/L)
Ci	:	Constant for Intraparticle diffusion model (mg/g)

Co	:	Initial adsorbate concentration (mg/L)
DOE	:	Design of experiment
FE-SEM	:	Field Emission Scanning Electron Microscope
FTIR	:	Fourier Transform Infrared
GAC	:	Granular Activated Carbon
GLFSAC	:	Granular Longan Fruit Shell activated carbon
ICP	:	Inducedly Coupled Plasma
IR	:	Impregnation ratio
IUPAC	:	International Union of Pure and Applied Chemistry
K_1	:	Adsorption rate constant for pseudo-first-order kinetic model (1/h)
K_2	:	Adsorption rate constant for pseudo-second-order Kinetic model (g/mg h)
K_F	:	Adsorption or distribution coefficient for Freundlich Isotherm [mg/g(l/mg)$^{1/n}$]
K_L	:	Rate of adsorption for Langmuir isotherm (L/mg)
K_{PI}	:	Adsorption rate constant for intraparticle diffusion model (g/mg h$^{1/2}$)
LFS	:	Longan Fruit Shell
LFSAC	:	Longan fruit shell Activated carbon
LFSC	:	Longan Fruit Shell Char
N	:	Total number of experiments required

PAC : Powdered Activated Carbon

R : Universal gas constant (8.314 J/mol K)

R_2 : Correlation coefficient

R_L : Separation factor

RS : Rattan sawdust

RSAC : Rattan Sawdust Activated Carbon

RSC : Rattan Sawdust char

RSM : Surface Response Methodology

S_{BET} : BET surface area (m2/g)

STP : Standard temperature and Pressure

T : Absolute temperature (K)

TGA : Thermo-gravimetric Analysis

V : Solution volume (L)

V_T : Total pore volume (cm3/g)

V_{meso} : Mesopore Volume (cm3/g)

W : Dry weight of adsorbent (g)

W_{after} : Dry weight of activated carbon after washing (g)

W_{before} : Dry weight of activated carbon before washing (g)

W_{char}	:	Dry weight of char (g)
W_o	:	Dry weight of precursor (g)
X	:	Activated carbon preparation variable
Y	:	Response
n	:	Constant for Freundlich isotherm
q_e	:	Amount of adsorbate adsorbed per unit mass of adsorbent at equilibrium (mg/g)
q_m	:	Maximum amount of adsorbate adsorbed per unit mass of adsorbent at equilibrium (mg/g)
q_t	:	Amount of adsorbate adsorbed per unit mass of adsorbent at time, t (mg/g)
q_t,cal	:	Calculated adsorption uptake at time, t (mg/g)
q_t,exp	:	Experimental adsorption uptake at time, t (mg/g)
t	:	Time (h)
ΔGo	:	Changes in standard free energy (KJ/mol)
ΔHo	:	Changes in standard enthalpy (KJ/mol)
ΔSo	:	Changes in standard entropy (J/mol K)

LIST OF APPENDICES

CHAPTER 1: INTRODUCTION

1.1 Research Overview

In this chapter, the general outline of the research is presented. The covered scope include the general problem associated with treatment of wastewater from industries with specific aim of_removing inorganic pollutants. Since so many wastewater treatment technologies have been used in the past decades with each having its shortcomings, this research therefore provides a means to a more effective way of solving the problems associated with wastewater treatment by adopting adsorption technique using activated carbons produced from biomass materials (agricultural waste). The problems associated with environmental pollution as a result of industrial activities, the heavy metal pollutants, the problem statements, the research objectives as well as the organization of the thesis are hereby presented.

1.2 Research Background:

Since the period of industrial revolution all over the world, all efforts geared towards removing industrial pollutants from the environment have not yielded the desired result (Amuda, Giwa, & Bello, 2007). This was partly due to increasing wastes being generated on daily basis and the growing population which normally takes its toll on the already aggravated situation. Accumulation of heavy metals in lakes, rivers and coastal waters has seriously disrupted the ecological balance of the aquatic environment. With industrial development and technological growth, two groups of materials that have debilitating effects on eco-system came into being. These are nutrients which encourage unrestricted biologic growth leading to oxygen depletion and sparingly degradable chemical substances which usually bring serious adverse effects to the eco-system. These chemical substance causing serious environmental hazards to man are classified as chemical pollutants (Harrison, 2001). It has been estimated by various experts that over a million different pollutants are introduced into water bodies (Ghrefat & Yusuf, 2006; Jain & Ram,

1997; Modak, Singh, Chandra, & Ray, 1992). These include both organic and inorganic pollutants some of which are not considered dangerous even though they may introduce unpleasant odour and or taste to the water, they do not have direct harmful effect to humans. Others on the other hand have direct and indirect negative or harmful effects on humans as they are capable of causing serious damage to human health or even can lead to death.

Heavy metals are discharged into water bodies through various activities of industries especially in the manufacturing and mining industries. Heavy metals are highly toxic and usually constitute health hazards when consumed beyond the permissible and tolerable level. Among these heavy metals pollutants, the divalent cations are considered as major pollutants (Abdel-Halim, Shehata, & El-Shahat, 2003). Thus among the highly toxic metals are lead (Pb), manganese (Mn), copper (Cu), mercury (Hg), arsenic (As), zinc (Zn) cadmium (Cd) and others in the group (Ahluwalia & Goyal, 2007). The presence of lead (Pb) in water, even at very low concentration, can lead to kidney, nervous system and reproductive system damage in humans (Z. Z. Chowdhury, Zain, Khan, Rafique, & Khalid, 2012). According to World Health Organization (WHO), lead has a maximum recommended acceptable concentration of 0.1- 0.05 mg L^{-1} in drinking water (K. Zhang, Cheung, & Valix, 2005). Zinc is known to be discharged into waterways by industries especially those involved in acid mines drainage, galvanizing plants, natural ores and municipal wastewater treatment plants (Moreno-Barbosa, López-Velandia, del Pilar Maldonado, Giraldo, & Moreno-Piraján, 2013). As essential as zinc in food to humans is, its presence above the tolerable dose could pose problems due to the fact that it is highly toxic to both humans and animals (Y. Wang, Qiao, Liu, & Zhu, 2012). Zinc is a non-biodegradable metal with 5.0 mg L^{-1} maximum tolerable concentration in drinking water (A. Hawari, Rawajfih, & Nsour, 2009). Heavy metal pollutants have been removed from wastewaters using various technologies ranging from precipitation, ion exchange,

membrane filtration and reverse osmosis (Baccar, Bouzid, Feki, & Montiel, 2009). These methods, good as they are, have several disadvantages which include; requirement of costly equipment and the need for continuous use of chemicals which may become water pollutants themselves. Due to these limitations, the need therefore arise for a more environmental friendly method which will at the same time be cost effective. Efforts were then geared towards the use of adsorption process. The use of adsorbents for heavy metal removal in wastewaters has not only been found to be superior to other conventional methods, it has equally been found to be cost-effective, simple in design, easy to operate and much more users friendly (Moreno-Barbosa et al., 2013).

1.3 Wastewater Treatment Technology

Industrial wastewaters are generally considered as serious agents of environmental pollution. They require special care for their efficient treatment and disposal. Wastewater can either be domestic or industrial. Whereas domestic wastewater is discharged from residential and commercial establishment, industrial wastewater on the other hand is discharged from industries. The composition of domestic wastewater is relatively constant, the composition of industrial wastewater varies from industry to industry and also from plant to plant depending on the activities of such industry (Dinesh Mohan, Singh, & Singh, 2008).

Industries have adopted various techniques in the treatment of wastewater generated by them with physicochemical methods being the most widely used. These methods include but not limited to the following; adsorption, chemical reaction, ion-exchange, ultrafiltration, coagulation/flocculation, reverse osmosis and electro dialysis (Amuda & Ibrahim, 2006; Cassini, Tessaro, Marczak, & Pertile, 2010; Dinesh Mohan et al., 2008; J.-P. Wang, Chen, Wang, Yuan, & Yu, 2011). The physicochemical technologies enjoy a number of advantages over the biological method of treatment as they remain unaffected

by toxic materials that may be present in such wastewater, whereas the biological methods cannot operate in case of wastewater containing inorganic or non-degradable materials (Dinesh Mohan et al., 2008).

The adoption of adsorption technique in the heavy metals removal from wastewater has become widely accepted. This led to several studies focusing on utilization of commercial activated carbon for adsorbing heavy metals from wastewater for years but it has a great limitation in that it is too expensive (Depci, Kul, & Önal, 2012). In an attempt to resolve this limitation, research interest shifted to the production of adsorbents from renewable sources which will at the same time be abundant at little or no cost (A. Ahmad, Hameed, & Ahmad, 2009; Gratuito, Panyathanmaporn, Chumnanklang, Sirinuntawittaya, & Dutta, 2008; Hameed, Tan, & Ahmad, 2009; Q.-S. Liu, Zheng, Wang, & Guo, 2010; Sumathi, Bhatia, Lee, & Mohamed, 2009). The production of adsorbents for heavy metal adsorption from agricultural by-products (waste), is a research area of high interest that deals with solving problems associated with waste disposal as well as producing value added products that can be applied in a number of ways environmentally.

Moreover, the conversion of these biomass wastes would lead to production of low cost adsorbents and equally divert the wastes from the usual landfill and burning practices (Nahil & Williams, 2012). This will provide a big alternative source of commercial activated carbons as they are readily available and renewable.

Activated carbon is a carbon-containing material that is extensively utilized in the treatment and purification of wastewater. It is usually amorphous in nature. Its effectiveness in water purification is dependent on its surface characteristics which is usually unique. These include an enhanced surface area between 500 and 2000 m^2/gm, favourable pore size distribution, favourable pore volume and a high degree surface

reactivity (Z. Z. Chowdhury, Zain, Khan, Arami-Niya, & Khalid, 2012). Activated carbons have complex and heterogeneous structure mainly due to the presence of micropores, mesopores and macropores of different sizes and shapes (A. Ahmad et al., 2009). Activated carbons are known to have been produced from non-renewable sources, such as coal, lignite and peat, on commercial basis. The use of commercial activated carbons in the treatment of wastewater has been limited by its high cost of production. In an attempt to resolve this limitation, there is a growing interest in research activities in the activated carbon production by making use of renewable, abundantly available materials at little or no cost, especially from biomass materials (ligno-cellulosic) as a results of its attendant high carbon compared to its low ash contents (Egila, Dauda, Iyaka, & Jimoh, 2011).

Activated carbons have found wide range of applications either as an adsorbent, a catalyst or a catalyst support. In industries, activated carbon has become a highly important adsorbent as it has found its uses in separating and purifying mixtures of gaseous and liquid materials. Industries such as food processing, pharmaceuticals, chemical, beverages, petroleum, nuclear, automobile and so on are all concerned with the application of activated carbons primarily due to their high adsorptive properties enhanced by their well- developed surface area and high porosity. The high porosity of activated carbon is dependent upon two main factors, that is, the nature of the starting material (precursor) and a balanced process conditions. Activated carbons have equally found their uses in environmental processes either in the general cleaning of the environment by mopping up of toxic gases from it and or wastewater and portable water treatments (El-Hendawy, 2005). Thus in recent times, several agricultural wastes have been engaged in the production of activated carbon – coconut shells, coconut shell fibers and rice husk (Dinesh Mohan et al., 2008), olive stones and walnut shells (Martinez, Torres, Guzman, & Maestri, 2006), jatropha curcas fruit shell (Tongpoothorn, Sriuttha,

Homchan, Chanthai, & Ruangviriyachai, 2011), mangostania garcinia (Z. Z. Chowdhury, Zain, Khan, Rafique, et al., 2012), cassava peel (Sudaryanto, Hartono, Irawaty, Hindarso, & Ismadji, 2006), silk cotton hull, coconut tree sawdust, sago waste, maize cob and banana pith (Kadirvelu et al., 2003), cornelian cherry, apricot stone and almond shell (Demirbas, Kobya, Senturk, & Ozkan, 2004) and many others.

1.4 Problem Statement

As desirable and inevitable as industrialization is, the occurrence of many devastating ecological and human disasters over the years in both developing and developed nations have pointed accusing fingers to industries as main contributors to environmental pollution of varying magnitude (Triantafyllou, 2001). Wastes and emissions from industries have been found to be toxic and hazardous and are highly detrimental to life. The list may include heavy metals like mercury, cadmium, lead, zinc, manganese including others. It has also been reported that irrigation of soil using wastewater is capable of accumulating heavy metals in the soil surface (Chary, Kamala, & Raj, 2008). When the soil could no longer retain such accumulated heavy metals, they are drained into ground water or soil solution for later uptake by plants. Heavy metals can also get into the soil through other sources which may include fertilizers application on the soil, sewage sludge or by direct irrigation using wastewater (Devkota & Schmidt, 2000). A number of authors from both the developing and developed countries have reported heavy metal pollutions in wastewater (Adeniyi & Anetor, 1998; Bansal, 1998; Chary et al., 2008; Chauhan & Chauhan; Chung, Song, Park, & Cho, 2011; Dooyema et al., 2011; Huang, Zhou, Sun, & Zhao, 2008; Järup, 2003; Khan, Cao, Zheng, Huang, & Zhu, 2008; Lăcătuşu & Lăcătuşu, 2008; Mapanda, Mangwayana, Nyamangara, & Giller, 2005; Nriagu, Oleru, Cudjoe, & Chine, 1997; Sharma, Agrawal, & Marshall, 2007; Sobukola, Adeniran, Odedairo, & Kajihausa, 2010; Venkateshwarulu & Kumar).

The use of adsorption on activated carbon in the treatment of wastewater has become widely recognized and accepted. The adoption of commercial activated carbon has however become limited due to the cost of production which is on the high side. This has in recent years necessitated more efforts towards the use of highly cost-effective, abundantly available, renewable with low or no cost, materials for production of adsorbents that can effectively be applied in the treatment of wastewater to remove organic pollutants such as dyes and inorganic pollutants (heavy metals). Several efforts have been reported on the production of adsorbents from agricultural waste, no studies have however been reported on the production of adsorbents from banana empty fruit bunch (BEFB), rattan sawdust (RS) and longan fruit shells by phosphoric acid (H_3PO_4) activation and the application of the adsorbents on heavy metals adsorption. Equally, very few authors have reported the activation effect of hydrothermal char materials with acid activating agent with subsequent study of the physiochemical characteristics of the porous activated carbon, hence the justification for and uniqueness of this research.

The raw materials employed in this research are purely agricultural by-products (wastes). These are wastes that are generated as a result of engaging in agricultural activities which may include cropping, animal husbandry, fishery, piggery, poultry, and other farming activities. The choice of precursors is based on both environmental and economic considerations. Environmental consideration is aimed at solving problems associated with the disposal of the by-products by mopping up of the waste from the environment, thereby reducing potential hazards they may cause to human beings. Economic consideration on the other hand involves the availability of these materials, all year round, at no or low cost and the production of value-added products from them.

Based on the above considerations, rattan sawdust, banana empty fruit bunch (BEFB) and longan fruit shells have been carefully chosen for the study. This is a bold attempt geared

towards replacing the production of activated carbon from non- renewable sources to renewable materials. Rattan (*Palmae/Arecaceae* family), has been described as a spiny climbing plant and a prominent member of the palm trees family. Thus the plant is considered to be important in the Peninsular Malaysia as a non-wood forest product (A. Ahmad, Hameed, & Ahmad, 2008). Accordingly, the world has about 600 species of rattan out of which we have 106 in Peninsular Malaysia (Hameed, Ahmad, & Latiff, 2007). Of this number, only 16 species are utilized and marketed. They are usually utilized in household items manufacture in rural communities (Dransfield, 1992). Malaysia has about 653 rattan mills which are involved in the manufacture of rattan furniture and other products including mats, walking sticks, baskets, toys and rattan balls (Latif, Mohd, & Husain, 1990). These industries generate a high amount of sawdust as residues. Rattan is widely available in Nigeria especially in southern region, where the fibre from the stalk is used in weaving mats, baskets, fans, pot stands, drink covers, furniture and other crafts (Obute & Ekiye, 2008). Bananas are an important food crop cultivated in the subtropics and tropics of Malaysia and are equally routinely cultivated for ornamental purposes and for fibre (Wong et al., 2001). The crop has been listed as one of the priotized crops cultivated for commercial purposes by the third National Agricultural Policy of Malaysia (Hassan, 2005). Moreover, the crop which is widely cultivated for both domestic and exportation purposes, occupies about 10-12% of the total acreage under fruit and according to available data, more than one-half million tonnes banana is produced annually for both domestic consumption and exportation (Hassan, 2005). Longan fruit (Dimocarpus longan), belongs to the same family as lychee and rambutan and it is widely cultivated in Indochina and Malaysia (Ampthill, 2010).

1.5 Research Objectives

(i). To prepare, optimize and characterize powdered activated carbons from Banana Empty Fruit Bunch (BEFB) and Rattan Sawdust (RS), using 2-step of hydrothermal pre-treatment and chemical activation with H_3PO_4 acid.

(ii). To prepare granular activated carbon from Longan Fruit Shell (LFS) and investigate its application in the removal of Pb(II) and Zn(II) in a single and binary solute systems.

(iii). To study the kinetics, isotherms and thermodynamics of adsorption of Pb(II) and Zn(II) onto the prepared powdered and granular activated carbons.

1.6 Thesis Layout

This thesis is comprised of seven chapters;

Chapter one (Introduction) presents the general overview of the research. This include the research background where problems usually associated with generation and discharge of pollutants into the environment through the activities of various industries were highlighted. To effectively tackle these problems, there is the need to produce activated carbons from biomass (agricultural wastes). The research objectives were equally enumerated while the last part contained the overall structure of the thesis.

Chapter two (Literature Review) presents the importance of adsorption technique in the treatment of industrial wastewaters especially the activated carbon adoption for removing heavy metals from wastewaters from the views of previous researchers as presented in their publications. Information on utilization of biomass in activated carbon preparation, various activation methods available, optimizing the preparation conditions, activated carbon classification as well as hydrothermal pre-treatment method was

presented. The last section of the chapter provides information on the adsorption kinetics, isotherms and thermodynamics in a single solute system and binary system.

Chapter three (Materials and Methods) gives detail description of all the required materials including methods employed in carrying out the activities. These include the collection and initial treatment of the precursors, the hydrothermal pre-treatment of the samples, the preparation of the activated carbons, characterization as well as adsorption studies. The experimental design used was also explained in both the preparation and the adsorption studies which include the design of experiment, model fitting and statistical analysis. Carbon regeneration as well as binary adsorption studies procedure are presented. At the end of the chapter, a schematic flow chart of the experimental activities performed in the study was shown.

Chapter four (Results and Discussion- preparation and characterization of powdered activated carbon from BEFB and RS and granular activated carbon from LFS). This chapter contains the experimental results from the BBD experimental design used in preparing powdered activated carbon from BEFB and RS. The results of optimization based on the removal strength (adsorption capacity) for Pb(II) and Zn(II) as well as the percent yield (%) of carbon were stated and discussed. The statistical parameters for model verification for the powdered activated carbons, the analysis of variance (ANOVA), the effects of process parameters as well as results of characterization of both the powdered (PAC) and granular activated carbon (GAC) are presented as obtained and discussed.

Chapter five (Batch Adsorption Studies). In this chapter, the experimental results obtained from batch adsorption studies of Pb(II) and Zn(II) on BEFBAC and RSAC are presented and discussed. Equally presented in the chapter are the results of the effects of the process conditions of solution temperature, solution pH and the amount of adsorbent

taken (dose) on percent removal of Pb(II) and Zn(II0 by BEFBAC and RSAC. Finally, the chapter contains the results and discussion of adsorption isotherms, kinetics, thermodynamic and de-sorption studies for BEFBAC and RSAC.

Chapter six (Binary Adsorption Study). The results obtained from the binary adsorption of Pb(II) and Zn(II) onto granular activated carbon prepared from longan fruit shell (GLFSAC) are presented and discussed.

Chapter seven (Conclusions and Recommendations). Here the findings of the research study are concluded. While the conclusions presents the reflections of the achievements of the research objectives obtained in the course of the study, recommendations for further future research are given. The recommendations made are such that will strengthen future research in the area.

CHAPTER 2: LITERATURE REVIEW

In this chapter, previous reports and publications on the preparation, characterization and application of activated carbon is reviewed and presented. A general overview of the precursors for preparing activated carbons, the activation methods and the process conditions are equally reviewed. Moreover, the adoption of activated carbon for removing heavy metals removal from wastewater including the adsorption isotherms, kinetics and thermodynamics are all presented. Finally, in the chapter, information on binary adsorption system is presented. At the end, a summary of all of these is given.

2.1 Utilization of Biomass Materials in the Preparation of Activated carbon.

Fossil fuel reserves depletion, high cost of energy, and concerns for the environment due to the effect of global warming have led the world towards alternative energy sources that are renewable and sustainable (Abioye & Ani, 2015). Prominent among the suitable alternative is biomass waste, also called stored energy, which is mainly carbohydrate. Biomass wastes have the least energy storage among other alternative sources like wind and solar (Saidur, Abdelaziz, Demirbas, Hossain, & Mekhilef, 2011). These wastes include wastes from municipal, agricultural/agro-industries, and energy crops such as sago, corn, sugarcane, wheat.

Biomass waste materials are increasingly gaining ground as remarkable precursor for synthesis of activated carbon (AC) due to their low cost in addition to the ease of access. The AC from this precursor is of high quality due to its high adsorptive capacity as enabled by its outstanding textural property. This quality makes AC attractive for several applications such as heavy metal removal, electrochemical applications, catalyst support, gas adsorption (methane), and waste water treatment (Katsigiannis, Noutsopoulos, Mantziaras, & Gioldasi, 2015; Lee, Zubir, Jamil, Matsumoto, & Yeoh, 2014). The procedure for the synthesis of AC from biomass waste generally includes thermochemical

carbonization via pyrolysis or combustion and subsequent activation of the resulting char. The pyrolysis of the biomass waste, which was aimed to produce carbon rich residue occurs in the absence of oxygen (Silva et al., 2014). Rather, combustion takes place in the presence of oxygen to extract energy from biomass wastes of diverse forms. It could also be termed as oxidative pyrolysis (Sanchez-Silva, López-González, Garcia-Minguillan, & Valverde, 2013). Both carbonization strategies leads to formation of a carbon rich solid residue called char, which is the main precursor for AC.

Unlike pyrolysis, carbonization via combustion occurs at a lower temperature, from140 to 400 C. A temperature above that decomposes the resulting secondary organic matter due to the presence of oxygen, thereby affecting the morphology of the produced char (Dorez, Ferry, Sonnier, Taguet, & Lopez-Cuesta, 2014; Lee, Ooi, Othman, & Yeoh, 2014).

Char activation by chemical method involves reaction between the chemical reagent and the surface of the char. The reagent can be acid, base or other relevant chemicals. Acid activation can be carried out with mineral acid such as phosphoric acid, nitric acid, sulphuric acid and hydrochloric acid (F. Ahmad, Daud, Ahmad, & Radzi, 2013; Nahil & Williams, 2012; Tseng & Wey, 2006). The main aim of the activation is to enhance the textural properties such as the pore structure and surface area of the char. The effect of the activation varies from acid to acid as well as the activation procedure. Yin et al. (Yin, Aroua, & Daud, 2007) reviewed the effect of acid modification on the textural properties of AC compared to that of the precursor. They reported that activation with nitric acid reduces the pore volume and surface area by 8.8% and 9.2%, respectively. The reduction is due to the severity of the activation, which destroys the pore structure of the material by complete or partial blockage with excess oxygen complexes.

2.2 Types of Carbon

Carbon exists in a stable form of diamonds, bulky balls, nanotubes, and graphene (Dahl, Liu, & Carlson, 2003; Novoselov et al., 2004). The myriad of its stability is due to its hybridization capability in a multiple stable bonding states, ability to form a strong bond with other atoms, as well as hydrogen. The direct compositional variables are the distribution of the hybridization states of carbon and sp2 versus sp3 bonds. Figure 2.1 presents the compositional phase space. Properties such as electrical conductivity, surface energy, and mechanical properties can be modified with dopants like F, O, Si, N, and B. Further, carbon materials can be grouped into (Grierson & Carpick, 2007; Lifshitz, 1999; Robertson, 1998, 2002):

(i) ordered, sp^2-bonded carbon (liken graphite);

(ii) diamond-like carbon (DLC), which consists of a mixture of sp^2 and sp^3 bonded amorphous films stabilized with H;

(iii) ordered, highly sp^3-bonded materials (like polycrystalline form or diamond in single crystal); and

(iv) tetra-hedral amorphous carbon (ta-C) made-up of highly bonded sp^3 amorphous materials.

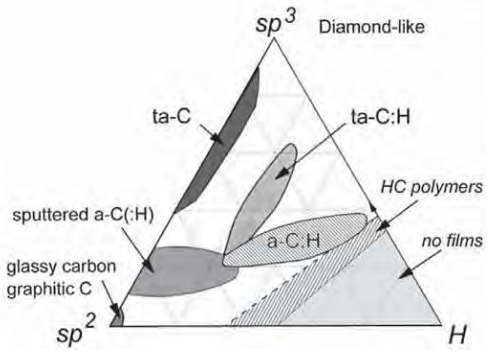

Figure 2.1: Robertson diagram illustrating the different compositions of common carbon-based materials (Grierson & Carpick, 2007).

2.3 Adsorption

Adsorption has been defined as a process of capturing of molecules of dissolved solids, liquids or gases onto the surface of an active solid material (Cheremisinoff, 2001). It occurs when the surface of the solid material is brought in contact with either a gas or a liquid. Its importance in modern technology cannot be underestimated as some adsorbents have found their uses in desiccants, as catalysts or as catalyst supports while others have been found to be useful in separation or storage of gases, liquids purification and pollution control processes (Rouquerol, Rouquerol, Llewellyn, Maurin, & Sing, 2013). Adsorption can either be physical (physisorption) or chemical (chemisorption). A physical adsorption occurs when weak inter-particle bonds such as Van der Waals, Hydrogen and dipole-dipole are involved between the liquid phase (adsorbate) and the solid phase (adsorbent) whereas chemical adsorption would only occur when strong inter-particle bonds exist between the two phases involved which usually has to do with transfer of electrons between them. Adsorption is an effective method currently being employed for removing heavy metals. This popularity of adsorption arises mainly from its ease of operation, wide pH range, low cost with high binding capacities for metals. This proves it as a highly effective and very economical technique for contaminants removal from water (C. Liu, Bai, & San Ly, 2008; Mobasherpour, Salahi, & Ebrahimi, 2012; S. Yang, Li, Shao, Hu, & Wang, 2009) . The adsorbents used for adsorption of heavy metals include activated carbons (Al-Khaldi et al., 2015; Di Natale, Erto, Lancia, & Musmarra, 2011; Goyal, Bhagat, & Dhawan, 2009; Ihsanullah et al., 2015; ShamsiJazeyi & Kaghazchi, 2010), crab shell (An, Park, & Kim, 2001), granular biomass (A. H. Hawari & Mulligan, 2006), modified chitosan (Justi, Fávere, Laranjeira, Neves, & Peralta, 2005), sewage sludge ash (Pan, Lin, & Tseng, 2003), activated carbon cloths (Kadirvelu, Faur-Brasquet, & Cloirec, 2000), fly ash (Ayala, Blanco, Garcìa, Rodriguez, & Sancho, 1998; Weng & Huang, 2004), peat (Ho & McKay, 1999), sugar beet pulp (Reddad, Gerente, Andres, & Le

Cloirec, 2002), biomaterials (Ekmekyapar, Aslan, Bayhan, & Cakici, 2006; Q. Li et al., 2004), zeolite (Biškup & Subotić, 2005), kaolinite (Alaba, Sani, & Daud, 2015; Yavuz, Altunkaynak, & Güzel, 2003) , bagasse (M. Rao, Parwate, & Bhole, 2002), recycled alum sludge (Chu, 1999), peanut hulls (Brown, Jefcoat, Parrish, Gill, & Graham, 2000), manganese oxides (Kim, Lee, Chang, & Chang, 2013), resins (Diniz, Doyle, & Ciminelli, 2002), and olive stone waste (Fiol et al., 2006). Contained in table 2.1 below is a list of some Biomass waste materials that have been adopted for the production of activated carbon.

2.4 Activated Carbon

Activated Carbon (AC) is a carbon-containing material, which is mainly amorphous in nature and possesses remarkable textural properties resulting from its production process and treatment. The properties of AC such as chemical polarity, pore structure and surface area largely depend on the activation process and the precursor (González-García, Centeno, Urones-Garrote, Ávila-Brande, & Otero-Díaz, 2013; SE, Gimba, Uzairu, & Dallatu, 2013). Generally, commercial ACs are not environmentally benign, and are costly because they are sourced from coal and petroleum, which are classified as fossil fuel. Recently, biomass precursors have gained much attention because they are abundant, low-cost, environmentally benign, renewable and sustainable (Farma et al., 2013). Prominent among biomass precursors are agricultural wastes which include oil palm empty fruit bunch (Farma et al., 2013; Foo & Hameed, 2011d), palm kernel shell (Foo & Hameed, 2013; SE et al., 2013), bamboo species (González-García et al., 2013), waste coffee beans (Rufford, Hulicova-Jurcakova, Zhu, & Lu, 2008), apricot shell (Xu et al., 2010), cassava peel waste (Ismanto, Wang, Soetaredjo, & Ismadji, 2010), rice husk (Foo & Hameed, 2011e; He et al., 2013; Kalderis, Bethanis, Paraskeva, & Diamadopoulos, 2008), sugarcane bagasse (Kalderis et al., 2008; Rufford, Hulicova-Jurcakova, Khosla, Zhu, & Lu, 2010; SI, WU, XING, ZHOU, & Zhuo, 2011), coffee

endocarp (JM Valente Nabais, Teixeira, & Almeida, 2011), sunflower seed shell (X. Li et al., 2011), rubber wood sawdust (Taer et al., 2011), and argan seed shell (Elmouwahidi, Zapata-Benabithe, Carrasco-Marín, & Moreno-Castilla, 2012). Activated carbon is usually prepared by carbonization of the starting material (precursor) at high temperature within an inert environment. This is then followed by activating the carbonized product. Three main methods of activation are available. These include physical, chemical and physicochemical methods (Z. Z. Chowdhury et al., 2013).

2.4.1 Activated Carbon – Demand and Applications

The demand for activated carbon in recent past has been on the high side. They have been widely employed in adsorption, as catalyst or as a catalyst-support. The use of activated carbon in industries cannot be underestimated where they are employed either in separation and purification processes of mixtures of gases and liquids, recovery of substances and removal of organic and inorganic pollutants from wastewaters from such industries(Khalili, Campbell, Sandi, & Golaś, 2000). Activated carbon is widely employed in the treatment of wastewater and effluents of textile industry especially effluents generated during dyeing and finishing processes which usually contain coloured substances, surfactants, dissolved solids and heavy metals. Apart from the fact that the coloured wastes are aesthetically displeasing, they equally hinder light penetration and therefore very disturbing to aquatic eco-system(El Nemr, Abdelwahab, El-Sikaily, & Khaled, 2009). Priorities are being given to regulate the discharge of some pollutants into the environment especially inorganic pollutants such as chromium (VI) ions. Chromium (VI) ions can get to the environment through the activities of industries such as dyes, pigments, metal cleaning, plating, leather and mining industries. The world Health Organization standard limit for chromium (VI) ions in drinking water is 0.05mg/l and anything above this becomes highly hazardous(Acharya, Sahu, Sahoo, Mohanty, &

Meikap, 2009). Heavy metals have become relatively more significant as pollutants because of their persistence, high toxicity and bio-magnification (Kadirvelu, Thamaraiselvi, & Namasivayam, 2001). They exist in aqueous wastes of many industries like radiator manufacturing, mining, metal plating, storage batteries manufacture, alloy and smelting industries. Due to its cost effectiveness, the use of adsorbents for removing heavy metals, compared to other techniques, including precipitation, membrane filtration, ion exchange, co-precipitation/adsorption, has gained prominence in recent times (Kadirvelu et al., 2001).

Other areas in which activated carbon has become excellent and versatile as an adsorbent are in the removal of color, odor, taste, organic pollutants and inorganic impurities contained in drinking waters and in the purification processes in many chemical, food and pharmaceutical products (Gottipati, 2012). Several authors have reported the application of activated carbon in removing metal pollutants from aqueous phases (Table 2.2).

Table 2.1: Some Biomass Waste Materials Utilized for the Production of Activated Carbon

Precursor	References
Macadamia nutshell	(Ahmadpour & Do, 1997)
Palm tree trunks, Waste cartoons and plastics	(AlOthman, Habila, & Ali, 2011)
Coconut shell	(Amuda et al., 2007)
Tunisian olive waste cakes	(Baccar et al., 2009)
Mangostania garcinian shell	(Z. Z. Chowdhury, Zain, Khan, Rafique, et al., 2012)
Kenaf core	(Z. Z. Chowdhury, Zain, Khan, Rafique, et al., 2012)
Vetch biomass	(Ceyhan, Şahin, Saka, & Yalçın, 2013)
Elaeagnus angustifolia seeds	(Şahin, Saka, Ceyhan, & Baytar, 2015)
Cow dung	(S. Elaigwu, Usman, Awolola, Adebayo, & Ajayi, 2010)
Prosopis Africana shell	(S. E. Elaigwu, Rocher, Kyriakou, & Greenway, 2014)
Cotton stalk	(El-Hendawy, Alexander, Andrews, & Forrest, 2008)

'Table 2.1, Continued'

Precursor	References
Date stones	(Bouchelta, Medjram, Bertrand, & Bellat, 2008)
Rice husks	(Herrera, Anaguano, & Suarez, 2013)
Pistachio nut shell	(Foo & Hameed, 2011a)
Sunflower seed oil residue	(Foo & Hameed, 2011b)
Oil palm empty fruit bunch	(Hidayu, Mohamad, Matali, & Sharifah, 2013)
Palm kernel shell and coconut shell	(Hidayu & Muda, 2016)
Soybean oil cake	(Tay, Ucar, & Karagöz, 2009)

Table 2.2: Application of activated carbon in the removal of metal pollutants from aqueous phase.

Pollutant	Precursor	Source
Hg, Ni	Silicon cotton hull, coconut tree sawdust, sago waste, maize cob and banana pith	(Kadirvelu et al., 2003)
Cu, Zn, Cr, CN	Commercial activated carbon	(Monser & Adhoum, 2002)
Hg, Cd, Pb, Ni, Cu	Waste coir pith	(Kadirvelu et al., 2001)
Cd, Zn	Bagasse	(Dinesh Mohan & Singh, 2002)
Cr	Coconut tree sawdust	(Selvi, Pattabhi, & Kadirvelu, 2001)
Cd, Pb, Hg, Cu, Ni, Mn, Zn	Carbon Aerogels	(Meena, Mishra, Rai, Rajagopal, & Nagar, 2005)
Cr, Hg, Fe	Cassava peel	(Sivakumar, Senthilkumar, & Subburam, 2001)
Cr	Jackfruit peel	(Narayanan & Ganesan, 2009)
Cr	Coconut shell charcoal and commercial activated carbon	(Babel & Kurniawan, 2004)
Cr	Terminalia arjuna nuts	(Mohanty, Jha, Meikap, & Biswas, 2005)
Cu, Ni, Pb	Activated carbon cloths	(Kadirvelu et al., 2000)
Cd, Cu, Ni, Pb, Zn	Peanut shells	(Wilson, Yang, Seo, & Marshall, 2006)
Pb	Mangostana garcinia shell	(Z. Z. Chowdhury, Zain, Khan, Rafique, et al., 2012)
Zn	Coconut shell	(Amuda et al., 2007)
Pb, Zn	Watermelon and walnut shell	(Moreno-Barbosa et al., 2013)

2.4.2 Preparation of Activated Carbon

The procedure for synthesis of AC consist of two phases, carbonization and activation. The two phases can occur sequentially or simultaneously. The carbonization can either be by pyrolysis or combustion (oxidative pyrolysis) (Abioye & Ani, 2015). The temperature for pyrolysis ranges between 400 and 850^{o}C while that of combustion is usually between 140- 400^{o}C.

The combustion temperature is lower than pyrolysis to prevent secondary reaction associated with the presence of oxygen (Dorez et al., 2014; Lee, Ooi, et al., 2014). The activation process converts the product of carbonization (char) to AC. The methods of activation could be chemical, physical, physiochemical or microwave-assisted activation (Table 2.3).

2.4.2.1 Physical Activation

Physical activation also known as thermal activation entails carbonization of the precursor at the range of 400-850^{o}C and subsequent controlled oxidation in a controlled environment. The oxidizing agents used for this process include air, carbon dioxide, steam as a mixture of gases at a temperature between 600 and 900^{o}C (Abioye & Ani, 2015). Prominent among the oxidizing agents is CO_2 due to its purity and ease of handle, which is evident in slow rate of reaction at about 800 C temperature (Ioannidou & Zabaniotou, 2007). The study of Nabais et al. (J. M. V. Nabais et al., 2008) indicates that activation with CO_2 produced AC with better pore volume and BET surface area as compared with samples activated with steam. However, Activation with steam exhibits higher activation rate than with CO_2.

Table 2.3: Activation methods for AC synthesis.

Activation method	Activating Agent	Lignocellulosic material	Reference
Chemical	$ZnCl_2$	Date stones, waste coffee beans, sugarcane bagasse, waste camellia oleifera	(Cruz et al., 2012; Rahim, Aqmar, & Dewi, 2010; Rufford et al., 2010; Rufford et al., 2008; Theydan & Ahmed, 2012; J. Zhang, Gong, Sun, Jiang, & Zhang, 2012)
	KOH	Bamboo species, distillers dried grains with soluble, waste tea-leaves, oil palm empty fruit bunches, argan seed shells, sunflower seed shell, coffee endocarp, cassava peel waste, soybean oil cake.	(Cruz et al., 2012; Elmouwahidi et al., 2012; Farma et al., 2013; González-García et al., 2013; Ismanto et al., 2010; X. Li et al., 2011; JM Valente Nabais et al., 2011; SE et al., 2013; Tay et al., 2009)
	NaOH	Apricot shell	(Xu et al., 2010)
	$FeCl_3$	Date stones	(Theydan & Ahmed, 2012)
	K_2CO_3	Cocoa pod husk, straw pulping	(Cruz et al., 2012)
Physical	Steam, CO_2	Corncob, bagasse bottom ash, macadamia nut-shell, rice husk fly ash, sawdust fly ash	(Aworn, Thiravetyan, & Nakbanpote, 2008)
	CO_2	Coffee endocarp	(J. M. V. Nabais et al., 2008; Joao Valente Nabais, Carrott, Carrott, Luz, & Ortiz, 2008; JM Valente Nabais et al., 2011)
Physiochemical	KOH/CO_2	Oil palm empty fruit bunches, cassava peel waste	(Farma et al., 2013; Ismanto et al., 2010)
Microwave assisted	KOH	Date stone, oil palm empty fruit bunch, oil palm fiber, cotton stalk, oil palm shell	(Deng, Li, Yang, Tang, & Tang, 2010; Foo & Hameed, 2011c, 2011d, 2012a, 2013)
	ZnCl2	Cotton stalk, white pine wood, sugarcane bagasse, peanut shell, rice husk	(Deng, Yang, Tao, & Dai, 2009; He et al., 2013; SI et al., 2011; T. Wang, Tan, & Liang, 2009)
	NaOH	Langsat empty fruit bunch waste	(Foo & Hameed, 2012c)
	K_2CO_3	Cotton stalk, tobacco stems, wood sawdust	(Deng, Li, et al., 2010; Foo & Hameed, 2012b; W. Li, Zhang, Peng, Li, & Zhu, 2008)
	H_3PO_4	Waste tea, cotton stalk, bamboo	(Deng, Zhang, Xu, Tao, & Dai, 2010; Q.-S. Liu et al., 2010; Yagmur, Ozmak, & Aktas, 2008)
	Steam	Jatropha hull, coconut shells	(K. Yang et al., 2010)

Moreover, to achieve a remarkable textural property, oxidizing agent needs to be carefully selected based on previous experiences with the precursor material (Aworn et al., 2008). The oxidizing agent mainly helps to eliminate the volatile matters and facilitates carbon burn-off, thereby developing porosity on the carbon char. This is evident in the pore volume and the surface area of the resulting material. The quality of the synthesized AC largely depends on the furnace type, gas flow, activation temperature and time.

2.4.2.2 Chemical Activation

This method employs the activating agent both as an oxidizing agent and a dehydrating agent. The activating agent can be acid, base or salt. The activation process entails simultaneous carbonization and activation at a temperature between 300 and 950^{o}C. Therefore, the porosity development and carbon yield proceed via decomposition at the chosen temperature. Chemical activation produced AC with a more outstanding textural property but the process is more wearisome, energy and time consuming, which makes it more expensive (Abioye & Ani, 2015). This is due to the need for post-activation activities such as washing-off of ash and other reactant residues.

The report of Zheng et al., (J. Zhang et al., 2012) shows that the porosity of AC synthesized by chemical process is a direct function of the amount of activating agent used and the activation temperature. The work of Jin et al. (Jin, Wang, Gu, & Polin, 2013) produced the highest porosity of AC so far in the literature. They produced AC with pore volume and specific surface area of 1.65 $cm^3\ g^{-1}$ and 2959 $m^2\ g^{-1}$, respectively using KOH for the activation.

2.4.3 Structure of Activated carbon

The dependence of the effectiveness (adsorption capacity) of AC on its structure cannot be underestimated. Such structure include porous, crystalline and chemical structures.

2.4.3.1 Porous Structure

The importance of porous characteristics such as surface area, pore volume and pore size distribution in the adsorption capacities of ACs cannot be under estimated (Gottipati, 2012). The porous structure of AC is formed during carbonization and further enhanced during activation (Wu, Tseng, & Juang, 1999). During this period, the tars and other carbonaceous materials between the elementary crystalline are removed. It should be emphasized that the nature of pores and pore size distribution of AC are dependent on the nature of the starting material and the manipulation of the activation process. During activation, disorganized carbons are removed through exposure of the crystalline to the action of the activating agent which results in the development of pores with varying sizes and shapes (Gottipati, 2012). Pores are classified according to their average width (w) according to International Union of Pure and Applied Chemistry (IUPAC, 1972) as reported by Donald C et.al. (1994) (Donati, Drikas, Hayes, & Newcombe, 1994). Thus pores are classified accordingly as follow:

Table 2.4: Classification of Activated Carbon Pores (IUPAC, 1972)

Type of Pores	Width (w)
Micropores	<2nm (20Å)
Mesopores	2nm – 50nm (20 – 500 Å)
Macropores	> 50nm (> 500 Å)

2.4.3.2 Crystalline Structure

During carbonization process, the microcrystalline structure of ACs starts developing, while the free valences are developed as a result of regular bonding disruption. Moreover,

the manipulation of the process conditions as well as presence of interference in form of impurities could negatively affect the development of valences in the structure (Kennedy, Vijaya, Kayalvizhi, & Sekaran, 2007; Skubiszewska-Zięba, 2010; T. Yang & Lua, 2006). Considering their graphitizing ability, active carbons can be classified as either graphitizing or non-graphitizing. While graphitizing carbon is made up of a large number of graphite with the porous structure not well developed, the non-graphitizing on the other hand are hard as a result of strong cross-linking existing between the crystallites with a microporous structure that are well-developed (Gottipati, 2012).

2.4.3.3 Chemical Structure

In addition to the porous and crystalline structures of an activated carbon, the chemical structure is equally an important character that influence its adsorption capacity. Activated carbons contains heteroatoms mainly oxygen and hydrogen which are chemically bonded to the carbon atoms. Other heteroatoms that may be present are sulfur, nitrogen, phosphorous and the halogens (Valix, Cheung, & Zhang, 2006). These heteroatoms are either present in the raw material or chemically added during activation (Gottipati, 2012). The heteroatoms are either bonded to carbon atoms at the edges or at defect positions to form surface groups or complexes, such as carbon-hydrogen, carbon-oxygen, carbon-sulfur, carbon-phosphorous and carbon-halides (Castro-Muñiz, Suárez-García, Martínez-Alonso, & Tascón, 2011; Valix et al., 2006). Of all the heteroatoms, oxygen significantly influence the surface chemistry and other properties of activated carbon including its catalytic properties.

2.4.4 Activated Carbons Classification

Classification of activated carbons based on the preparation process, their physical properties and surface characteristics is difficult and cumbersome due to their complexities. For convenience, activated carbons are better classified based on their

particle size, hence they can be classified as Powdered Activated Carbon (PAC), Granular Activated Carbon (GAC) or Activated Carbon Fibres (ACF) (Babel & Kurniawan, 2003; Gottipati, 2012) (Table 2.5).

2.5 Hydrothermal Pretreatment

To be able to modify the surface chemistry of activated carbon, the precursors are usually pretreated using several methods including biological, physical, physio-chemical, chemical processes and hydrothermal technique. The process of preparing activated carbon through hydrothermal treatment followed by chemical activation is to enhance the surface chemistry of the carbon (Roman et al., 2013). During hydrothermal pretreatment stage, the precursor is carbonized at low temperature range usually between 150 – 250ºC and pressure generated within the system in the presence of deionized water as 'green' solvent. The advantages of this method are numerous including simplicity in design, high cost effectiveness, high energy efficiency and completely 'green' in nature (Titirici, Thomas, Yu, Müller, & Antonietti, 2007). All these give the method the advantage of being energy efficient under milder conditions as it produces one-third of the required energy for carbonization (Roman et al., 2013). Unlike conventional pyrolysis, it does not produce toxic gases and tars (Xiu, Shahbazi, Shirley, & Cheng, 2010). Furthermore, hydrothermal pretreatment of biomass leads to production of a new type of starting materials for the preparation of activated carbon (Hao, Björkman, Lilliestråle, & Hedin, 2014). Other advantages of the hydrothermal char include its self-binding properties which enhances peletilization (Amaya, Medero, Tancredi, Silva, & Deiana, 2007). Finally, the method does not require gas flow, thereby making it highly feasible economically (Amaya et al., 2007). However, other pretreatment methods have limitations which are summarized below:

Table 2.5: Classification of Activated Carbon.

Class of Carbon	Particle size	Application	Reference
Powdered Activated Carbon (PAC)	0.015-0.025mm	Industrial/Municipal wastewater treatment, sugar decolourization in food industry and in pharmaceutical industry.	(Foo & Hameed, 2009; Ormad, Miguel, Claver, Matesanz, & Ovelleiro, 2008; Satyawali & Balakrishnan, 2009)
Granular Activated Carbon (GAC)	0.6 – 4mm	Applied in continuous process of liquid and gas phase	(Gottipati, 2012; Hijnen, Suylen, Bahlman, Brouwer-Hanzens, & Medema, 2010)
Activated Carbon Fibre (ACF)	Heat-treated-carbonized in an oxidizing atmosphere	For adsorption in gas and aqueous phases, and in methane preservation	(Alcaniz-Monge, De La Casa-Lillo, Cazorla-Amorós, & Linares-Solano, 1997; Gottipati, 2012; Suzuki, 1994)

Table 2.6: Issues with Current Pre-Treatment Methods

Method	Limitations
Biological technique or the use of fungi	Requires long treatment time
Physical technique such as milling, chipping and grinding)	Too expensive to be used at full scale
Physico-chemical processes e.g. steam explosion	High pressure and temperature required
The use of chemicals such as dil. acid, alkali, organic solvents	Involve toxic materials and environmentally unfriendly.
Torrefaction	Requires significant capital and energy

2.6 Optimization of process conditions for activated carbon preparation

The production of activated carbon for a specific application has a great challenge. The effectiveness of an activated carbon in adsorption process is highly influenced by two main factors namely the nature of the precursor and the preparation conditions (Tan, Ahmad, & Hameed, 2008). The manipulation of the preparation conditions of carbonization temperature, holding time and impregnating agent/impregnation ratio so as

to produce activated carbon with target application, is very important. To achieve this, the use of an appropriate experimental design becomes germane and to this end, the use of surface response methodology (RSM) as a statistical technique for developing, improving and optimizing processes becomes a useful tool (Karacan, Ozden, & Karacan, 2007). To this end, the use of Box Behnken Design (BBD) having three factors and five replicates at the center point to appraise errors, was employed to determine the effects (main and interactive) of the variables with a view to develop a second-order polynomial model having linear, interaction, and quadratic terms. The number of experimental runs (N) which the BBD design required is expressed by Eq. 2.1

$$N = 2k\,(k-1) + C_0 \qquad 2.1$$

where k stands for the factors number while Co represents the central point number. The method is less time consuming as less number of experimental run is required, especially when k is not too large (Ferreira *et al*., 2007).

2.7 Adsorption of heavy metals on various adsorbents

The presence of heavy metal ions in wastewater constitutes environmental challenge because of their harmful effects to human health and the health of other living organisms (Fu & Wang, 2011; S. Wang, Soudi, Li, & Zhu, 2006). Several strategies such as adsorption, membrane separation (Ciardelli, Corsi, & Marcucci, 2001), flocculation and coagulation (Panswad & Wongchaisuwan, 1986), ion exchange (Körbahti, Artut, Geçgel, & Özer, 2011) and chemical precipitation (Bilgiç, 2005; Roy, Adhikari, & Majumder, 2013; Tong, Li, Yuan, & Xu, 2011) have been employed for removing heavy metals pollutants. Adsorption method has proved to be an attractive and effective method for metal ions removal (Alslaibi, Abustan, Ahmad, & Foul, 2013). One of the most popularly used adsorbents for this course is AC because of its fast rate of removal and high adsorption capacity (Rafatullah, Sulaiman, Hashim, & Ahmad, 2010). AC possesses an

aromatic molecular structure of graphene layers, highly functional groups which contains oxygen and porous structure (Luo et al., 2015). Further, AC exhibits varied and complex interaction during adsorption due to its non-uniform active sites.

2.8 Activated Carbon Regeneration

Investigation of the possibility of reusability of spent AC to remove heavy metal ions in wastewater treatment is essential towards determination of its economic viability. This investigation is done via appropriate desorption route or by chemical regeneration, and it is extremely effective and economical (G. P. Rao, Lu, & Su, 2007). Prominent among the possible strategies is activation with carbonic acid in the presence of a supercritical mixture of CO_2 and water at high pressure. The use of this strategy in different areas have been deeply investigated by several scholars (Jessop & Leitner; Marr & Gamse, 2000). Some other regeneration strategies include thermal volatilization, chemical activation and bio-regeneration.

2.9 Summary

The high cost of commercial activated carbon has called for shifting of attention to preparation of activated carbon from a more economical and environmental friendly precursors, thereby leading to the use of biomass (agricultural waste). Biomass waste materials have gained ground as remarkable precursor for synthesis of activated carbon due to their low cost and ease of access. Activated carbons from biomass have been discovered to be of high quality standard in terms of their adsorptive capacity. Adsorbents have become highly important in modern technology as they have found their uses in desiccants, as catalysts and or as catalysts supports. The popularity of adsorption as a method of removing metals from wastewaters is a result of the ease with which it can be operated, wide pH range, highly affordable cost and extremely high binding capacities for metals, thereby making the demand for activated carbon in recent times to be on the

high side especially when removing of heavy metals is of interest. It could be affirmed that the effectiveness of an activated carbon in the removal of pollutants could be enhanced by the type of starting material (precursor) coupled with the appropriate modifications of preparation process. Therefore, in order to enhance the adsorption capacity of an activated carbon, there is the need to employ an appropriate mode of preparation by choosing an appropriate activation method and the optimization of the operating conditions of carbonization temperature, holding time and activating agent/concentration. The preparation of activated carbon through the 2-step of hydrothermal pretreatment followed by acid activation and carbonization has not been well reported in literature but has been found to improve significantly the surface structure and pore characteristics of activated carbon, thereby enhancing its adsorption capacity.

CHAPTER 3: MATERIALS AND METHODS

This chapter provides list of chemicals, reagents and the methodology which were used to carry out the research. The chapter is subdivided into three sections. The first section contains the list of chemicals and reagent. The second section gives the description of experimental procedure for preparing adsorbent by using design of experiment (DOE), model development and ANOVA analysis. It provides the characterization system of the prepared activated adsorbent at different stages. The third section provides the batch sorption studies, kinetics and thermodynamics studies. The process used for regeneration of the cations loaded sorbent in batch sorption system is described. The chapter ends with a schematic flow chart reflecting generally the experimental activities undertaken to carry out the project.

3.1 Materials

The Carbonaceous precursors used in the studies are Banana Empty Fruit Bunch (BEFB), Rattan Sawdust (RS) and Longan Fruit Shell (LS). Banana empty fruit bunch (BEFB) was collected from Bangladesh Scientific Institute of Research (BCSIR), Dhaka, Bangladesh. Rattan core was collected from the premises of the Federal School of Agriculture, Akure, Nigeria, The BEFB and RS were mechanically cut into small sizes, thoroughly washed in hot deionized water to rid them of mud, dusts and other forms of dirt. They were then sun-dried for 4 weeks and finally oven-dried in the laboratory at 80^{o}C for 24h. The samples were then crushed using a ball mill. The powdered sample was sieved to remove large particles, washed, dried, and stored in a sealed container for further processing. Each precursor so prepared was packed in plastic container tightly covered and labeled accordingly .However, Longan Fruit was purchased from a popular night market in Banda Sunway, Petaling Jaya, Malaysia. After deshelling the fruit, the pulp covering the shell was carefully removed while the shell was cut into small sizes,

washed thoroughly using hot deionized water, followed by oven drying at 80ºC for 24 h. Moreover, all the chemical agents used were supplied by Chemlab SDN BHD, Petaling Jaya, Malaysia. The cleaned, dried materials were pulverized to <1μm mesh size with the aid of a jaw crusher (Denver Product, Dagenham, U.K).

3.2 Methodology

3.2.1 Pre-treatment of Precursors

After the initial washing and oven drying, in order to ensure a more homogeneous mixing and produce samples with required particle size, banana empty fruit bunch and rattan sawdust were crushed using a ball mill and sieved. The samples were then washed and dried again and finally stored for further processing. However, the longan fruit shell was cut to appropriate size of 2mm for preparation of granular activated carbon and washed, dried and stored for further experiments.

3.2.2 Preparation of Hydro-char

The hydro-char of the various samples (BEFB, RS and LS) were prepared as a middle product to improve both the physical and chemical properties of the precursors as adsorbents. To achieve this, 5g of each of the precursor was mixed with 50ml of deionized water and vigorously stirred to ensure homogeneity. The mixed samples were then transferred into an autoclave lined with Teflon (100ml) while the temperature was adjusted to 220ºC and carbonized for 12h. The char produced was then thoroughly washed using deionized water to obtain neutral pH. The hydro-char was then stored in an air-tight stoppered container for both characterization and further adsorption studies.

3.2.3 Preparation of Powdered Activated Carbon

20g of hydro-char was impregnated with 100 ml of H_3PO_4 using variable concentration according to the design of experiment (ratio1:5 solid to liquid) and heated to 90-100ºC for 4h. This was then followed by oven-drying at 90ºC for 24 h. The sample was then fed

into the urns of about 150mm length and 40mm diameter. The urns were then transferred into the calcination furnace (Bamstead/Thermolyne 48000) fitted with a temperature knob to regulate the temperature. The urns was equally connected to nitrogen gas cylinder while the pyrolysis of the sample was carried out using a continuous nitrogen gas flow at 100 ml/min. The carbonization was carried out at varying temperature and time based on response surface methodology using Box Behnken design matrix (Table 3.1). Upon attaining the regulated holding time, the sample was allowed to cool to room temperature under inert atmosphere and then raked from the vessel. The sample was then thoroughly washed using hot deionized water to remove residual chemical agents until the pH became neutral and then dried at 65^{o}C for 12 h. This was then stored for characterization and further adsorption studies accordingly.

3.2.4 Preparation of Granular Activated Carbon

The fruits of longan were opened mechanically to separate the fruit cover, the edible pulp and the shells. The shells were then crushed and cut into size using stainless steel scissors while the resulting product was sieved into 15-50 mesh (1500-250 microm) size. This was then stored in a desiccator prior to the preparation of the granular activated carbon. The granular activated carbon was then prepared as was done for powdered activated carbon above.

3.2.5 Experimental Design

The secondary stage of pyrolysis was carried out in the presence of nitrogen gas flow at varying temperatures, based on the basic design matrix (Tables 3.1 and 3.2

Table 3.1: Independent Variables for Box Behnken Design

Variables	Code	Coded Variable Levels		
		-1	**0**	**+1**
Temperature (°C)	x_1	500	650	800
Carbonization Time (h)	x_2	1	2	3
H_3PO_4 Concentration (%)	x_3	25	37.5	50

The RSM technique was used to examine the impact of the major operating factors on Pb(II) and Zn(II) cation removal. The experimental runs number (N) required for the BBD design is expressed by Eq. 2.1, (Ferreira et al., 2007).

The Box Behnken Design (BBD) having three factors with five replicates at the center point specifically designed for errors appraisal, was used to estimate the main and interaction effects of the variables and to develop a second-order polynomial model with linear, interaction, and quadratic terms. To carry out the equilibrium adsorption studies, three important effective parameters—temperature (x_1), time (x_2), and activating agent concentration (x_3)—were the independent variables, while Pb(II) removal (Y_1), Zn(II) (Y_2) removal, and carbon yield (Y_3) were the response variables (dependent variables). The variations were as follows: temperature, 500 to 800 °C; time, 1 to 3 h; and concentration of acid, 25 to 50%. The low, middle, and high levels of each variable were indicated as -1, 0, and +1, respectively. The order of the experimental runs was randomized, and the responses were used to develop empirical models using a second-degree polynomial equation Eq. 3.1: (Gunaraj & Murugan, 1999)

$$Y = b_0 + \sum_{i=1}^{n} b_1 x_1 + \sum_{i=1}^{n} b_{11} x_i^2 + \sum_{i=1}^{n} \sum_{j>1}^{n} b_{ij} x_i x_j \qquad 3.1$$

where Y stands for the predicted response, b_0 represents the constant coefficient, b_i defines the linear coefficient, b_{ij} denotes the interaction coefficients, b_{ii} is the quadratic

coefficient, while x_i, and x_j stand for the coded values of adsorption. For the three variables, the suggested number of experiments at the center point was five, and the total number of experiments (N) required was 17 (Table 3.2). Table 3.2 summarizes the coded and actual levels of the three independent variables together with the responses obtained from the BBD experimental run represented by the design matrix.

3.2.5.1 Effect of H_3PO_4 Concentration

The effect of H_3PO_4 acid concentration on the yield and porous characteristics of BEFB, RS, and LS activated carbons were studied. 20g of the samples hydro-char was impregnated with H_3PO_4 in varying impregnation ratio ranging from 30% - 50%, according to Table 3.2 above. For each activation, 20g of the hydro-char was impregnated with 100ml of different percentage concentration of H_3PO_4 (ratio1:5 of solid to liquid). This can be represented mathematically by the following equation

$$\text{impregnation ratio} = \frac{W}{V} \qquad 3.2$$

Where w = weight of solid sample, and

v = volume of H_3PO_4

3.2.5.2 Effect of Carbonization Temperature

The influence which carbonization temperature has on the yield and adsorption characteristics of activated carbon during activation process is important. This was studied by varying the carbonization temperature within the range of 500 to 800^{o}C for each of the chemical activations (Table 3.2).

3.2.5.3 Effect of holding time

The holding time was the time the sample was held in the oven at a carbonization temperature. The holding time was varied between 1 – 3h to determine the effect of this

on the yield and removal percentages of Pb(II) and Zn(II) cations by the activated carbons (Table 3.2).

3.2.6 Characterization of the Precursors, Hydro-char and Activated Carbons

3.2.6.1 Proximate Analysis

The proximate analysis of the raw materials, hydro-char and the activated carbons were subjected to thermo-gravimetric analysis (TGA). The parameters analyzed include moisture, volatile matter, fixed- carbon and ash contents. The TGA analysis provided the opportunity to study the pyrolysis behaviour of the samples, biochar and the activated carbons. In evaluating the moisture content, the oven-drying test method was used while the ash content was evaluated by heating for 8h at 650^{o}C until consistent mass was obtained. The fixed carbon was estimated by difference, according to Duran Valle *et al*., 2005 (Durán-Valle, Gómez-Corzo, Pastor-Villegas, & Gómez-Serrano, 2005).

Fixed carbon (%) =100–(moisture % + ash % + volatile matter %). 3.3

3.2.6.2 Elemental (Ultimate) Analysis

CHNS analyser was used in carrying out the elemental analysis. However, the percentage oxygen present was evaluated by difference as follow

Oxygen (%) = 100 – (C % + H% + N % + S %) 3.4

Table 3.2: Experimental Design for Preparation of Activated Carbon from Banana Empty Fruit Bunch (BEFB), Rattan Sawdust (RS) and Longan Fruit Shell (LS) using Box-Behnken Factorial Design.

Sample ID	Run	Type of Point	Reaction Variables			Pb(II) Removal (%)	Zn(II) Removal (%)	Yield (%)
			Temp x_1 (^oC)	*Time* x_2 *(h)*	*Concentration* x_3 *(%)*	Y_1	Y_2	Y_3
1	1	Center	650	2	37.50	-	-	-
2	2	Center	650	2	37.50	-	-	-
3	10	Center	650	2	37.50	-	-	-
4	11	Center	650	2	37.50	-	-	-
5	17	Center	650	2	37.50	-	-	-
6	3	IBFact	500	1	37.50	-	-	-
7	4	IBFact	650	1	25.00	-	-	-
8	5	IBFact	650	3	50.00	-	-	-
9	6	IBFact	500	3	37.50	-	-	-
10	7	IBFact	650	1	50.00	-	-	-
11	8	IBFact	800	3	37.50	-	-	-
12	9	IBFact	500	2	50.00	-	-	-
13	12	IBFact	800	2	37.50	-	-	-
14	13	IBFact	800	1	50.00	-	-	-
15	14	IBFact	500	2	25.00	-	-	-
16	15	IBFact	800	2	50.00	-	-	-
17	16	IBFact	650	3	25.00	-	-	-

3.2.6.3 Yield

The yield of activated carbon is important and usually estimated on a chemical free basis. The chemical activation process efficiency is determined by the yield of activated carbon and calculated as the weight of the activated carbon obtained divided by the weight of the raw sample, multiplied by 100

$$\text{Yield } \% = \frac{\text{Weight of activated carbon obtained}}{\text{Weight of raw material}} \text{ X } 100 \qquad 3.5$$

3.2.6.4 Surface Porosity Characterization

The surface porosity of the raw materials, hydro-chars and the prepared activated carbons was carried out using the Nitrogen Adsorption-Desorption isotherm at 77.313 K with surface area analyzer (Trister II BET Surface Area Analyzer). The BET model was applied to fit nitrogen adsorption isotherm with the surface area of the sorbent evaluated according to (Vernersson, Bonelli, Cerrella, & Cukierman, 2002). The BET equation was used to calculate the surface area. The BET equation (Bigham, Schwertmann, Traina, Winland, & Wolf, 1996) is given as follows (eq. 3.6).

$$\frac{\mathrm{P}}{\mathrm{V}(\mathrm{P}^0-\mathrm{P})} = \frac{1}{V_m \mathrm{C}} + \frac{\mathrm{C}-1\,(\mathrm{P})}{V_m \mathrm{C}(\mathrm{P}^0)} \qquad 3.6$$

where,

V = volume adsorbed at STP (cm^3g^{-1})

V_m = volume of monolayer capacity at STP (cm^3g^{-1})

C = BET constant.

The total pore volume was calculated as the as the total volume of N_2 adsorbed at relative pressure of 0.995. In order to overcome the problem usually encountered when the linear form of Dubinin-Radushkevich (DR) equation is used, a more generalized equation known as Dubinin-Astakhov (DA) is employed in calculating the micropore surface area and the pore volume.

$$\ln \mathrm{W} = \ln (\mathrm{V}^{\mathrm{o}}\,\mathrm{P}) - \mathrm{K}[\frac{\ln(v^0)}{p}]^{\mathrm{n}} \qquad 3.7$$

where,

K = empirical constant.

n = Dubinin-Astakhov parameter (usually used for homogeneous micropore structure).

3.2.6.5 Microscopy

The surface of the precursors, hydro-chars and the final products (Activated Carbons) were analysed using the Field Emission Scanning Electron Microscope (FESEM) (Zeiss SUPRA #%VP; Germany). The FESEM was coupled with Energy Dispersive X-Ray for carrying out the elemental analysis.

3.2.6.6 Surface Chemistry Determination

The surface functional groups and structure of the raw materials, hydro-chars and the activated carbons were estimated using the Fourier Transform Infrared (FTIR) spectroscopy (FTIR – BRUKER FTIR IFS 66/S). The FTIR spectra were recorded between 400 and 4000cm^{-1}.

3.2.7 Adsorption Experiments

3.2.7.1 Preparation of Adsorbates Solutions

Prior to adsorption studies, stock solution of Pb (II) and Zn (II) ions were prepared from $Pb(NO_3)_2.2H_2O$ and $Zn(NO_3)_2.6H_2O$ respectively. While Pb (II) adsorbate was prepared by dissolving 1.77g of its salt, Zn (II) was prepared by dissolving 4.55g of its salt (to make 1000ppm) in some deionized water in a 1000ml Standard volumetric flask, shaken thoroughly to ensure homogeneous solution and then made up to mark with deionized water. The test solutions used in the study, that is, 150mg/L, 200mg/L, 250mg/L, 300mg/L and 350mg/L initial concentrations were then made from the stock solution by serially diluting the mother solution (stock solution). The solutions were usually prepared freshly from stock solution for each adsorption study. The pH of the initial concentrations was usually adjusted by adding in drops either 0.1M NaOH or 0.1M HCl using a pH meter (Mettles Toledo, Ross FE 20 Model, USA).

3.2.7.2 Batch Adsorption Studies

The sorption of the adsorbates onto the adsorbents was studied through batch adsorption study. Variation of uptake level of Pb (II) and Zn (II) ions with contact time was determined for each of the adsorbent. This was required in other to establish the equilibrium time (time for the adsorbent to reach sorption equilibrium). To accomplish this, 0.2g each of the adsorbent were dispersed in 50cm^3 of each of the initial concentrations of 150, 200, 250, 300 and 350mg/L solutions in well stoppered plastic containers. The mixture was then thoroughly agitated using a water bath shaker set at 150rpm and at room temperature (30^{o}C). After attaining the set contact time, the mixture was filtered while the residual concentration of the Pb (II) or Zn (II) ions (as the case may be) in the filtrate was determined by ICP (APHA 3125B, 20th edition, 1998). The amount of Pb (II) or Zn (II) adsorbed at equilibrium (qe) was calculated using the equation below,

$$q_e = \frac{(C_o - C_e)\,v}{W} \qquad 3.8$$

where,

q_e (mg/g) = the amount of adsorbate (Pb (II) or Zn (II) ions) adsorbed at equilibrium.

C_o (mg/L) = initial concentration of adsorbate.

C_e (mg/L) = final concentration of adsorbate after adsorption at equilibrium.

V (L) = Volume of solution taken.

and W (g) = Mass of adsorbent (activated carbon) taken.

3.2.7.3 Adsorption Kinetics

To be able to determine the adsorption kinetics in this study, three kinetic models were used. These are the pseudo-first-order kinetic model, the pseudo-second-order kinetic model and the Elovich equation model. Furthermore, the diffusion mechanism for the process was studied by using intraparticle diffusion model.

3.2.7.4 Adsorption Isotherms

To be able to explain the adsorbate interaction with the adsorbent during the adsorption process, adsorption isotherms were applied as this is highly significant in the adsorption process design. In the study, Langmuir, Freundlich and Temkin isotherms were applied.

Langmuir, $\frac{C_o}{q_e} = \frac{1}{K_L} + \frac{aL}{K_L} C_e$ 3.9

Freundlich, $\ln q_e = \ln K_F + (1/n) \ln C_e$ 3.10

Temkin, $q_e = B_T \ln A_T + B_T \ln C_e$ 3.11

3.2.7.5 Adsorption Thermodynamics

The study of the thermodynamic behaviour of the process of adsorption of Pb (II) and Zn (II) ions is equally important. To do justice to this, the obtained experimental data from the batch adsorption experiments were analyzed using the following thermodynamic equations, ΔG^o (Gibb's free energy), ΔH^o (Change in enthalpy of reaction) and ΔS^o (Change in entropy) for adsorbate-adsorbent interaction.

$$\frac{\ln K}{R} = \frac{\Delta S}{RT} + \Delta H \quad 3.12$$

$$\Delta G = RT \ln K_L \quad 3.13$$

where, K_L (L/mg) = langmuir isotherm constant obtained from 3 different temperatures of 30ºC, 60ºC and 80ºC.

R = universal gas constant (8.314 j/mol K).

T = temperature in Kelvin

3.2.7.6 Binary Adsorption Study

To study the effect of the competing ion, Zn(II) on the adsorption of Pb(II) in binary solute system of Pb(II) and Zn(II), the initial concentrations of each of the cations in solution was varied from 150mg/L to 350mg/L at equilibrium conditions of 5.5 pH, 210min and 30ºC. 0.2g of the adsorbent, longan fruit shell granular activated carbon

(LFSAC) were dispersed in 100cm^3 containing a mixture of 50cm^3 each of the adsorbate {Pb(II) and Zn(II)}s. The volume of each of the adsorbate in the mixture was varied in such a way as to be able to determine the effect such will have on the adsorption studies.

3.2.7.7 Desorption Study

Desorption study is also known as regeneration study which is normally carried out to regenerate the spent activated carbon to make it reusable. In this study, regeneration experiment was carried out with 1M solutions of hydrochloric acid, sulphuric acid, nitric acid, acetic acid and deionized water. The adsorbent, after adsorption process has been completed, was removed by filtration and transferred into stoppered containers while 50ml of each of the solutions was added and shaken at room temperature using water shaker for 210min (adsorption equilibrium time) and the initial concentration of 350mg/l. The adsorbent was then removed and filtered. The concentration of lead and zinc in the aqueous solutions (filtrate) was then determined using ICP method. Finally, the recovery efficiency (RE) of the adsorbent for the metal ions was calculated using the following equation

$$\text{Recovery Efficiency, RE (\%)} = \frac{C_e\ (des)}{C_o - C_o\ (ads)}\ X\ \frac{100}{1} \qquad 3.14$$

where, C_o = Adsorbate initial concentration.

C_e (ads) = Adsorbate final concentration after adsorption.

Ce (des) = Final concentration of adsorbate after desorption.

3.2.8 Scope of Work

The scope of activities involved in this study are illustrated by the flow chart presented in Figure 3.1

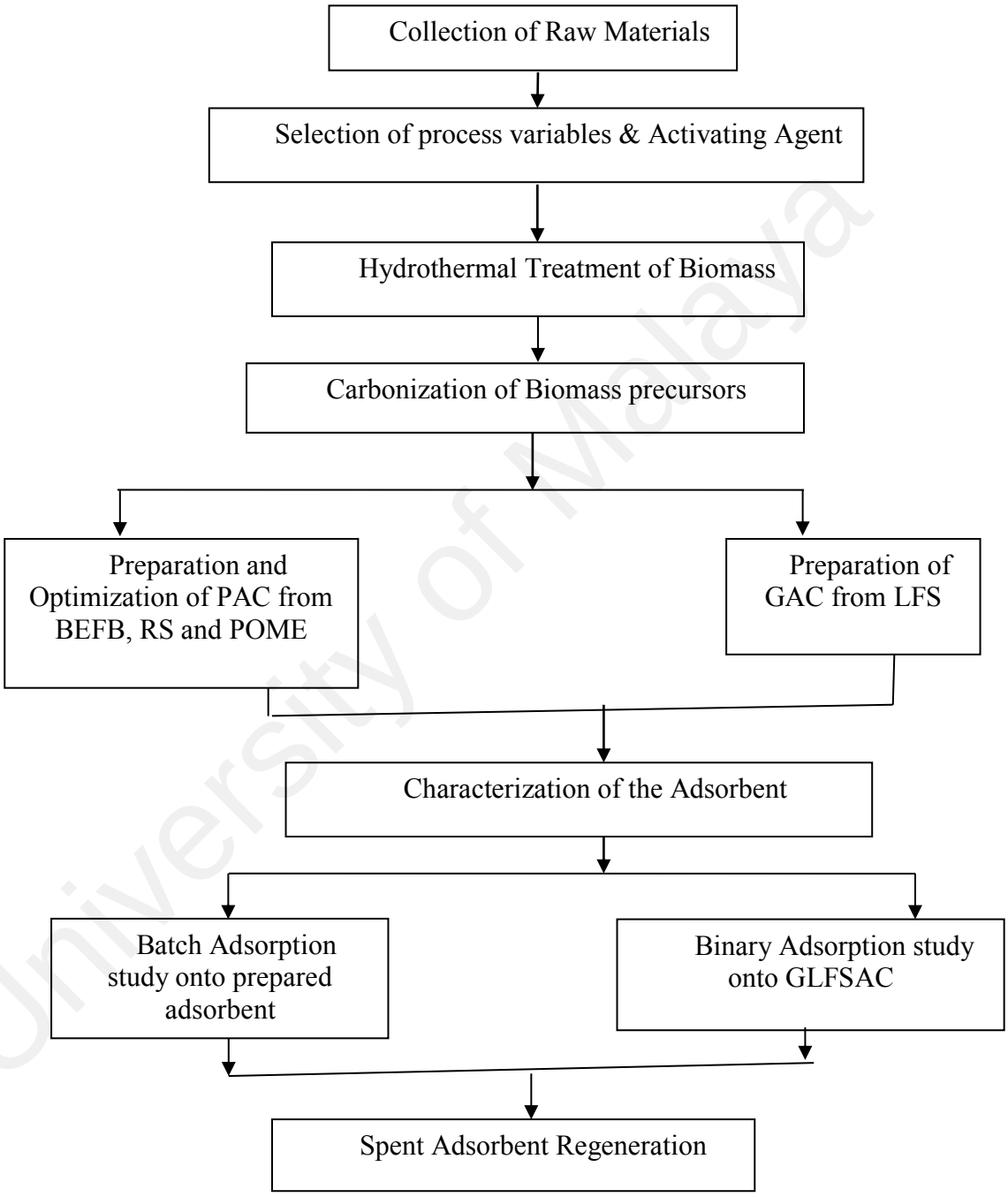

Figure 3.1 Schematic Flow Chart of Experimental Activities

CHAPTER 4: RESULTS AND DISCUSSION

PREPARATION AND CHARACTERIZATION OF POWDERED ACTIVATED CARBONS FROM BEFB AND RS AND GRANULAR ACTIVATED CARBON FROM LFS.

The results obtained from all the experiments carried out in this study were presented and discussed in the following chapter, in line with the design and optimization of the process conditions used in preparing the powdered activated carbons from banana empty fruit bunch (BEFB) and rattan sawdust (RS). The chapter is comprised of five sections with section one presenting and discussing the development of regression model, section two presents the results of preparation of powdered activated carbon from Banana empty fruit bunch and rattan sawdust. Section three shows the statistical analysis done while sections four and five present effects of the process parameters and characterization of the activated carbons respectively.

4.1 Development of the Regression Model

Linear, interactive, quadratic, and cubic functions were applied to the analytical data for ion removal and yield to develop regression equations. To check the adequacy of the models, three different tests were used: sequential model sum of squares, lack of fit, and model summary statistics. A cubic model was not suggested for the removal percentage and yield because of insufficient points for the calculation of the coefficients. Based on the sequential model sum of the squares and model summary statistics models, the quadratic model showed the best fit with the experimental data, having the lowest standard deviation and the highest correlation coefficient and adjusted R^2 values, including the lowest P-value for Pb(II) and Zn(II) removal. A linear model was chosen for the carbon yield calculation. The experimental data were used for developing the models shown in Eqs. 4.1 to 4.3.

$$Y_1 = +80.99 + 4.97x_1 + 0.65x_2 - 3.74x_3 - 4.97x_1x_2 - 0.76x_1x_3 - 0.50x_2x_3 - 9.61x_1^2 - 9.20x_2^2 - 3.70x_3^2 \quad 4.1$$

$$Y_2 = +63.71 + 3.01x_1 + 1.11x_2 - 0.89x_3 - 2.39x_1x_2 - 4.00x_1x_3 - 0.56x_2x_3 - 8.58x_1^2 - 5.19x_2^2 + 1.25x_3^2 \quad 4.2$$

$$Y_3 = +36.43 - 9.25x_1 - 1.57x_2 - 2.57x_3 \quad 4.3$$

The coefficients containing independent variables of temperature (x_1), time (x_2), and concentration of H_3PO_4 acid (x_3) denote the effects of the individual parameters on the response variables of Pb(II) removal (Y_1), Zn(II) removal (Y_2), and carbon yield (Y_3). Multiplication values between the two factors and others with second order terms exhibited the interaction and quadratic effect respectively (Arami-Niya, Abnisa, Sahfeeyan, Daud, & Sahu, 2011; ZZ Chowdhury et al., 2011). A constant having a positive value indicates that a synergistic effect has occurred, while a negative value indicates that the effect is antagonistic in nature (Anderson & Whitcomb, 2000). Figures 4 . 1(a), 4 . 1(b), 4.1(c) and 4.2(a), 4.2(b), 4.2(c) show the data obtained from the experiments versus the values predicted for BEFBAC and RSAC respectively. The high values of the regression coefficient for all response variables indicated that the predictions made in the model fit reasonably well with observations made in the experiments (Tables 4.2 and 4.4).

4.2 Preparation of Powdered Activated Carbon from Banana Empty Fruit Bunch (BEFB) and Rattan Sawdust (RS)

Powdered activated carbons were obtained from the two biomass materials through two steps of hydrothermal treatment and carbonization of the resulting hydro-char. While the hydro-char obtained was dark brown in colour, the final product (activated carbon) was completely black. The carbons were obtained in accordance with the experimental design matrix (Tables 4.1, 4.3 and 4.5 below).

Table 4.1: Independent Variables for Box Behnken Design

Variables	Code	Coded Variable Levels		
		-1	0	+1
Temperature (°C)	x_1	500	650	800
Carbonization Time (h)	x_2	1	2	3
H_3PO_4 Concentration (%)	x_3	25	37.5	50

Standard deviation was calculated to validate the quality of the models (Tables 4.2 and 4.4). The experimental R^2 values reasonably agreed with the values of adjusted R^2. The values obtained for the coefficient of variation (CV) and standard deviation were small, suggesting reproducibility of the developed models. The adequate precision values were calculated based on the signal-to-noise ratio. For effective model simulation, adequate precision should be greater than 4; the adequate precision observed for Pb(II) removal, Zn(II) removal, and carbon yield were 18.49, 22.81, and 26.65 for BEFBAC and 20.37, 14.41 and 20.01 for RSAC respectively. Thus, the experimental data was statistically significant to confirm the experimental layout of the design.

Table 4.2: Statistical Parameters for Model Verification (BEFBAC)

Statistical Parameters	Pb(II) Removal (%)	Zn(II) Removal (%)	Yield (%)
	Y_1	Y_2	Y_3
Standard Deviation, SD	2.07	1.03	1.83
Correlation Coefficient, R^2	0.977	0.988	0.945
Adjusted R^2	0.948	0.973	0.933
Mean	70.40	57.82	36.43
Coefficient of Variation	2.94	1.79	5.02
Adequate Precision	18.49	22.81	26.65

Table 4.3: Experimental Responses from the Preparation of Banana Empty Fruit Bunch Activated Carbon (BEFBAC)

Sample ID	Run	Type of Point	Reaction Variables (Actual Factors)			Lead Removal (%)	Zinc Removal (%)	Carbon Yield (%)
			Temp. X_1 (°C)	Time X_2 ,(h)	Concentn X_3 (%)	Y_1	Y_2	Y_3
B-1	1	Center	650	2	37.50	80.88	63.88	36.66
B-2	2	Center	650	2	37.50	82.77	63.55	36.88
B-3	10	Center	650	2	37.50	79.77	63.23	37.76
B-4	11	Center	650	2	37.50	80.99	63.88	38.99
B-5	17	Center	650	2	37.50	80.56	63.99	37.88
B-6	3	IBFact	500	1	37.50	53.66	49.66	47.88
B-7	4	IBFact	650	1	25.00	68.77	57.77	39.99
B-8	5	IBFact	650	3	50.00	66.43	60.66	33.66
B-9	6	IBFact	500	3	37.50	61.44	55.88	44.67
B10	7	IBFact	650	1	50.00	62.66	58.77	31.66
B11	8	IBFact	800	3	37.50	60.77	45.44	22.66
B-12	9	IBFact	500	2	50.00	59.22	61.88	42.66
B-13	12	IBFact	800	2	25.00	77.67	58.88	30.66
B-14	13	IBFact	800	1	37.50	72.88	48.77	29.88
B-15	14	IBFact	500	2	25.00	65.54	57.32	46.77
B-16	15	IBFact	800	2	50.00	68.33	47.44	24.77
B-17	16	IBFact	650	3	25.00	74.54	61.88	35.88

Table 4.4: Statistical Parameters for Model Verification (RSAC)

Statistical Parameters	Pb(II) Removal (%)	Zn(II) Removal (%)	Yield (%)
	Y_1	Y_2	Y_3
Standard Deviation, SD	1.63	2.11	1.56
Correlation Coefficient, R^2	0.9861	0.9333	0.9538
Adjusted R^2	0.9682	0.8477	0.9261
Mean	74.52	57.80	38.44
Coefficient of Variation	2.18	3.65	4.05
Adequate Precision	20.365	14.405	20.012

Table 4.5: Experimental Responses from the preparation of Rattan Sawdust Activated Carbon (RSAC)

Sample ID	Run	Block	Reaction Variables (Actual Factors)			Lead Removal Y_1 (%)	Zinc Removal Y_2 (%)	Yield Y_3 (%)
			Temp X_1 (°C)	Time X_2 ,(h)	Concentn X_3 (%)			
14	1	B1	650	2	37.50	83.89	61.87	38.69
13	2	B1	650	2	37.50	84.77	60.99	39.88
1	3	B1	500	1	37.50	59.65	43.88	48.54
9	4	B1	650	1	25.00	69.88	53.77	43.99
12	5	B1	650	3	50.00	70.43	60.66	37.99
3	6	B1	500	3	37.50	63.34	56.89	42.67
11	7	B1	650	1	50.00	72.66	51.77	33.66
4	8	B1	800	3	37.50	80.77	51.64	28.68
7	9	B1	500	2	50.00	64.22	58.88	39.68
15	10	B1	650	2	37.50	86.77	59.22	39.76
16	11	B1	650	2	37.50	83.99	60.77	39.09
6	12	B1	800	2	25.00	79.67	64.88	33.68
2	13	B1	800	1	37.50	74.88	59.77	31.88
5	14	B1	500	2	25.00	60.52	52.33	47.79
8	15	B1	800	2	50.00	68.33	63.44	28.79
10	16	B1	650	3	25.00	79.54	60.89	38.89
17	17	B1	650	2	37.50	83.56	60.98	39.89

4.3 Statistical Analysis

Statistical analysis for the developed models for all three responses was analyzed using analysis of variance (ANOVA). The analysis results are summarized in tables 4.6 to 4.11.

Based on model F values, it can be concluded that temperature (x_1) had greatest influence on the response of removal percentage of Pb(II) cations, Y_1, time (x_2), and ratio (x_3) had moderate influences on the removal percentage (Table 4). However, between time and H_3PO_4 concentration, the concentration of H_3PO_4 acid played vital role to enhance the quality of the prepared activated carbon. The interaction influences of temperature and time (x_1x_2) was more prominent than the other interaction factors associated with the percentage removal of Pb(II) cation, Y_1. In this case, x_1, x_3, the

quadratic terms of x_1^2, x_2^2, x_3^2 including interaction terms of x_1x_2 are significant model terms (Tables 4.3 and 4.4).

Table 4.6: Analysis of Variance (ANOVA) and Lack of Fit Test for the Removal of Pb(II) onto BEFBAC (Y_1)

Source	Sum of Squares	Degrees of Freedom	Mean Square	F Value	Prob> F
Model	1296.56	9	144.06	33.54	<0.0001*
x_1	197.91	1	197.91	46.08	0.0003
x_2	3.39	1	3.39	0.79	0.4036
x_3	11.60	1	11.60	25.98	0.0014
x_1x_2	98.90	1	98.90	23.03	0.0020
x_1x_3	2.28	1	2.28	0.53	0.4899
x_2x_3	1.00	1	1.00	0.23	0.6442
x_1^2	388.71	1	388.71	90.50	<0.0001
x_2^2	356.24	1	356.24	82.94	<0.0001
x_3^2	57.51	1	57.51	13.39	0.0081
Residuals	30.06	7	4.29		
Lack of Fit	25.21	3	8.40	6.93	0.0462*
Pure Error	4.85	4	1.21		

* significant

For Zn(II) removal percentage, Y_2, temperature (x_1) and time (x_2) had larger influence than ratio (x_3) whereas cumulative effect of temperature and ratio (x_1x_3) had greatest impact on removal percentages. In this case, x_1, x_2, x_3, the quadratic terms of x_1^2, x_2^2, x_3^2 including interaction terms of x_1x_2 and x_1x_3 are significant model terms (Tables 4.8 and 4.9).

Table 4.7: Analysis of Variance (ANOVA) and Lack of Fit Test for the Removal of Pb(II) onto RSAC (Y_1)

Source	Sum of Squares	Degrees of Freedom	Mean Square	F Value	Prob> F
Model	1314.94	9	146.1	55.18	<0.0001
x_1	390.88	1	390.8	147.6	<0.0001
x_2	36.17	1	36.17	13.66	0.0077
x_3	24.40	1	24.40	9.21	0.0190
x_1x_2	1.21	1	1.21	0.46	0.5207
x_1x_3	56.55	1	56.55	21.36	0.0024
x_2x_3	35.34	1	35.34	13,35	0.0081
x_1^2	415.95	1	415.9	157.1	<0.0001
x_2^2	105.13	1	105.1	39.71	0.0004
x_3^2	176.35	1	176.3	66.61	<0.0001
Residuals	18.53	7	2.65		
Lack of	11.84	3	3.95	2.36	0.2129
Pure	6.70	4	1.67		

*significant

For yield percentage (Y_3), x_1, x_2 and x_3 are significant model terms. Tables 4.10 and 4.11 reveal that temperature (x_1) and H_3PO_4 acid concentration (x_3) had more dominating effect for yield calculation. The F-test values representing the variation in the data about the mean were determined to check the competence of the models. Based on a 95% confidence interval, the model F-values for Pb(II) removal, Zn(II) removal, and carbon yield were 33.54, 64.87, 73.52 and 55.18, 10.89, 34.41 for BEFBAC and RSAC respectively. This is an indication that the models were significant. However, the P-values obtained for all the three responses were less than 0.05, thereby indicating that the model terms considered for the response analysis were significant. However, the P-values obtained for all the three responses were less than 0.05, thereby indicating that the model terms considered for the response analysis were significant.

Table 4.8: Analysis of Variance (ANOVA) and Lack of Fit test for the Removal of Zn(II) onto BEFBAC (Y_2)

Source	Sum of Squares	Degrees of Freedom	Mean Square	F Value	Prob> F
Model	622.71	9	69.19	64.87	<0.0001*
x_1	73.33	1	73.33	68.75	<0.0001
x_2	9.88	1	9.88	9.26	0.0188
x_3	6.32	1	6.32	5.92	0.0452
x_1x_2	22.80	1	22.80	21.38	0.0024
x_1x_3	63.92	1	63.92	59.93	0.0001
x_2x_3	1.23	1	1.23	1.16	0.0181
x_1^2	309.82	1	309.82	290.46	<0.0001
x_2^2	113.44	1	113.44	106.35	<0.0001
x_3^2	6.63	1	6.63	6.29	0.0414
Residuals	7.47	7	1.07		
Lack of Fit	7.07	3	2.36	24.05	0.0051*
Pure Error	0.39	4	0.098		

* significant

Table 4.9: Analysis of Variance (ANOVA) and Lack of Fit test for the Removal of Zn(II) onto RSAC (Y_2)

Source	Sum of Squares	Degrees of Freedom	Mean Square	F Value	Prob> F
Model	431.31	9	48.48	10.89	0.0024*
x_1	96.26	1	96.26	21.63	0.0023
x_2	54.55	1	54.55	12.26	0.0100
x_3	1.04	1	1.04	0.23	0.6441
x_1x_2	111.72	1	111.72	25.10	0.0015
x_1x_3	15.96	1	15.96	3.59	0.1001
x_2x_3	0.78	1	0.78	0.18	0.6874
x_1^2	22.38	1	22.38	5.03	0.0599
x_2^2	123.48	1	123.48	27.74	0.0052
x_3^2	8.51	1	8.51	1.91	0.2092
Residuals	31.16	7	4.45		
Lack of	27.45	3	9.15	9.88	0.0254*
Pure	3.70	4	0.93		

* significant

Table 4.10: Analysis of Variance (ANOVA) and Lack of Fit test for the Percent Yield of BEFBAC (Y_3)

Source	Sum of Squares	Degrees of Freedom	Mean Square	F Value	Prob> F
Model	757.13	3	252.38	73.52	<0.0001*
x_1	684.69	1	684.69	204.88	<0.0001
x_2	19.66	1	19.66	5.88	0.0306
x_3	52.79	1	52.79	15.80	0.0016
Residuals	43.45	13	3.34		
Lack of Fit	40.01	9	4.45	0.26	5.18
Pure Error	3.43	4	0.86		

*significant

Table 4.11: Analysis of Variance (ANOVA) and Lack of Fit test for the Percent Yield of RSAC (Y_3)

Source	Sum of Squares	Degrees of Freedom	Mean Square	F Value	Prob> F
Model	499.21	6	83.20	34.41	<0.0001*
x_1	387.12	1	387.12	160.08	<0.0001
x_2	12.10	1	12.10	5.00	0.0492
x_3	73.39	1	73.39	30.35	0.0003
Residuals	24.18	10	2.42		
Lack of Fit	23.00	6	3.83	12.98	0.0134*
Pure Error	1.18	4	0.30		

*significant

For further assessnent, studentized residuals were plotted versus experimental runs for all the responses. The experimental points for residuals were randomly scattered around zero (Figures 4.3 and 4.4). Most of the standard residuals fell within the interval range of ± 3.00. This indicated that the experimental design requires no response transformation.

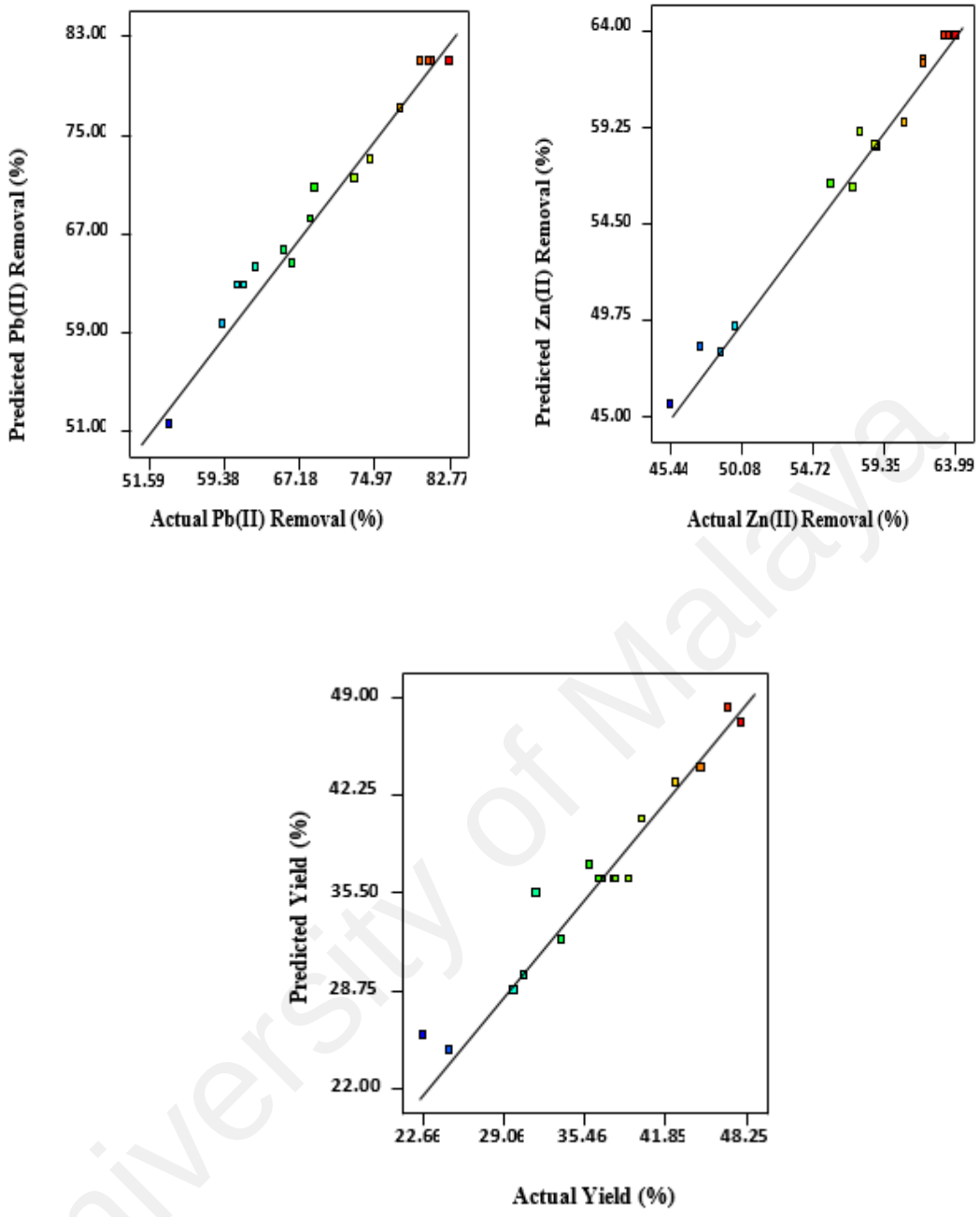

Figure 4.1: Predicted versus actual (a) % removal, of Pb (II), *Y1* (b) % removal of Zn(II), *Y2* and (c) % yield of BEFBAC, *Y3*

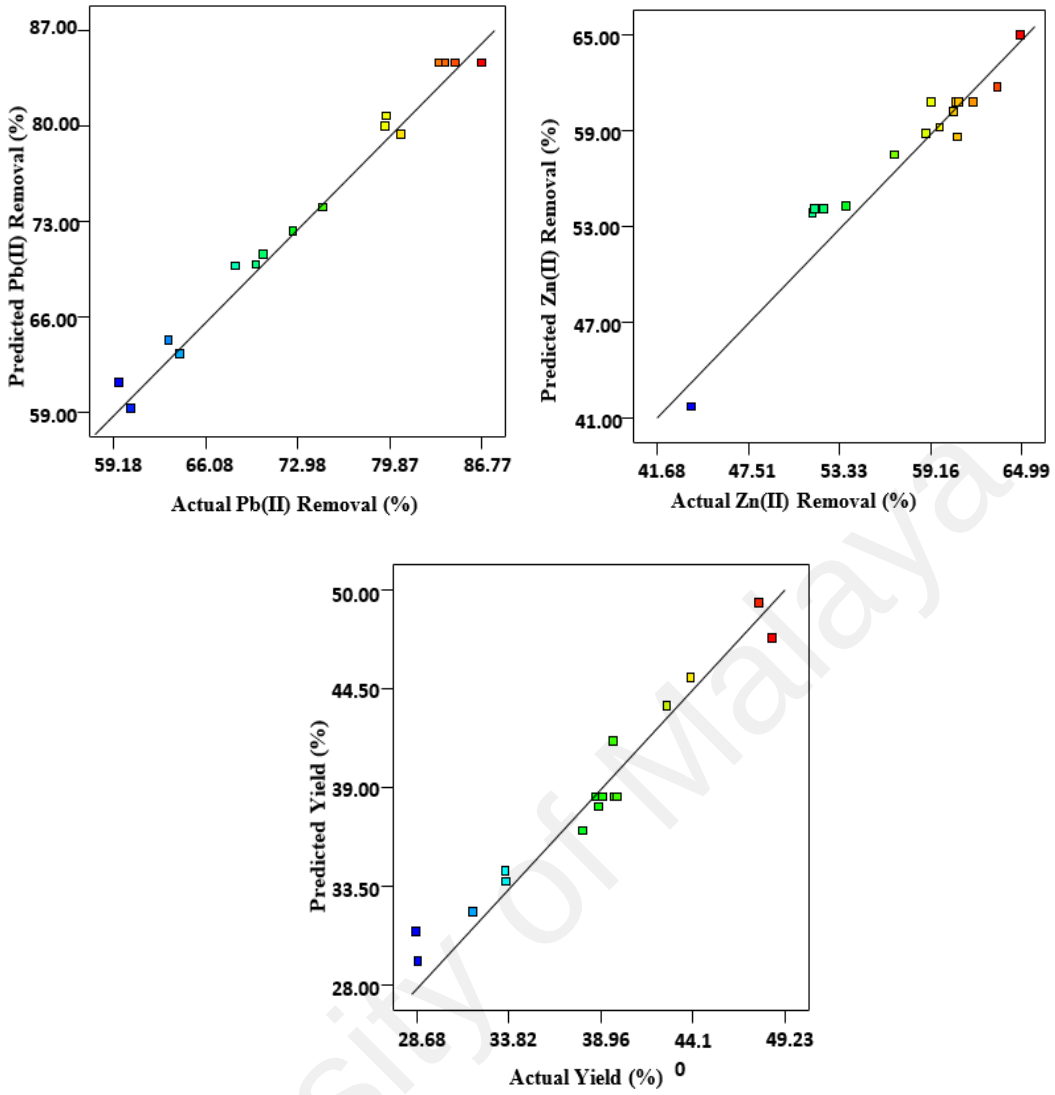

Figure 4.2: Predicted versus actual (a) % removal, of Pb (II), Y_1 (b) % removal of Zn(II), Y_2 and (c) % yield of RSAC, Y_3

For the robustness of experimental design to manufacture carbon, relatively high removal efficiencies, along with satisfactory carbon yields, were expected for targeting pollutants under optimum conditions. When the independent variables of temperature, time, and acid concentration were increased, the percentage removal increased up to a certain point, whereas the yield decreased. The converse effects were also observed. To optimize the char activation process, maximum values for removal were set as the targets, while the three variables (temperature, time, and acid concentration) were set within the studied ranges. A 1.0-g sample was used as the input for each parameter to control the

desirability function (Khandanlou et al., 2015).The desirability function for optimization and error percentage were estimated [Tables 4.12(a) and 4.12(b)].

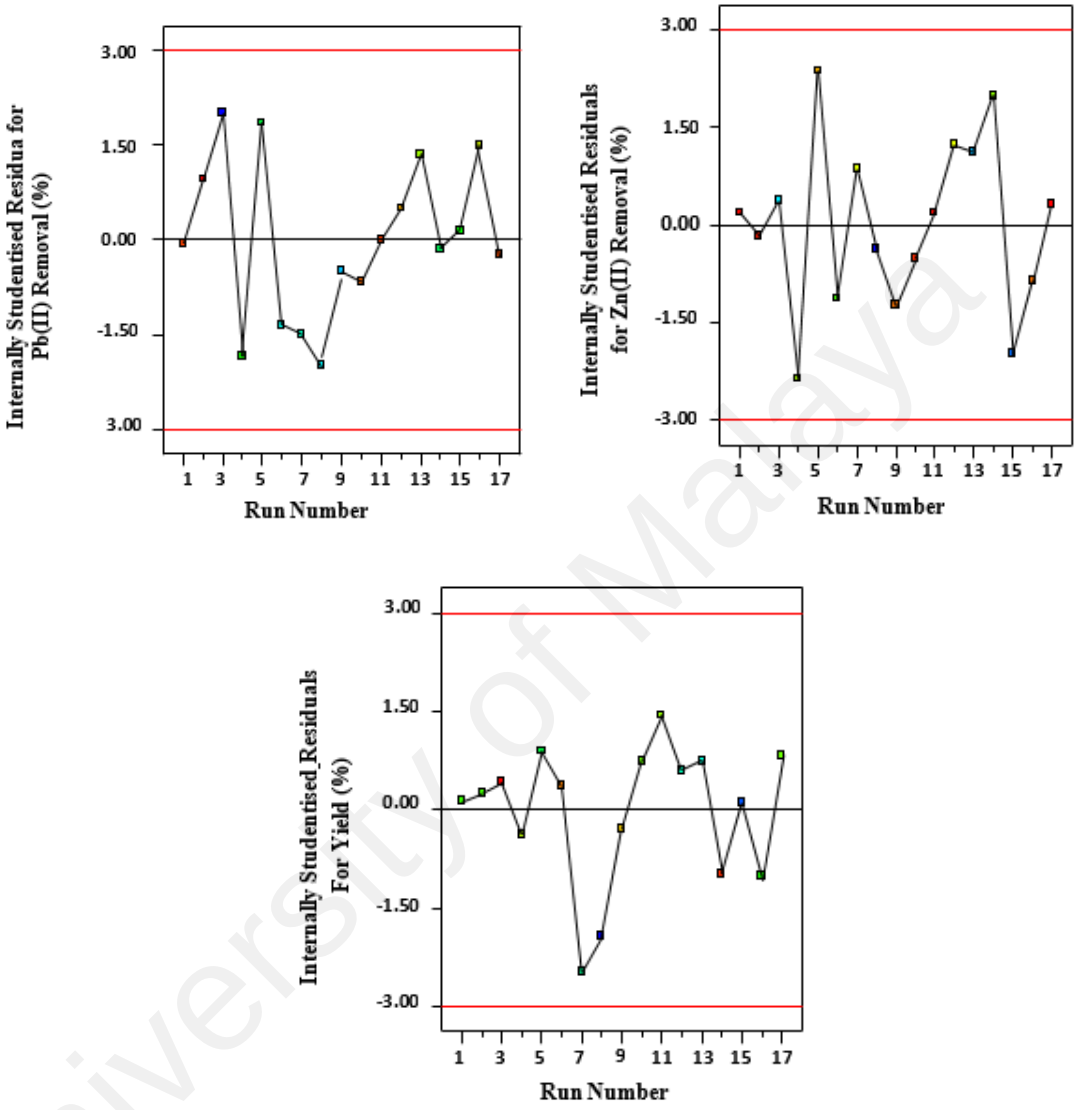

Figure 4.3: Studentized residuals versus experimental run (a) % removal, of Pb(II), *Y1* (b) % removal of Zn(II), *Y2* and (c) % yield of BEFBAC, *Y3*

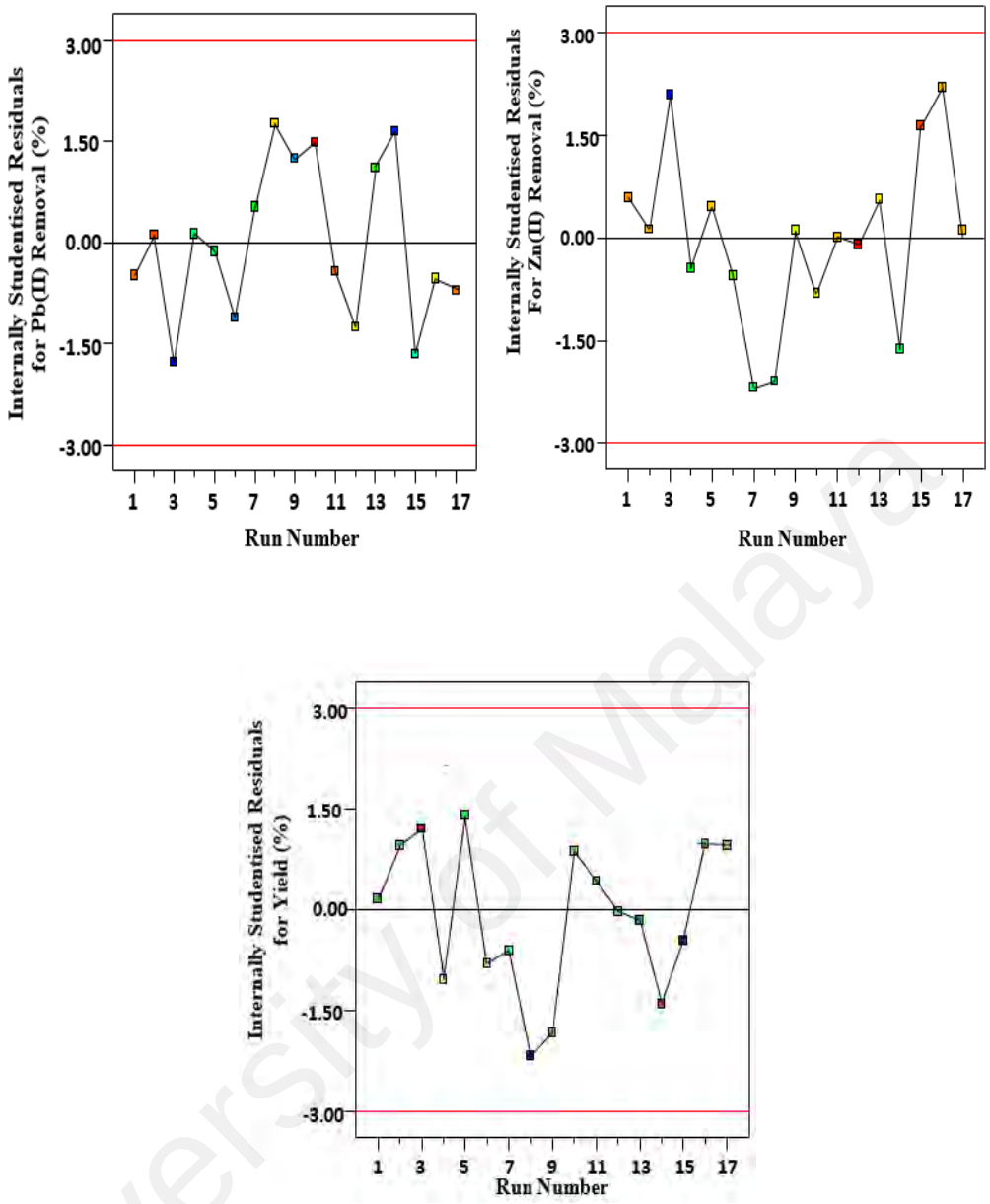

Figure 4.4: Studentized residuals versus experimental run (a) % removal, of Pb(II), *Y1* (b) % removal of Zn(II), *Y2* and (c) % yield of RSAC, *Y3*

4.4 Effect of Process Parameters

4.4.1 Effect of Process Parameters on Removal Percentages

Figures 4.5(a) and 4.7(a) show the three-dimensional response surface plots of the collective impact of temperature ($\boldsymbol{x_1}$) and time ($\boldsymbol{x_2}$) on the removal of Pb(II) cations (Y_1) by BEFBAC and RSAC respectively when the H_3PO_4 concentration ($\boldsymbol{x_3}$) was fixed at the center point (37.50%). Figures 4.5(b) and 4.7(b) display the influence of temperature ($\boldsymbol{x_1}$)

and H_3PO_4 acid concentration (x_3) on the removal of Pb(II) cations, when the activation time for the two hydro-chars (BEFBC and RSC) were kept at the center point (2 h). Figures 4.6(a), 4.6(b), 4.8(a) and 4.8(b) are constructed to reveal the interaction of (Y_2) by BEFBAC and RSAC respectively. In all cases, the third variable was fixed at the center point.

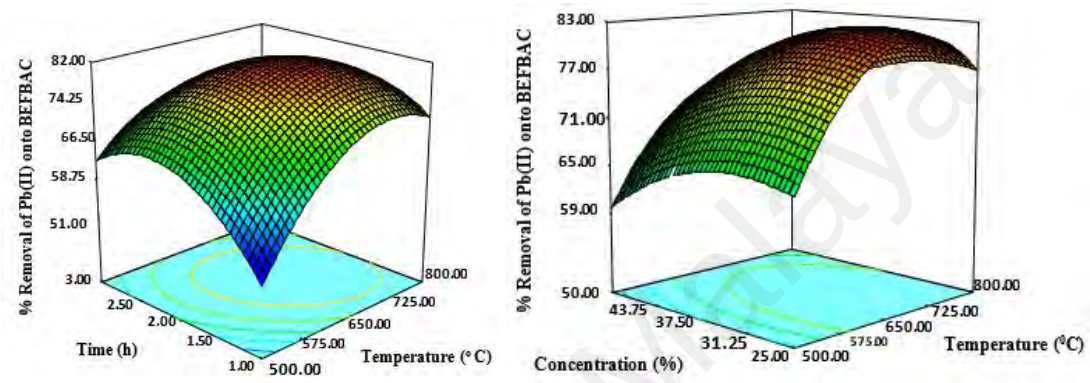

Figure 4.5: Three dimensional response surface contour plots of the combined effects of (a) temperature (x_1) and time (x_2) and (b) temperature (x_1) and H_3PO_4 acid concentration (x_3) on the percent removal of Pb(II) cations by BEFBAC (Y_1), when the third variable was fixed at the center point

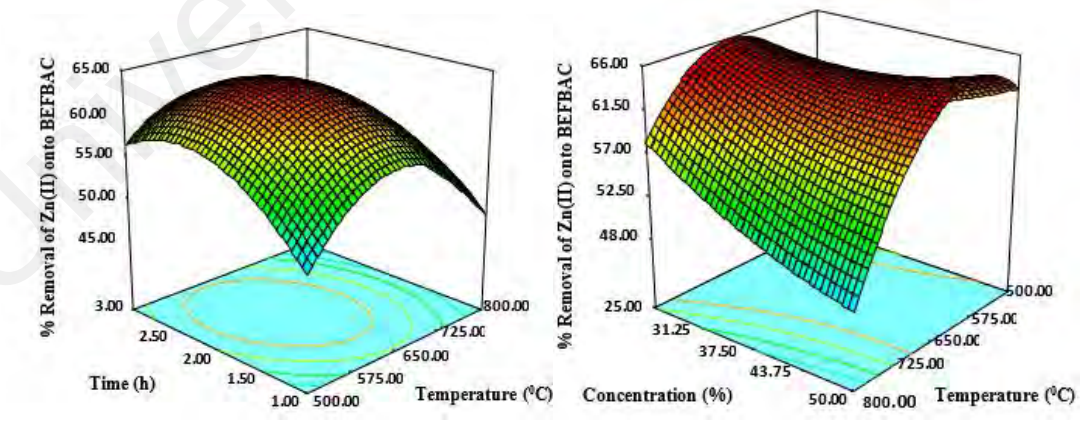

Figure 4.6: Three-dimensional response surface contour plots of the combined effects of (a) temperature (x_1) and time (x_2) and (b) temperature (x_1) and H_3PO_4 acid concentration (x_3) on the percent removal of Zn(II) cations by BEFBAC (Y_2), when the third variable was fixed at the center point.

Table 4.12(a): Process Parameter Optimization for BEFBAC

Temperature °C	Time (h)	Concentration (%)	Percentage Removal Pb(II)			Percentage Removal Zn(II)			Percentage Yield			Desirability
			Predicted	Experimental	Error	Predicted	Experimental	Error	Predicted	Experimental	Error	-
599.45	2.04	25.97	78.39	82.85	5.68	64.49	61.02	5.38	41.45	42.76	3.16	0.87

Table 4.12(b): Process Parameter Optimization for RSAC

Temperature oC	Time (h)	Concentration (%)	Percentage Removal Pb(II)			Percentage Removal Zn(II)			Percentage Yield			Desirability
			Predicted	Experimental	Error	Predicted	Experimental	Error	Predicted	Experimental	Error	-
657.63	2.04	40.54	84.12	86.77	3.15	61.18	64.88	5.97	47.34	48.04	1.48	0.75

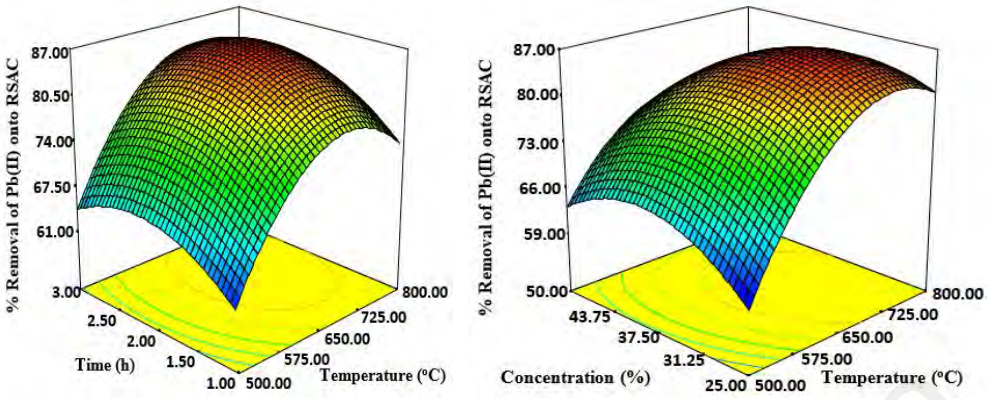

Figure 4.7: Three dimensional response surface contour plots of the combined Three-dimensional response surface contour plots of combined effects of (a) temperature (x_1) and time (x_2) and (b) temperature (x_1) and H3PO4 acid concentration (x_3) on the percent removal of Pb(II) cations by RSAC (Y_1), when the third variable was fixed at the center point.

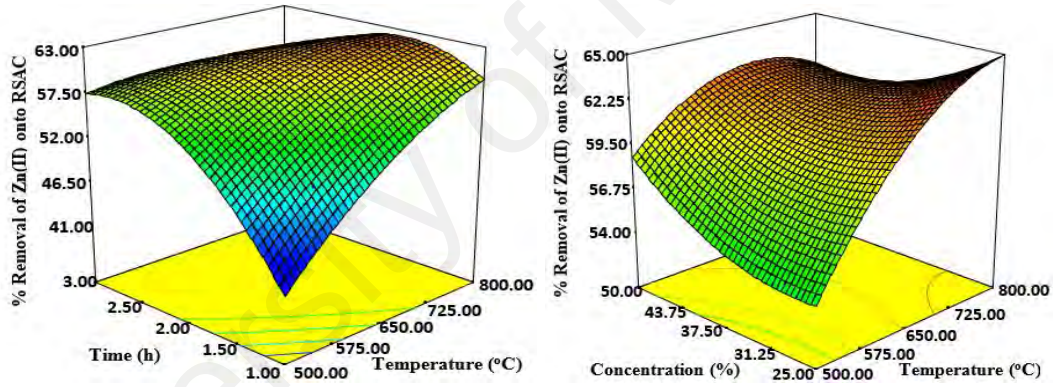

Figure 4.8: Three dimensional response surface contour plots of the combined effects of (a) temperature (x_1) and time (x_2) and (b) temperature (x_1) and H_3PO_4 acid concentration (x_3) on the percent removal of Zn(II) cations by RSAC (Y_1), when the third variable was fixed at the center point.

The curvature observed in the Figures 4.5 to 4.8 represent the prominent effect which the activation temperature has on the removal of both cations, irrespective of the time and concentration of H_3PO_4. The plots revealed that the temperature and concentration of the impregnating acid was proportional to the percentage removal. Up to a certain limit, increasing of temperature and acid concentration enhanced the reaction, resulting in more surface area with a porous texture, which is desirable for adsorption. ANOVA also showed that the activation temperature had the highest impact on ion removal. In previous

studies, the activation time exhibited a moderate to minimal impact on the development of the surface area and pore structure of the activated carbon prepared from cassava peel, whereas the pore distribution in terms of micropore and mesopore percentages were strongly influenced by the activating KOH impregnation ratio and the temperature (Sudaryanto et al., 2006). A short activation time and very low temperature might not be sufficient to enhance the surface area (Cao, Xie, Lv, & Bao, 2006). After a certain limit, increasing the temperature and concentration both exhibited a detrimental effect on the percentage removal; high temperature or acid concentration might destroy some surface functional groups. In addition, these conditions might compromise the integrity of the porous texture of AC by thermal annealing, which destroys the walls of the micropores to form more mesopores, which are suitable for liquid phase adsorption. However, in that case, the pore size distribution is not suitable, because larger mesopores fail to adsorb and retain smaller cations, resulting in lower removal efficiency (Z. Z. Chowdhury, Zain, Khan, Arami-Niya, et al., 2012). At very high temperatures and longer residence times with highly concentrated acid, the carbon skeleton might burn into ash, which also compromises removal efficiency. A very long activation time is not beneficial, as it increases the liquid yield and reduces the carbon yield, with successive decreases in the removal efficiency. This trend was also observed during the preparation of activated carbon from oil palm fronds for the removal of Zn(II) cations (Zahangir, Suleyman, & Noraini, 2008).

4.4.2 Effect of Process Parameters on Carbon Yield

Figures 4.9(a) and 4.10(a) reveal the cumulative influence of two independent factors, temperature and time, on percentage yield of carbon when the H_3PO_4 concentration was fixed at the center point (37.50%). Figures 4.9(b) and 4.10(b) show the combined impact of temperature and H_3PO_4 concentration over yield percentage, where time was kept at

the center point of 2 h. All three parameters exhibited a synergistic effect on percentage yield.

In general, the yield decreased with increasing temperature, time, and acid concentration. Temperature had the highest impact on the yield percentage, which was earlier shown by the highest F-value of 684.69 and 387.12 for BEFBAC and RSAC respectively (Tables 4.10 and 4.11), whereas the activation time was not as noteworthy compared to the temperature and acid concentration. Temperature was the dominant factor relative to the yield, as supported by the ANOVA data (Tables 4.10 and 4.11). The lowest yields (22.66% and 26.68% for BEFBAC and RSAC respectively) were obtained at 800 °C for 3 h with 37.50% acid concentration [Sample B-11(Table 4.3) and sample B-8(Table 4.5)]. With increased temperature, the contact time and concentration intensified the diffusion of acidic solution inside the hydro-char matrix, leading to conversion of carbon to ash. This effect initiated the disintegration of the crystalline region of hydro-char and formed amorphous carbon, which is desirable for adsorbent preparation. Thus, the optimum reaction condition should be determined to enhance the surface area of the carbon sample with the highest possible yield. Consequently, the removal efficiency would also be higher.

This observation is consistent with previous study on cassava peel (Sudaryanto et al., 2006), where it was observed that activation temperature stands out as the most important factor, whereas role and activation time had the least impact on the carbon yield. Increasing the temperature beyond a certain point enhanced dehydration and elimination reactions to release additional volatile organic fractions from the hydro-char matrix as gaseous and aqueous products, rather than as solid activated carbon.

4.5 Characterization of Activated carbon

4.5.1 Surface Area Porosity

The surface area, pore volume and pore size distribution of the hydro-char and the prepared activated carbons were analyzed using surface area analyzer (Trister II BET Surface Area Analyzer) with nitrogen Adsorption-Desorption isotherm at 77.313 K.

Table 4.13. below presents the obtained BET results with the results showing a wide gap between the surface areas of the hydro-chars and the activated carbons, an indication that chemical activation using phosphoric acid greatly enhance the surface area enlargement. The result further showed the BET surface area obtained for RSAC is 1,151.23 m^2/g which is comparable to most commercial activated carbon (J. Wang, 2005) and higher than the BET values obtained for Watermelon shell and Walnut shell (710 $m2g^{-1}$ and 789$m2g^{-1}$ respectively) activated carbons prepared through chemical activation using phosphoric acid (Moreno-Barbosa et al., 2013) while the value obtained for BEFBAC is higher than that watermelon shell activated but slightly lower than the walnut shell activated carbon. Referring to the pore size as seen in table 4.13, RSC, RSAC, LFSC and LFSAC are mesoporous because their pore sizes all fall between the mesoporosity range of 2-50nm.

Quantitatively RSC, RSAC, LFSC and LFSAC pore sizes were found to be 2.970nm, 3.891nm, 3.497nm and 3.345nm respectively. Conversely, BEFBC and BEFBAC materials are both microporous because their pore sizes were found to be 0.101nm and 1.822nm respectively. Furthermore, the results showed that BEFBC, RSC and LFSC have lower BET surface areas compared to their corresponding activated carbons, an indication that they have undergone incomplete carbonization. However, after activation and further carbonization, the surface area and pore volume increased substantially.

4.5.2 Proximate Analysis (TGA Analysis)

The proximate components, in percentage, of the precursors, hydro-chars and their corresponding activated carbons are as presented in table 4.14 below. The result shows that the precursors are rich in volatile matters but their fixed carbon contents are equally high enough to support their conversion to carbons. Moreover, the result shows a significant drop in the volatile matter content after hydrothermal treatment and subsequent activation and carbonization processes. During this period, the fixed carbon contents of the hydro-char and the fixed carbon increased progressively due to breakdown of bonds and linkages of the molecules of organic compounds upon exposure to heat.

4.5.3 Ultimate Analysis

Contained in table 4.15 below are the results of the ultimate analysis of biomass, hydro-chars and their corresponding activated carbons. The results showed that while the carbon contents of biomass, hydro-chars and activated carbons increased progressively in that order, the hydrogen and oxygen contents decreased. Moreover, after activation with phosphoric acid, the increase in the carbon contents became very significant. Equally, a decrease in the H/O and O/C can be noticed after activation and carbonization due to decarboxylation reaction and aromatization process during these processes (F. Liu & Guo, 2015).

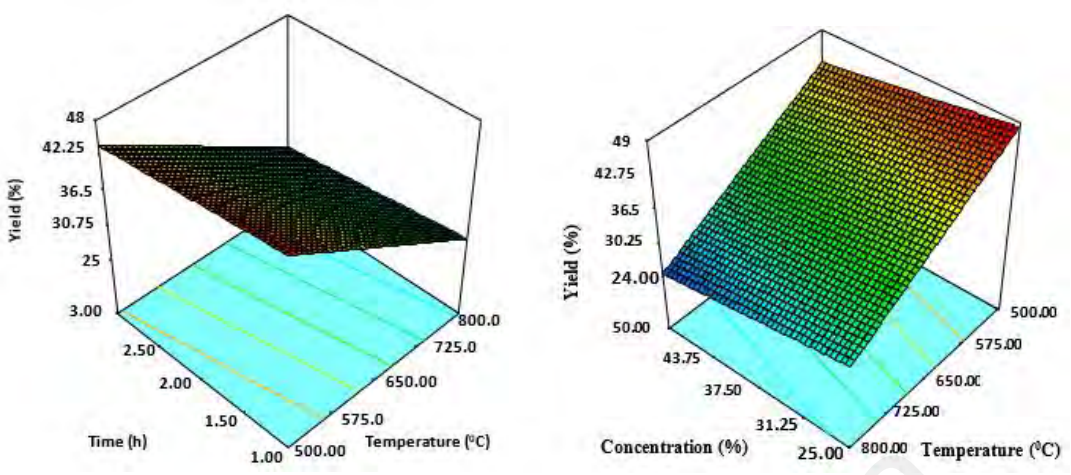

Figure 4.9: Three-dimensional response surface contour plots of the combined effects of (a) temperature (x_1) and time (x_2) and (b) temperature (x_1) and H_3PO_4 acid concentration (x_3) on the percent yield of BEFBAC (Y_2), when the third variable was fixed at the center point

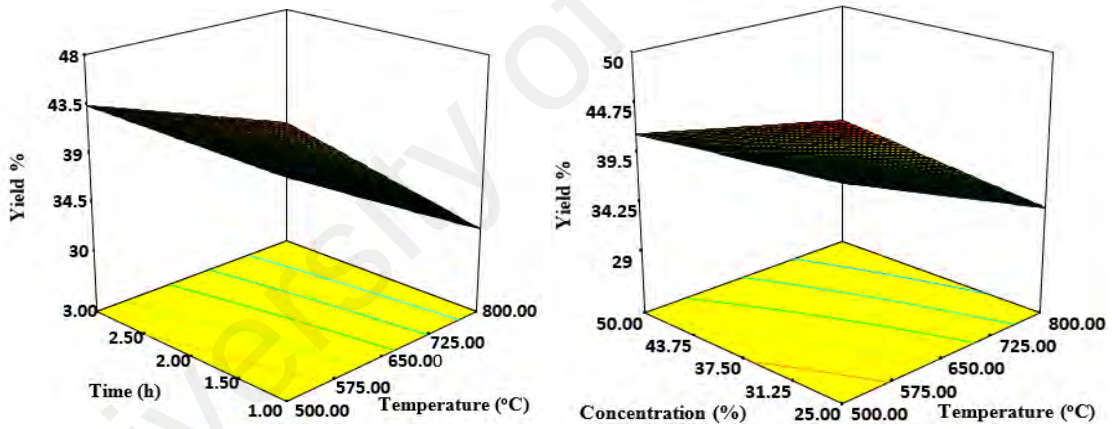

Figure 4.10: Three-dimensional response surface contour plots of the combined effects of (a) temperature (x_1) and time (x_2) and (b) temperature ($x1$) and H_3PO_4 acid concentration (x_3) on the percent yield of RSAC (Y_2), when the third variable was fixed at the center point

Table 4.13: Surface area and pore characteristics of the hydro-char and the prepared activated carbons of BEFB, RS and LFS.

Sample Properties	BEFBC	BEFBAC	RSC	RSAC	LFSC	LFSAC
BET Surface Area (m^2/g)	7.01	762.05	169.28	1,151.23	1.79	672.10
Micropore Surface Area (m2/g)	1.01	1004.30	147.66	37.66	0.85	472.58
Total pore Volume (cc/g)	0.10	0.43	0.13	0.95	0.0016	0.31
Average Pore size (^oA)	1.01	18.22	29.70	38.91	34.97	33.45
BJH Adsorption Cumulative Surface Area (m^2/g)	2.62	522.72	134.23	865.05	0.27	21.71

Table 4.14: The proximate composition (%) of BEFB, BEFBC, BEFBAC, RS, RSC, RSAC, LFS, LFSC and LFSAC.

Sample	Proximate Content (%)			
	Moisture	Volatile Matter	Ash	Fixed Carbon*
BEFB	17.58	27.49	14.51	40.42
BEFBC	14.57	19.87	23.56	42.00
BEFBAC	10.82	12.30	26.57	50.31
RS	17.87	27.98	14.15	40.00
RSC	15.00	19.05	19.78	46.17
RSAC	8.62	9.74	21.98	59.66
LFS	20.50	29.52	9.94	40.04
LFSC	17.78	22.85	16.98	42.39
LFSAC	16.95	11.08	21.63	50.34

*calculated by difference

4.5.4 Ultimate Analysis

Contained in table 4.15 below are the results of the ultimate analysis of biomass, hydro-chars and their corresponding activated carbons. The results showed that while the carbon contents of biomass, hydro-chars and activated carbons increased progressively in that order, the hydrogen and oxygen contents decreased. Moreover, after activation with phosphoric acid, the increase in the carbon contents became very significant. Equally, a decrease in the H/O and O/C can be noticed after activation and carbonization due to decarboxylation reaction and aromatization process during these processes (F. Liu & Guo, 2015).

Table 4.15: Ultimate Analysis of BEFB, BEFBC, BEFBAC, RS, RSC and RSAC

Ultimate Analysis	BEFB	BEFBC	BEFBAC	RS	RSC	RSAC	LFS	LFSC	LFSAC
Percentage Carbon	42.09	52.55	81.55	42.31	56.74	84.65	39.76	56.65	78.35
Percentage Hydrogen	5.99	4.56	3.51	6.00	3.12	2.29	3.95	3.60	3.25
Percentage Nitrogen	1.33	1.00	1.02	0.64	0.45	0.62	0.68	0.45	0.57
Percentage Oxygen	47.00	39.13	12.91	49.50	37.70	11.66	37.55	28.67	11.26
Others	3.59	2.76	1.01	2.55	1.00	0.78	18.06	10.63	6.57
H/C	0.142	0.086	0.043	0.142	0.055	0.027	0.100	0.064	0.041
O/C	1.11	0.744	0.158	1.170	0.664	0.138	0.94	0.51	0.14

.

4.5.5 Morphological Structures

The microscopic examination of the precursors, hydro-chars and their corresponding activated carbons were examined using the field emission scanning electron microscope (FESEM). Figures 4.11 (a) – (i) below show the micrographs obtained from the examination. As could be observed from the obtained micrographs, the precursors surface textures [figures 4.11 (a), (d) and (g)] are very rough and covered with extraneous matters which appear to be uneven and undulating.

(a)BEFB

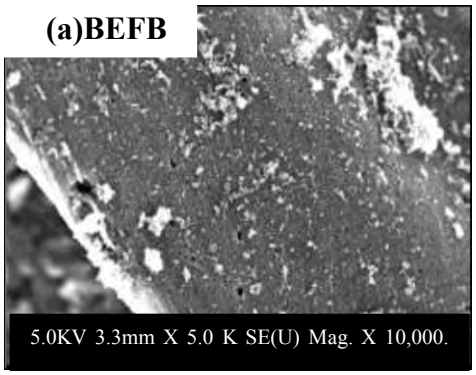

(b) BEFBC

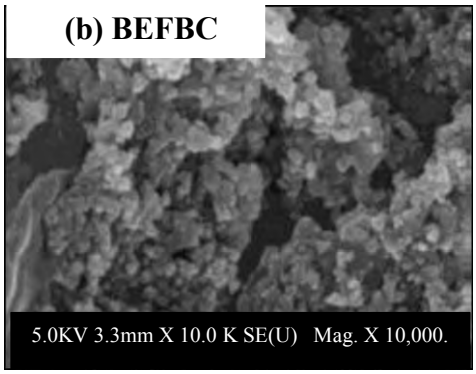

(c) **BEFBAC**

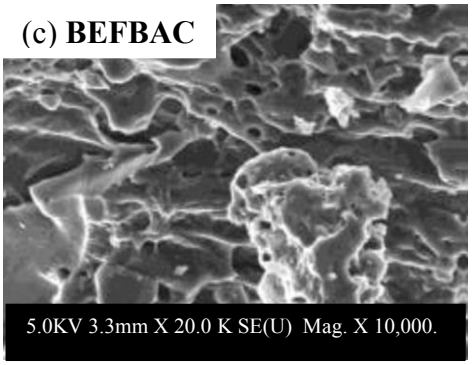

(d) RS

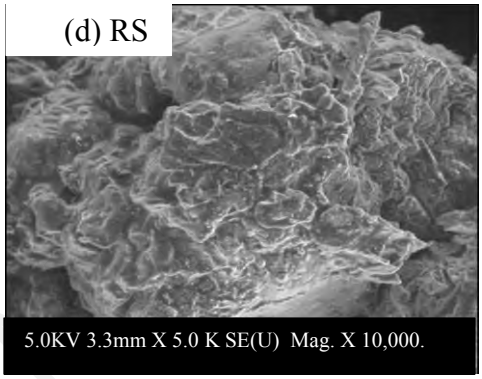

(e) RSC

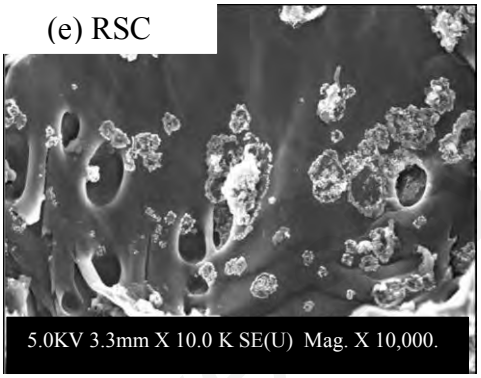

(f) RSAC

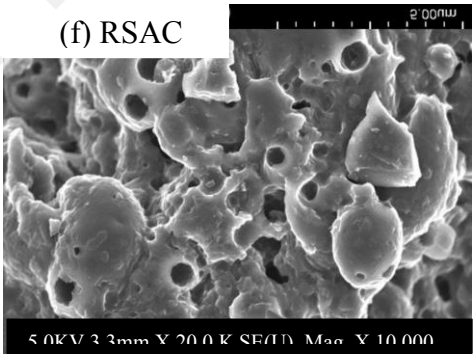

(g) LFS

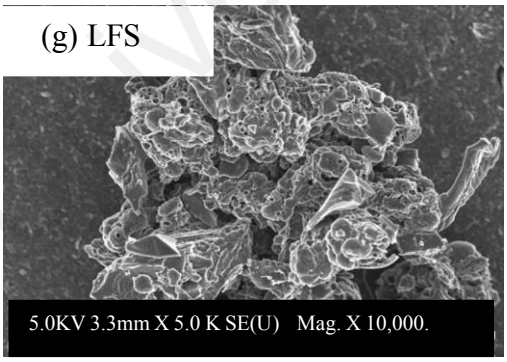

(h) LFSC

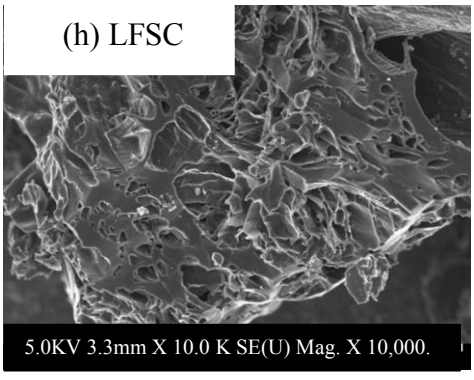

(i) LFSAC

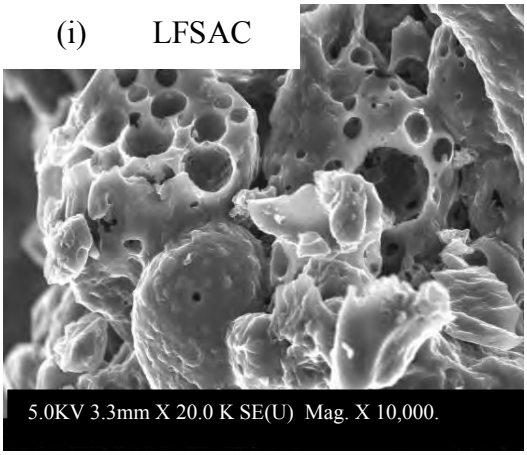

Figure 4.11: SEM micrographs (Mag. x 10,000) of (a) BEFB (b) BEFBC (c) BEFBAC (d) RS (e) RSC, (f) RSAC,(g) LFS, (h) LFSC and (i) LFSAC.

The images of the precursors have smooth, non-porous structures which changes significantly after carbonization. After hydrothermal carbonization, the formation of some pores could be noticed on the surfaces of the hydro-chars [figures 4.11 (b), (e) and (h)]. During hydrothermal carbonization, however, cellulose and hemicellulose were degraded yielding carbon microspheres (F. Liu & Guo, 2015). During this process, lignin components of the biomass precursors were just partially degraded, thus preserving the original skeleton of the particles (Gao, Wang, Yang, & Chen, 2012; Sevilla & Fuertes, 2009). After activation with phosphoric acid and subsequent carbonization, the pores became very clear as could be seen from figures 4.11 (c), (f) and (i). All the activated carbons contain homogeneous pore size distribution with uniform pore arrangements. However, to achieve this in RSAC [figue 4.11(f)] requires more heat to break the hard texture of the precursor [figure 4.11(d)] compared to the soft texture of BEFB [figure 4.11(a)]. After activation and subsequent carbonization, the pores on the surface of the three activated carbons became pronounced and well arranged, thereby leading to high adsorption capacity. This happened due to the fact that during activation with the acid, the materials which blocked the pores on the chars [Figures 4.11(b), (e) and (h)] have been carried away by gasification process. After pyrolysis, thin layers were observed in the char structure containing some rudimentary pores as a result of the release of volatiles.

4.5.6 Surface Chemistry

The adsorption capacity of an activated carbon is usually influenced by the presence of appropriate surface functional groups. Figures 4.12 – 4.14 above depict the spectra peaks obtained from the FTIR spectroscopic analysis of BEFB, RS and LFS together with their corresponding hydro=chars and activated carbons. The three precursors exhibit similar spectra peaks showing the presence of appropriate functional groups which include –C=O, -C-O-, C=C, -CH_2, -C-H, -OH and –N-H corresponding bandwidth for BEFB, RS and LFS respectively. The conversion of the precursors to hydro-chars and activated carbons leads to significant reduction in the intensities of the peaks as seen in the figures and much more reduced number of peaks and intensities as evident in the activated carbons picks (Figures 4.12 – 4.14).

There is similarity in the number and intensities of functional groups present on the surface of the activated carbons (BEFBAC, RSAC and LFSAC). This is due to the fact that they been activated using the same activating agent.

However, some differences can still be noticed due to the nature of the starting materials since BEFB contain more cellulose while RS and LFS contan more lignin. The dissociation of the functional groups to obtain the necessary surface electrical charge exert a great influence on the sorption and desorption properties of the sorbent on the target metal ions. In a situation whereby both the adsorbent and the adsorbate possess similar electrical charge, repulsion will take place which will lead to low adsorption of the metal ions. However, the above revealed the presence of fuctional groups that promotes affinity for adsorbing positive cations, that is, the metal ions.

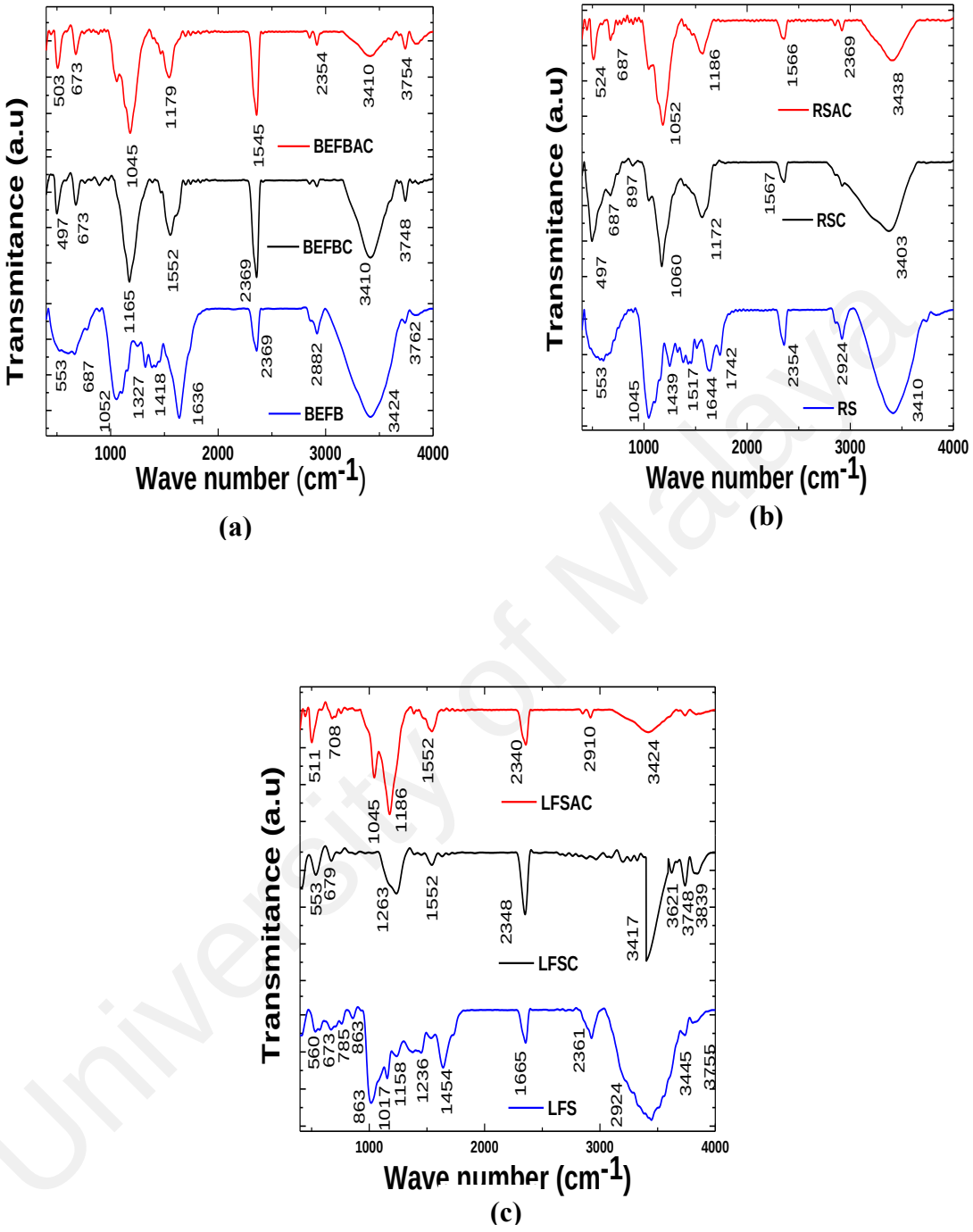

Figure 4.12: FTIR Spectra of (a) BEFB, BEFBC and BEFBAC; (b) RS, RSC and RSAC; (c) LFS, LFSC and LFSAC

Table 4.16: FTIR Spectrum of Banana empty fruit bunch (BEFB), Hydro-char (BEFBC) and Activated Carbon (BEFBAC)

IR Peak	Precursors	Frequency(cm^{-1})		Peak
Number	Banana empty fruit bunch(BEFB)	Hydrochar BEFB (BEFBC)	Activated BEFB (BEFBAC)	Assignment
1.	553	497	503	C-H out-of-plane bending of
2.	687	673.10	673.21	C-O-H
3.	895	886.94	895.35	C-H
4.	1052	1057.24	1045	C-O-C stretching of esters, ethyl or phenyl group
5.	-	1161.35	1178.83	-C-N stretching
6.	1327	-	-	CH_3 deformation
7.	1418	1551.81	1545.39	C=C
8.	1636.05	-	-	C=O
9.	2368.98	2368.77	2353.73	CO_2
10.	2881.97	-	-	-CH2, methylene groups
11.	2919.94	2918.71	-	-C-H (aliphatic)
12.	3424.05	3410.09	3410.24	-OH (Low)
13.	3761.64	3747.81	3753.69	-OH (Heavy)

Table 4.17: FTIR Spectrum of Rattan Sawdust (RS), Hydro-char (RSC) and Activated Carbon (RSAC)

IR Peak Number	Frequency(cm^{-1})			Peak Assignment
	Rattan Sawdust (RS)	Hydrochar RS (RSC)	Activated RS (RSAC)	
1.	553	456.94	524	C-H out-of-plane bending of benzene
2.	606.90	637.07	637.95	C-O-H
3.	-	897.01	-	C-H
4.	1045.44	1059.68	1052.09	C-O-C stretching of esters, ethyl or
5.	-	1172.35	1166.49	-C-N stretching
6.	1249.74	-	-	C-O stretching
7.	1438.98	-	-	CH_3 deformation
8.	1516.86	1567.83	1566.47	C=C
9.	1644.00	-	-	C=O
10.	1741.75	-	-	R-OR (ether)
11.	2353.85	-	2369.45	CO_2
12.	2923.50	-	-	-C-H (aliphatic)
13.	3410.18	3403	3438	-OH

Table 4.18: FTIR Spectrum of Longan Fruit Shell (LFS), Hydro-char (LFSC) and Activated Carbon (LFSAC)

IR Peak Number	Precursors			Peak Assignment
	Raw Longan Fruit	Hydro-char Material	Activated Longan Fruit Shell	
1.	560	553	511	C-H bending
2.	673.01	679.24		C-O-H
3.	785	-	708.03	C-H out-of-plane bending of benzene
4.	863	-	-	C-H O
5.	1017	-	1045.03	C-O-C stretching of esters, ethyl or phenyl
6.	1158.08	-	1186	-C-N stretching
7.	1235.76	1263	-	C-O stretching
8.	1454.36	1422.06	-	in-plane OH bending and C-O stretch of
9.	-	1551.99	1552	C=C ring stretching of benzene derivatives
10.	1664.53	-	-	C=O stretching
11.	2361.25	2348	2340.45	CO_2
12.	2924.10	-	2910	-C-H (aliphatic)
13.	3445.18	3417	3424	-OH
14.	3755.34	3748.01	3753.69	-OH (Heavy)

CHAPTER 5: BATCH ADSORPTION STUDIES

This chapter presents the experimental results obtained from the studies on Pb(II) and Zn(II) adsorption onto BEFBAC and RSAC and it is made up of five sections. Section one deals with the effects of processing conditions on the Pb^{+2} and Zn^{+2} adsorption onto the activated carbons. Sections two and three present the adsorption isotherms and kinetic studies respectively. The last two sections (iv and v) respectively discuss the adsorption thermodynamics and activated carbon regeneration.

5.1 Batch Adsorption Studies of Pb (II) and Zn (II) on BEFBAC and RSAC

To evaluate the adsorption isotherms, kinetics and thermodynamic characteristics of Pb^{+2} and Zn^{+2} on the activated carbons (BEFBAC and RSAC), batch adsorption studies were carried out.

5.1.1 Effect of Process Conditions

The effect of the process conditions on the equilibrium sorption are presented as follows:

5.1.1.1 Effect of contact time on the equilibrium sorption

The effect which the contact time exert on the equilibrium sorption process for the adsorbent (BEFBAC and RSAC) is as presented in figures 5.1 and 5.2. From the figures, it could be observed that the sorption level of the adsorbent increased as the initial sorption time increases up to about three and half hours (210 min) but remained relatively constant afterwards. The above trend suggested that at about three and half hours, all the active sites must have been saturated with the adsorbate [Pb (II) and Zn (II) ions as obtainable in each case]. A similar trend has been observed by (Khezami, Bessadok-Jemai, Al-Dauij, & Amami, 2012) and (Z. Z. Chowdhury, Zain, Khan, Rafique, et al.,

2012). The point of the observed saturation corresponds to the maximum sorption limit of the adsorbent.

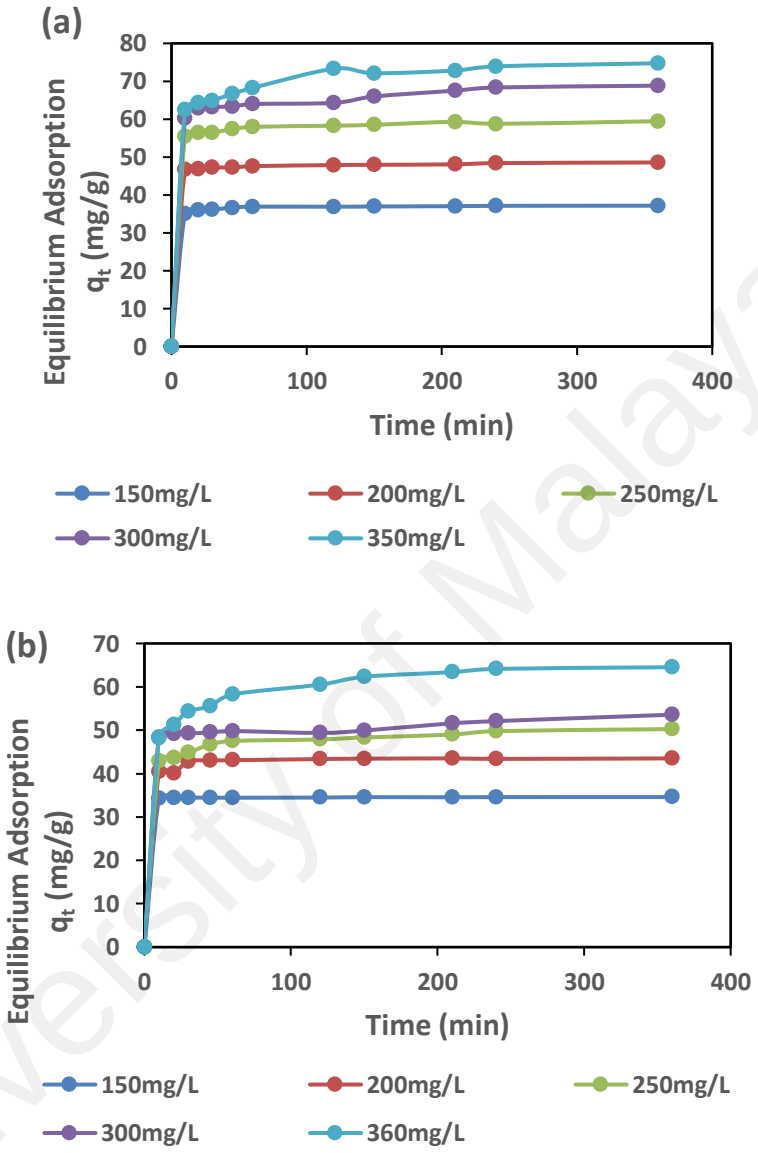

Figure 5.1: Adsorption of (a) Pb (II) and (b) Zn (II) versus adsorption time at various initial concentrations at 30°C on BEFBAC respectively

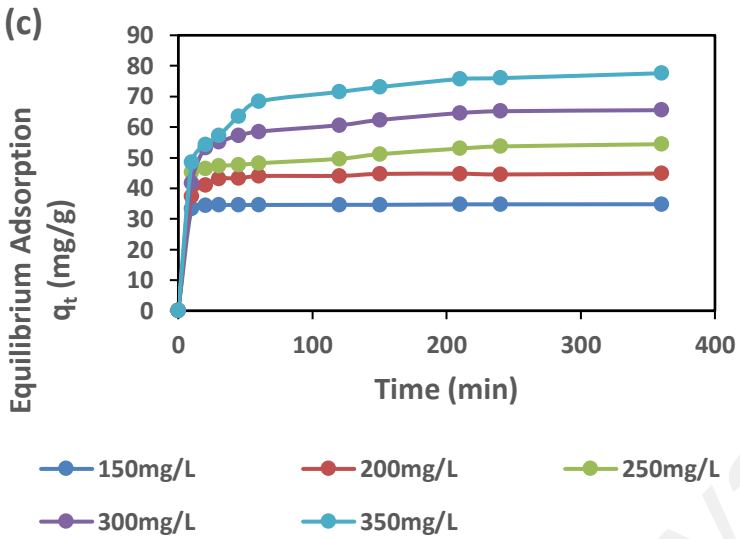

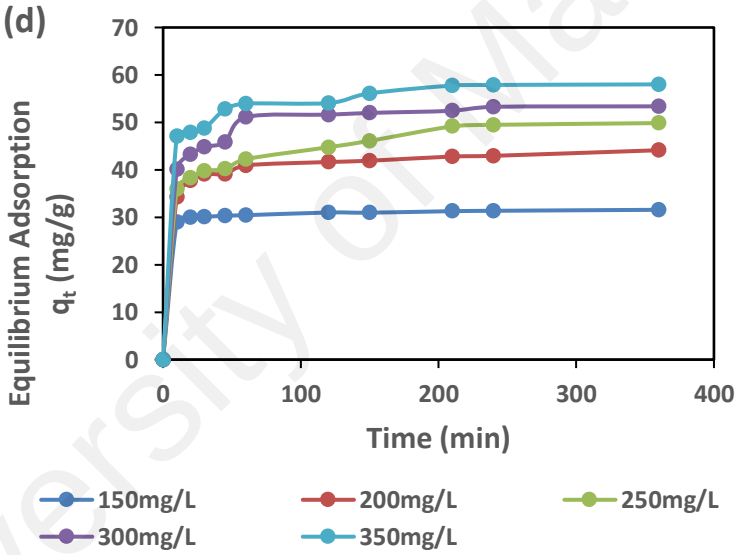

Figure 5.2: Adsorption of (c) Pb (II) and (d) Zn (II) versus adsorption time at various initial concentrations at 30°C on RSAC respectively

5.1.1.2 Effect of Solution Temperature

The effect which the solution temperature exert on the adsorption capacity of Pb(II) and Zn(II) ions in aqueous solution by BEFBAC and RSAC was studied. To do this, the solution temperature was varied between 30°C to 80°C with other process conditions kept at constant values, pH = 5.5, time = 210 min, initial concentration = 350 mg/l and adsorbent dosage = 0.2 g. Figures 5.3 and 5.4 below shows the graph of adsorption

capacity versus the solution temperature for Pb(II) and Zn(II) of BEFBAC and RSAC respectively. The extent to which the solution temperature affects the adsorption capacity depends majorly on the type of adsorbent-adsorbate system (Shrestha, Son, Lee, & Lee, 2013). In the figures, the adsorption capacity increased with steady increase in solution temperature, indicating the endothermic nature of the adsorption process is, thereby following a similar trend reported on the removal from aqueous solution, Pb(II) ions onto biomass-waste-derived activated carbon (Erdem, Ucar, Karagöz, & Tay, 2013).

5.1.1.3 Effect of Solution pH

In an effort to study the effect which the solution pH exert on the adsorption of Pb(II) and Zn(II) ions onto BEFBAC and RSAC, the solution initial pH was varied between 2 to 14 while other adsorption process conditions were kept constant at T = 30 ^{o}C, t = 210min, adsorbate initial concentration = 350 mg/l and adsorbent dosage = 0.2 g. The solution pH has the ability to either suppress or uplift the adsorption capacity of an adsorbate, usually attributed to change of the activated carbon charge when the solution pH is altered (Nguyen et al., 2013). Increase in pH up to between 5 and 7.5 leads to availability of more negatively charged surface thereby contributing to more metal adsorption (Chigondo, Nyamunda, Sithole, & Gwatidzo, 2013). The surface of an adsorbent is normally surrounded by the presence of hydroxonium ions (H^+) at lower pH values which usually block metal ions from binding onto adsorbents (Onundi, Mamun, Al Khatib, & Ahmed, 2010).

At pH lower than pH 4, there will be serious competition between the concentration of H^+ and H_3O^+ ions and M^{2+} cations present in solution which will lead to repulsion and thereby culminating into reduced adsorption of the cations by the adsorbents. Thus the adsorption of the metal ions under investigation are generally low at lower pH. Moreover, at pH higher than 8, the OH^- groups present will be precipitated thereby leading to

blockage of available sorption sites. This invariably resulted to reduced adsorption of the metal ions. Such similar trend has been reported (Nguyen et al., 2013).

5.1.1.4 Effect of Adsorbent dosage

From economic point of view, it is essential to evaluate the influence which adsorbent dosage has so as to determine the minimum weight of adsorbent required for effective metal ion removal. Figures 5.7 and 5.8 below present the influence of adsorbent dosage on sorption of Pb (II) and Zn (II) ions by BEFBAC and RSAC. It is evident that the uptake of both metal ions increased with increase in the quantity of adsorbent used. Moreover, increase in the amount of the adsorbent taken (dosage) also favors the equilibrium adsorption capacity (mg g^{-1}). However, economic viability of the process is of vital importance, therefore we used 0.2 g to investigate the feasibility of better adsorption performance by varying other parameters. This is done in order to use minimum amount of the sorbent to achieve maximum adsorption. This is in agreement with the submissions of several authors (Bhattacharya, Mandal, & Das, 2006; Mishra & Patel, 2009; M. M. Rao, Rao, Seshaiah, Choudary, & Wang, 2008).

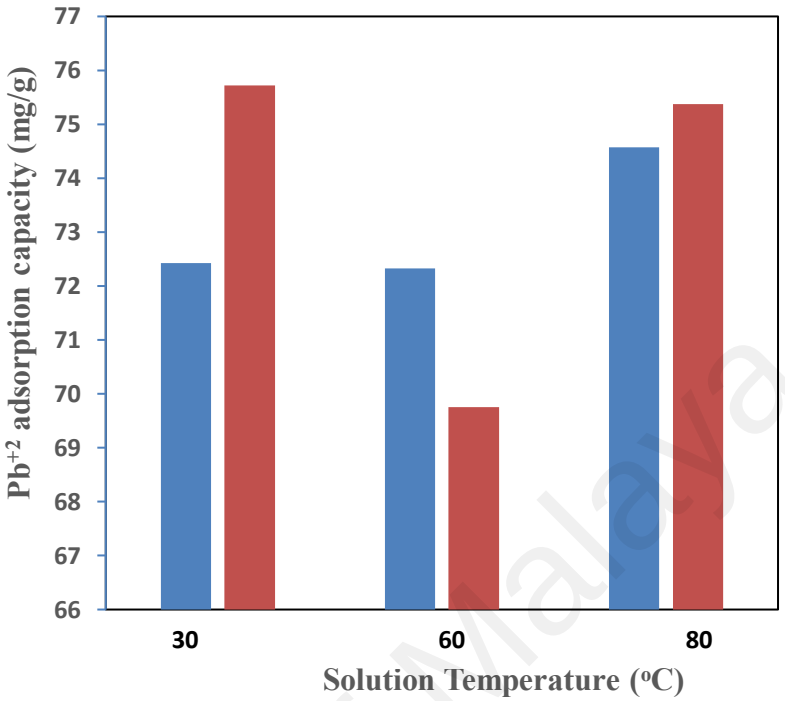

Figure 5.3: **Effect of solution temperature on Pb (II) adsorption capacity of BEFBAC and RSAC.**

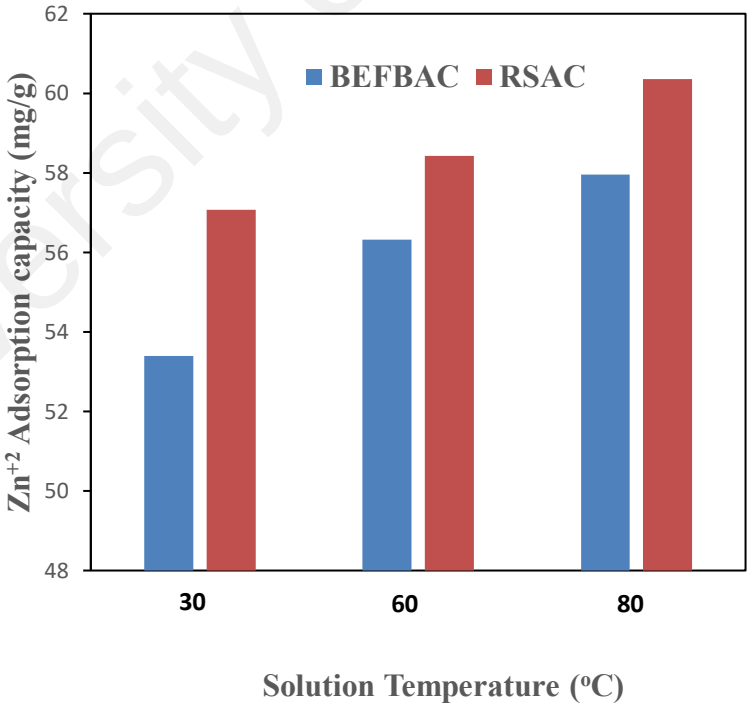

Figure 5.4: **Effect of solution temperature on Zn (II) adsorption capacity of BEFBAC and RSAC**..

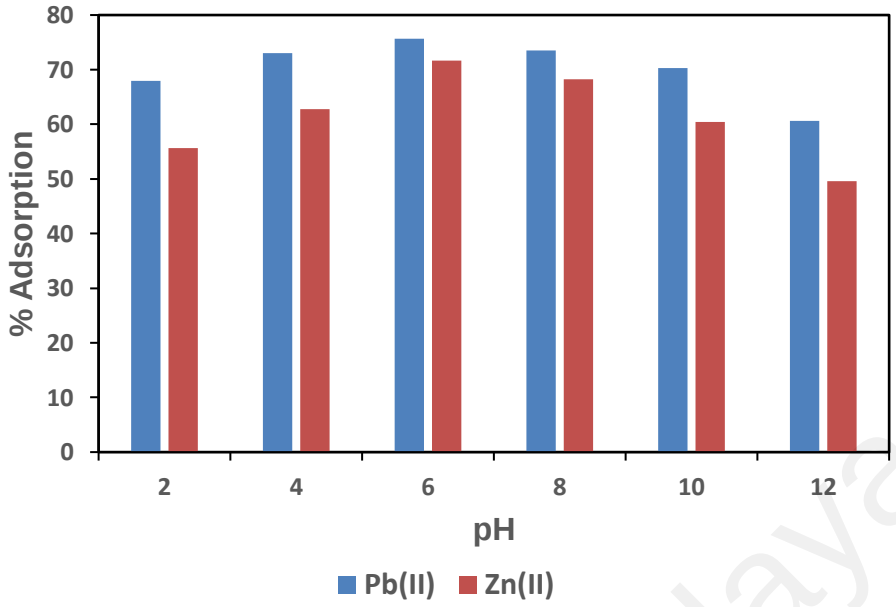

Figure 5.5: Effect of initial solution pH on adsorption of Pb(II) and Zn(II) onto BEFBAC.

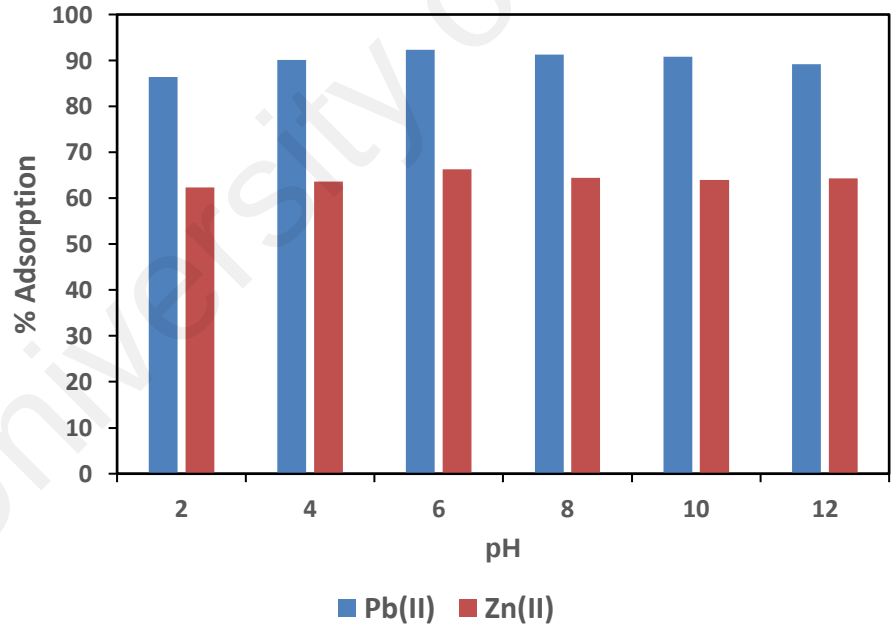

Figure 5.6: Effect initial solution pH on adsorption of Pb(II) and Zn (II) onto RSAC.

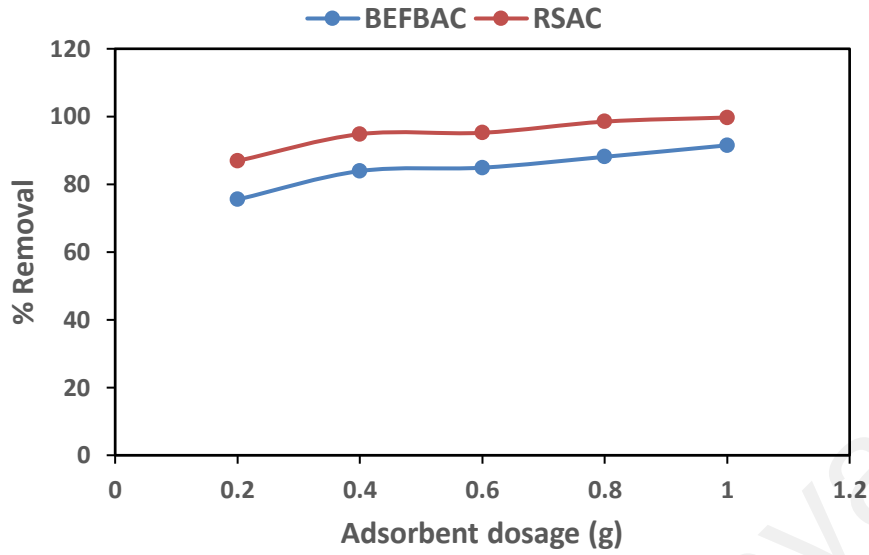

Figure 5.7: Effect of adsorbent dosage on adsorption of Pb (II) onto BEFBAC and RSAC.

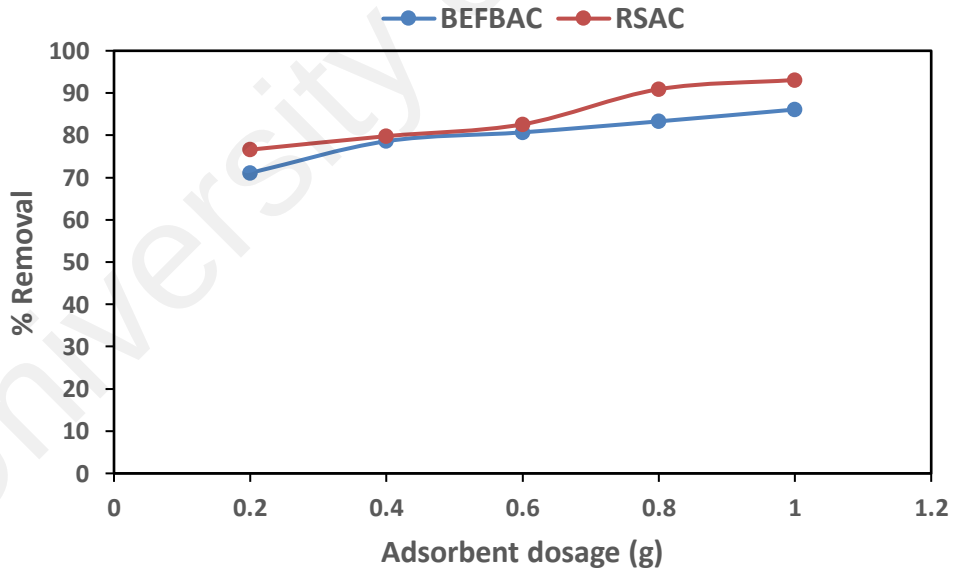

Figure 5.8: Effect of adsorbent dosage on adsorption of Zn (II) onto BEFBAC and RSAC.

5.2 Adsorption Isotherms

The adsorption isotherm represents the ratio of the distribution of the adsorption molecules between the adsorbate (liquid phase) and the adsorbent (solid phase) at

equilibrium state (Moreno-Barbosa et al., 2013). It is always important to subject kinetic experimental data to various adsorption isotherm models so as to be able to determine which of the models best describes the adsorption process, that is, which of the models the adsorption process best fits. For the present work, the experimental data was subjected to three isotherm models. These are Langmuir, Freundlich and Temkin isotherm models. The three models were compared to determine their applicability on the value of the various constants especially the closeness of their correlation coefficients, R^2 value, to unity since the closer the value of R^2 to one (unity), the better (Z. Z. Chowdhury, Zain, Khan, Rafique, et al., 2012).

Tables 5.1 and 5.2 represent the Langmuir, Freundlich and Temkin isotherm model parameters and correlation coefficients of adsorption of lead and zinc onto BEFBAC and RSAC at 30ºC, 60ºC and 80ºC respectively. In Langmuir model, K_L indicates the energy of adsorption while q_{max} shows the maximum monolayer adsorption capacity (mg g^{-1}) (Moreno-Barbosa et al., 2013). From the tables, it could be observed that the energy of adsorption, K_L at temperatures 30, 60 and 80ºC for BEFBAC are 0.3004, 0.4137 and 0.4452 and 0.0758, 0.0864 and 0.0710 for lead and Zinc respectively; and for RSAC are 0.0424, 0.0321 and 0.0353; and 0.0281, 0.0329 and 0.0334 for lead and zinc respectively. The maximum adsorption capacity, q_{max} as contained in the tables are 74.63, 78.74 and 79.37 and 77.52, 76.34 and 80.65 in the case of BEFBAC while for RSAC, it is 101.01, 133.33 and 129.87; and 96.25, 95.24 and 99.01 respectively for lead and zinc. Furthermore, the Langmuir isotherm is usually evaluated using the separation factor, R_L, which is normally dimensionless and used to determine whether an adsorption system is favourable or otherwise (Moreno-Barbosa et al., 2013). R_L is calculated using the following equation,

$$R_L = 1/1+K_LC_o \qquad 5.2$$

where, C_o = initial metal concentration.

K_L = Langmuir constant.

The value of R_L obtained is an indication of the type of isotherm and the nature of the adsorption process that occurred during the process (Moreno-Barbosa et al., 2013). The Langmuir R_L value can be described as follows: $R_L > 1$ is unfavourable, $R_L = 1$ is linear, $0 < R_L < 1$ is favourable and $R_L = 0$ is irreversible (Z. Z. Chowdhury, Zain, Khan, Rafique, et al., 2012). In the subsisting study, the values of R_L are 0.01, 0.01 and 0.01; 0.04, 0.03 and 0.04 for lead and zinc respectively for BEFBAC while for RSAC, it is 0.06, 0.08 and 0.07; and 0.09, 0.08 and 0.08 for lead and zinc respectively at temperatures 30, 60 and 80^{o}C. The result indicates that the values fall between 0 and 1, a confirmation that all R_L values are favourable. It further indicates that the process of adsorption fits satisfactorily into Langmuir isotherm model. Another confirmation of this deduction is the value of R^2 obtained at every temperature which is very close to unity (value one). This further confirms the fitness of the adsorption process into Langmuir model.

The Freundlich isotherm model describes the heterogeneity of the surface in an adsorption process (Z. Z. Chowdhury, Zain, Khan, Rafique, et al., 2012). The value of K_F in the model is the Freundlich constant and usually related to the distribution coefficient of the ions during the process of adsorption while n stands for the Freundlich exponent. All these values were obtained from the plot of log q_e against log C_e (Moreno-Barbosa et al., 2013). In Freundlich model, when the value of 1/n is very close to 0, it indicates that the process is becoming heterogeneous, when 1/n is less than 1, it signifies normal Langmuir isotherm and when the value is greater than 1, it is an indication of cooperative adsorption. From the table, the value of 1/n is less than 1, indicating that the adsorption process satisfactorily fits into normal Langmuir isotherm model. The fitness of Langmuir model into the experimental could be due to homogeneous distribution of active sites on

the adsorbent. Therefore, the applicability of the Langmuir isotherm model in the adsorption process is an indication of monolayer attachment of lead and zinc ions on the outer surface of adsorbents (BEFBAC and RSAC) (Chigondo et al., 2013).

Contained in tables 5.1 and 5.2 are the Temkin constants. Temkin isotherm signifies the occupation of the more energetic adsorption sites by the adsorbate, that is, the interaction between the adsorbate and the adsorbent (Z. Z. Chowdhury, Zain, Khan, Rafique, et al., 2012). The value of R^2 obtained for Temkin model at room temperature (30^{o}C) gives 0.9726 and 0.5881 for BEFBAC; and 0.8242 and 0.8094 for RSAC respectively for lead and zinc. This is far lower than the values obtained for Langmuir at the same temperature, an indication that the obtained experimental data best fits into the Langmuir model than it fits into either the Freundlich model or the Temkin model. For Langmuir model, the values of R^2 are consistently close to unity at the three temperatures under observation than what were obtained for Freundlich and Temkin isotherms. Thus it can be deduced from the experimental results that the Langmuir model is the most applicable model and therefore be concluded that monolayer adsorption process has taken place in the system.

5.3 Kinetics of Adsorption

Adsorption kinetics study is germane in determining adsorption efficiency during any adsorption process. It is usually employed in testing the obtained experimental data and used in determining both the adsorption mechanism as well as its potential rate controlling steps such as mass transfer and chemical reaction that have taken place during sorption process. Tables 5.3 to 5.8 below represent the results of adsorption kinetics models for adsorption of Pb^{2+} and Zn^{2+} ions from their aqueous solutions. The models include pseudo-first- order kinetic model, pseudo-second-order kinetic model, elovich equation model and intra-particle diffusion.

The adsorption kinetics elucidate the adsorption uptake of the adsorbates [(Pb (II) and Zn (II) ions] on the adsorbent (activated carbon). As stated earlier, the pseudo-first-order, pseudo-second-order and Elovich kinetic models were employed in studying the kinetics of the adsorption process in this work. Furthermore, the intra-particle diffusion model was applied to evaluate the mechanism of diffusion of the process being studied. For all the chosen models, the obtained kinetic data were analyzed while the various constants were computed using Microsoft Office Excel, version 2013. The pseudo-first-order model has been in use for many years to predict the sorption kinetics (Z. Z. Chowdhury, Zain, Khan, Rafique, et al., 2012) and usually expressed by equation;

$$\log(q_e - q_t) = \log q_e - K_1 \frac{t}{2.303} \quad 5.3$$

$$h = q_e cal \quad 5.4$$

where, q_e and q represent the amounts in mg/g of adsorbate [(Pb (II) and Zn (II) ions] adsorbed at equilibrium and 210 min respectively, h (mg/g min) stands for the initial rate of sorption, and K_1 denotes the adsorption rate constant. When the plot of log ($q_e - q_t$) versus t is made, a slope of K_1 and intercept log q_e were obtained. K_1 (1/h) is the pseudo-first-order adsorption constant. Tables 5.3 & 5.4 below presented the results of both the first order and second order constants obtained for adsorption of Pb (II) and Zn (II) ions onto BEFBAC and RSAC respectively. Unlike the pseudo-first-order model, the pseudo-second-order determines the behaviour of the adsorption process over a wide range of adsorption (Z. Z. Chowdhury, Zain, Khan, Rafique, et al., 2012) and represented by equation

$$\frac{t}{q_t} = \frac{1}{k_2 qe^2} + \frac{1}{q_e} t \quad 5.5$$

$$h = K_2 qe^2 cal \quad 5.6$$

K_2 (g/mg h) and h (mg/g min) denote the pseudo-second-order adsorption rate constant and initial rate of sorption respectively. All of these constants are contained in tables 5.3 & 5.4 below. It is clearly evident from the values obtained for the various constants as contained in the tables that overall, the kinetic data fitted into pseudo-second-order model. In this model, the values of the q_e exp agreed perfectly with q_e values calculated (q_e cal) which resulted in relatively low Δq_t. Apart from this, the R^2 (correlation coefficient) values obtained were unity at low initial concentrations (150mg/L and 200mg/L) and very close to unity at other initial concentrations for both lead and zinc. As noticed in the pseudo-first-order model, there was a wide gap between the q_e exp and q_e cal thereby resulting in large Δq_t values [above 90% by both adsorbents for Pb (II) and Zn (II) ions for all initial concentrations]. The results obtained for the pseudo-second-order model showed satisfactory agreement with previous research carried out on adsorption of Pb (II) and Zn (II) ions onto activated carbons synthesized from watermelon shell and walnut shell (Moreno-Barbosa et al., 2013), Penicillium simplicissimum (Fan et al., 2008) and low cost adsorbents (Mishra & Patel, 2009) where the processes of adsorption were all best defined by the pseudo-second-order kinetic model. It could also be observed from tables 5.3 & 5.4 that removal percent of Pb (II) ion for all the initial concentrations by both BEFBAC and RSAC were higher than obtained for Zn (II) ion by them. The reason for higher Pb (II) ion adsorption might be due to its ionic potential, electronegativity and softness parameters. Lead has electronegativity 2.33 while Zinc has 1.65 (Kalmykova, Strömvall, & Steenari, 2008). Since the electronegativity of lead was higher, its adsorption capacity will be greater (Depci et al., 2012). This result was in agreement with those obtained for watermelon shell and walnut shell (Moreno-Barbosa et al., 2013). Other reasons may be due to difference in ionic size, Irving Williiams series and higher reactivity of lead over zinc.

For proper description of the mode of adsorption that has taken place, the experimental data obtained was fitted into Elovich equation model. Contained in tables 5.5 and 5.7 below are the Elovich equation constants and the correlation coefficients obtained. The tables also show that there is a close gap between the uptake capacity and the theoretical uptake capacity leading to low values of Δqt%, indicating the fitness of the experimental data into Elovich equation model. This signifies that chemisorption has taken place.

The experimental data obtained were fitted with intra-particle diffusion equation model so as to observe the effect of the diffusion process since the other three models could not describe the diffusion mechanism of the sorbate onto the interior of the sorbent. In sorption process, the role of diffusion as the rate controlling step is examined by the intra-particle diffusion (Z. Z. Chowdhury, Zain, Khan, Rafique, et al., 2012). It is usually a general expectation that during adsorption process, uptake should be directly proportionally to the square root of time ($t^{1/2}$) but not with contact time (t). The intra-particle diffusion model is normally referred to as Weber and Morris (1962) model and usually represented by the following equations (Z. Z. Chowdhury, Zain, Khan, Rafique, et al., 2012);

$$q_t = K_{id}\, t^{1/2} + C \qquad 5.7$$

where, K_{id} (mg/g h) is the intra-particle diffusion rate constant and obtainable from the slope of curve of q_t against $t^{1/2}$. C provides information about the boundary layer's thickness. Information has been provided regarding the relationship between the intercept of the curve and the layer of the boundary. The larger the intercept, the greater the boundary layer (Kannan & Sundaram, 2001).

To establish intra-particle diffusion, the curve of q_t against $t^{1/2}$ should be linear and must pass through the origin for particle diffusion to be involved in the rate limiting step.

Otherwise, some other rate limiting mechanisms may have been involved. Tables 5.6 and 5.8 below contained the intra-particle diffusion constants and correlation coefficients for adsorption of lead and zinc onto BEFBAC and RSAC respectively. The plot of q_t versus $t^{1/2}$ (not shown) though linear, but did not pass through the origin, thereby making it difficult to establish that intra-particle diffusion is the only rate controlling step involved in the adsorption process. In the tables 5.6 and 5.8 below, the correlation constants, R^2 are not close to one (unity) for all the initial concentrations indicating that the adsorption process does not fit into inta-particle diffusion model.

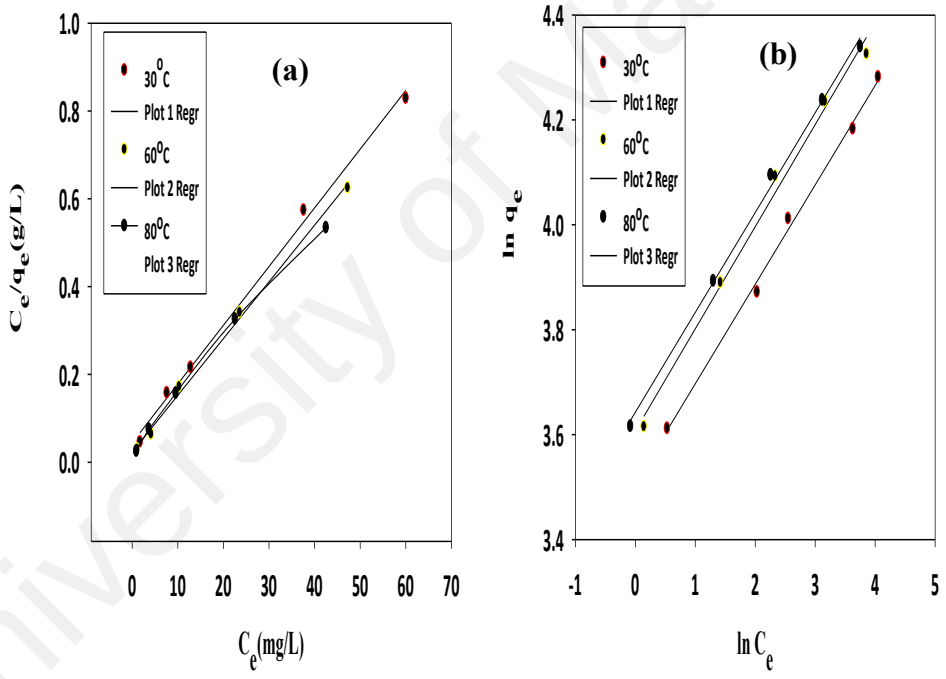

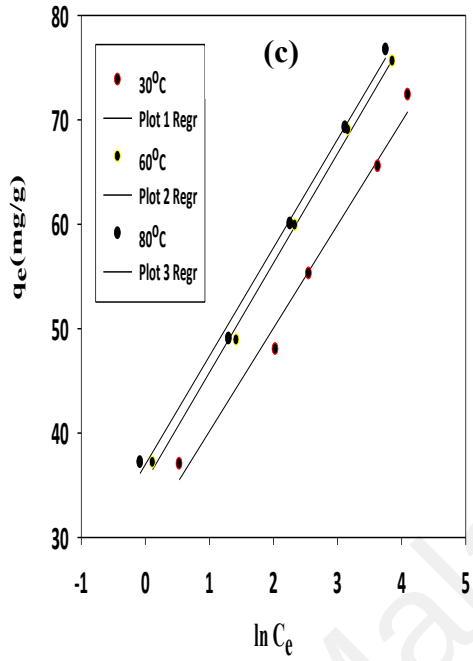

Figure 5.9: Plots of (a) Langmuir (b) Freundlich and (c) Temkin Isotherms for Pb(II) adsorption on BEFBAC at 30, 60 and 80ºC.

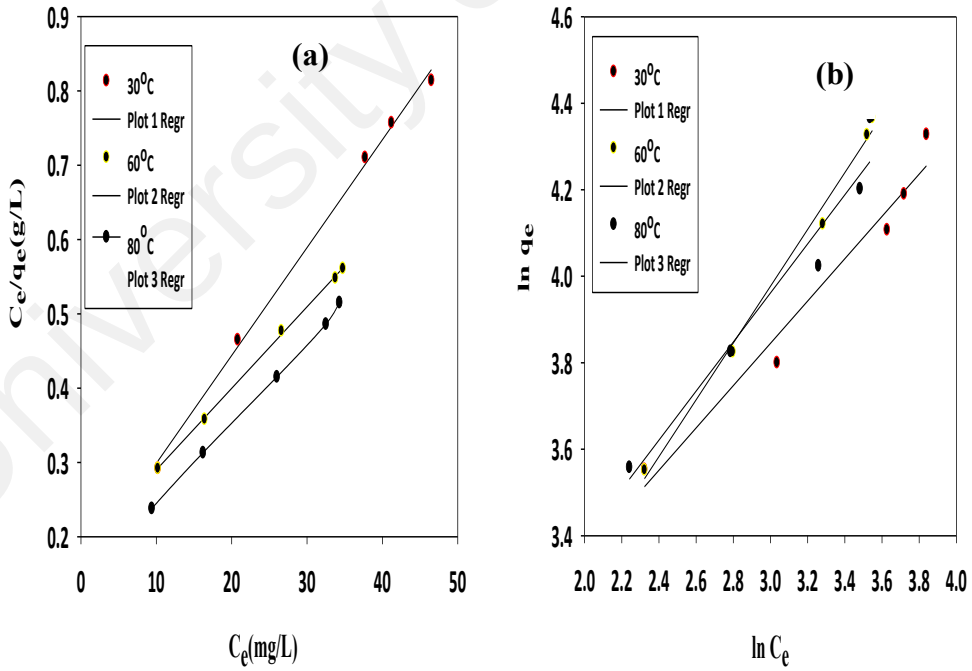

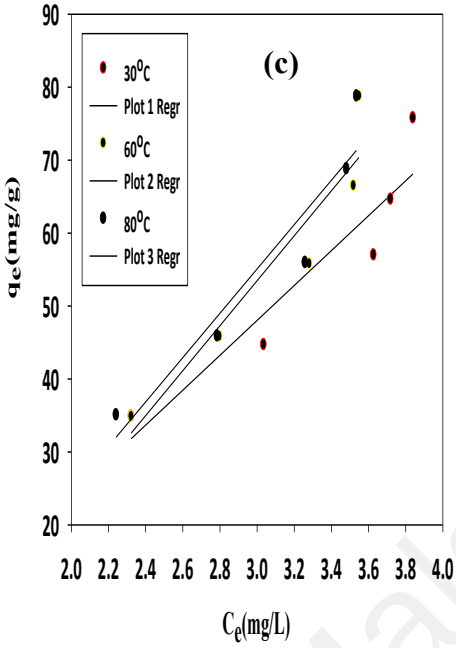

Figure 5.10: Plots of (a) Langmuir (b) Freundlich and (c) Temkin Isotherms for Zn(II) adsorption on BEFBAC at 30, 60 and 80°C.

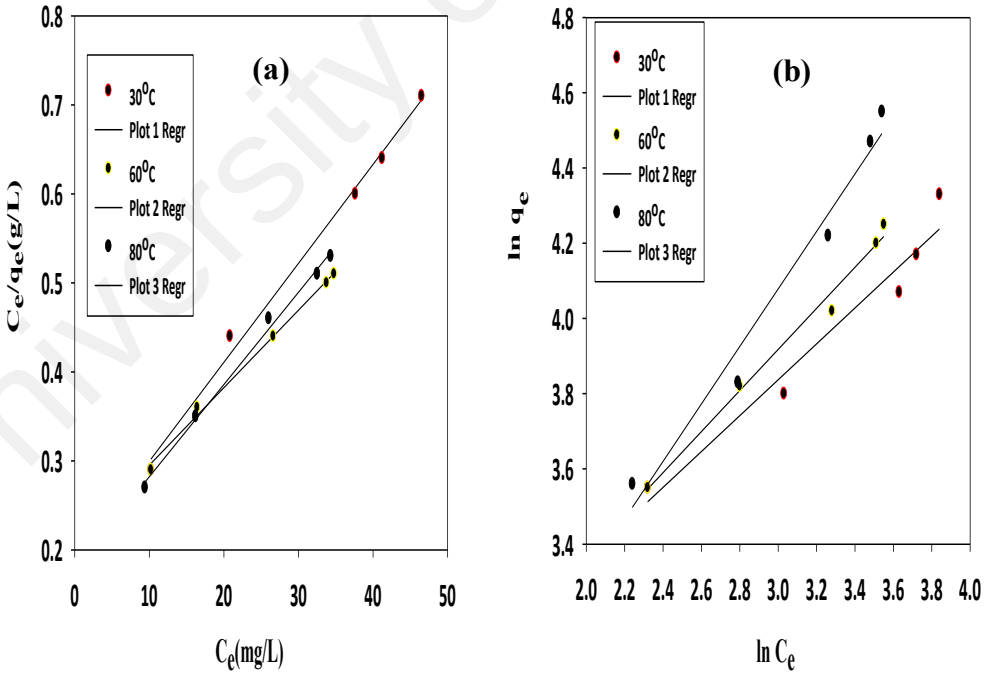

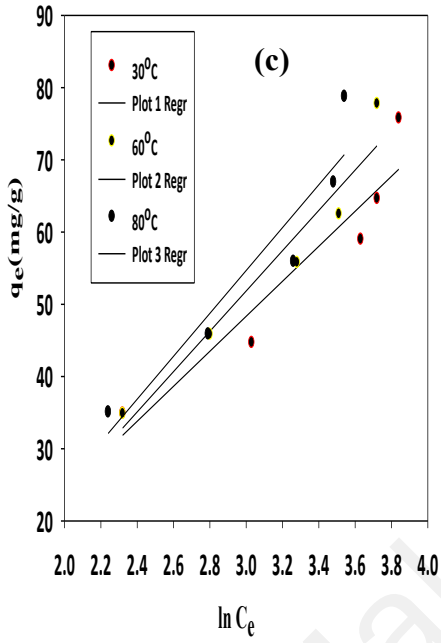

Figure 5.11: Plots of (a) Langmuir (b) Freundlich and (c) Temkin Isotherms for Pb(II) adsorption on RSAC at 30, 60 and 80°C.

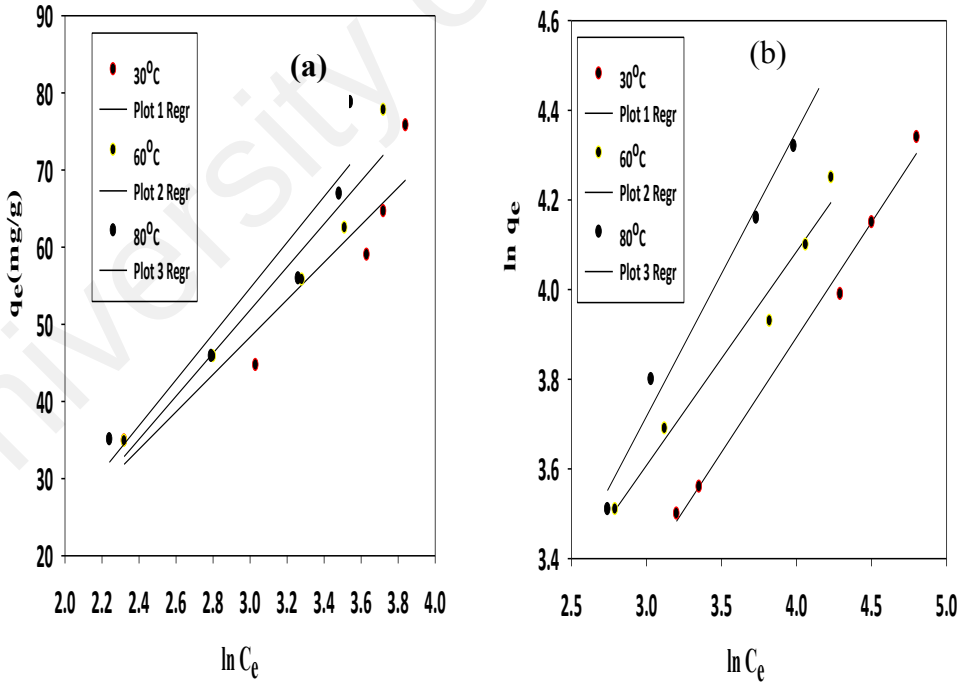

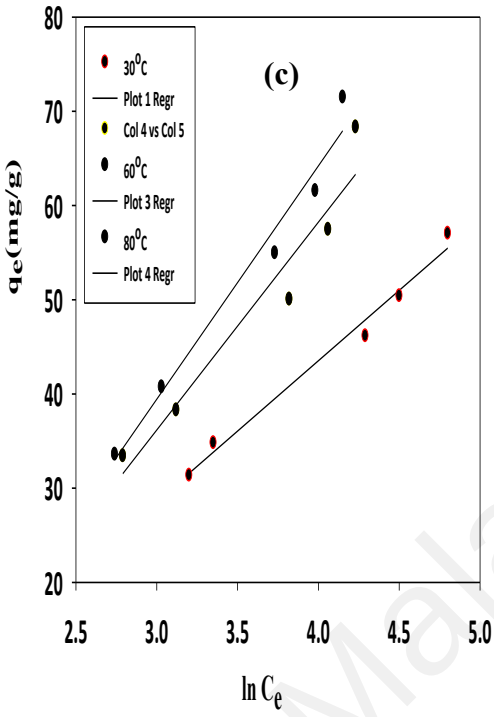

Figure 5.12: Plots of (a) Langmuir (b) Freundlich and (c) Temkin Isotherms for Zn(II) adsorption RSAC at 30, 60 and 80ºC.

Table 5.1: Langmuir, Freundlich and Temkin isotherms models parameters and correlation coefficients for adsorption of Pb (II) and Zn (II) on BEFBAC at 30°C, 60°C and 80°C

Pollutant	Isotherm										
	Temp (°C)	Langmuir Isotherm				Freundlich Isotherm			Temkin Isotherm		
		Maximum monolayer adsorption capacity q_{max} (mg/g)	Langmuir constant K_L (L/mg)	Correlation coefficient R^2	Separation FactorR_L (mg/g) $(L/mg)^{(1/n)}$	Affinity factor K_F	Freundlich exponent 1/n	Correlation coefficient R^2	Binding constant K_T (L/mg)	Temkin constant B	Correlation coefficient R^2
Pb (II)	30	74.63	0.30	0.996	0.009	33.93	0.187	0.971	23.28	9.88	0.973
	60	78.74	0.41	0.998	0.007	37.01	0.193	0.993	29.00	10.49	0.997
	80	79.37	0.45	0.997	0.006	38.19	0.190	0.997	35.23	10.38	0.996
Zn (II)	30	77.52	0.08	0.978	0.036	17.99	0.311	0.718	38.30	6.48	0.588
	60	76.34	0.09	0.973	0.032	19.45	0.295	0.060	1.32	14.80	0.714
	80	80.65	0.07	0.984	0.039	16.04	0.347	0.902	0.74	17.31	0.895

Table 5.2: Langmuir, Freundlich and Temkin isotherms models parameters and correlation coefficients for adsorption of Pb (II) and Zn (II) on RSAC at 30°C, 60°C and 80°C

Pollutant	Isotherm										
	Temp (°C)	Langmuir Isotherm				Freundlich Isotherm			Temkin Isotherm		
		Maximum monolayea adsorption capacity q_{max} (mg/g)	Langmuir constant K_L (L/mg)	Correlation coefficient R^2	Separation factor R_L(mg/g) $(L/mg)^{(1/n)}$	Affinity factor K_F	Freundlich exponent 1/n	Correlatio coefficient R^2	Binding constant K_T(L/mg)	Temkin constant B	Correlation coefficient R^2
Pb (II)	30	101.01	0.04	0.972	0.06	11.64	0.46	0.899	0.39	23.12	0.824
	60	133.33	0.03	0.925	0.08	8.74	0.59	0.950	0.28	30.83	0.892
	80	129.87	0.04	0.938	0.07	9.59	0.57	0.952	0.31	29.67	0.892
Zn (II)	30	96.25	0.03	0.964	0.09	14.05	0.29	0.785	0.69	12.48	0.809
	60	95.24	0.03	0.934	0.08	10.03	0.45	0.941	0.29	22.01	0.922
	80	99.01	0.03	0.935	0.08	9.98	0.46	0.939	0.29	23.04	0.926

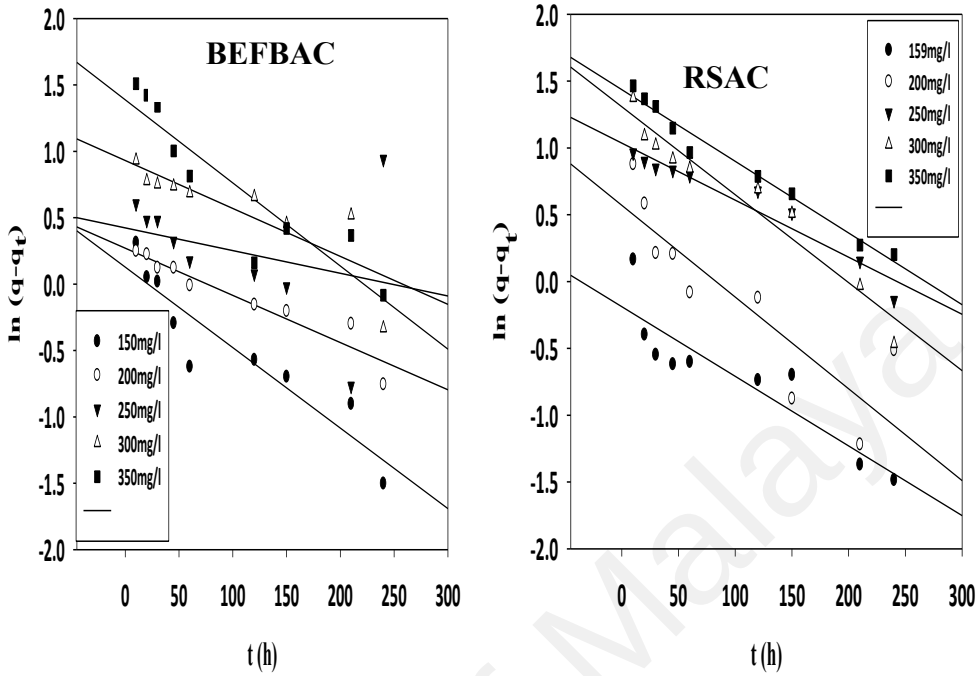

Figure 5.13: Linearized plots of pseudo-first-order kinetic model for Pb(II) adsorption on BEFBAC and RSAC at 30°C

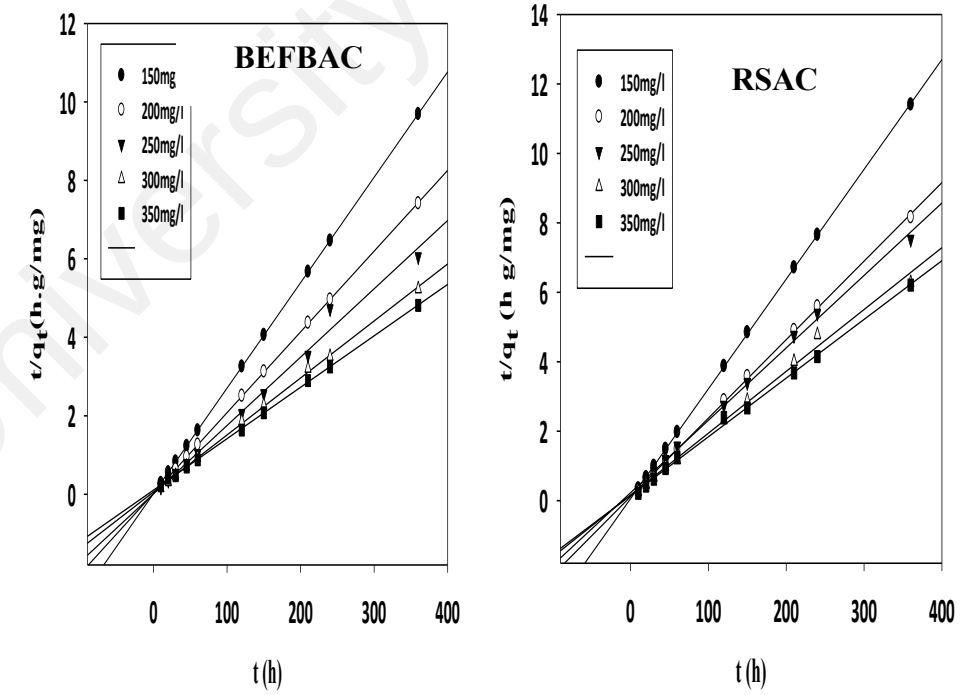

Figure 5.14: Linearized plots of pseudo-second-order kinetic model for Pb(II) adsorption on BEFBAC and RSAC at 30°C.

94

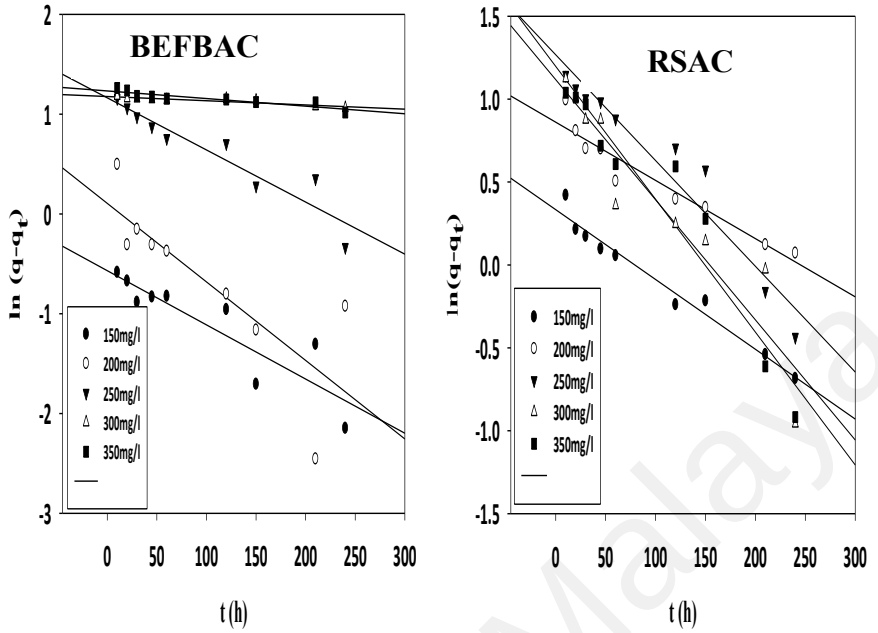

Figure 5.15: **Linearized plots of pseudo-first-order kinetic model for Zn(II) adsorption on BEFBAC and RSAC at 30ºC.**

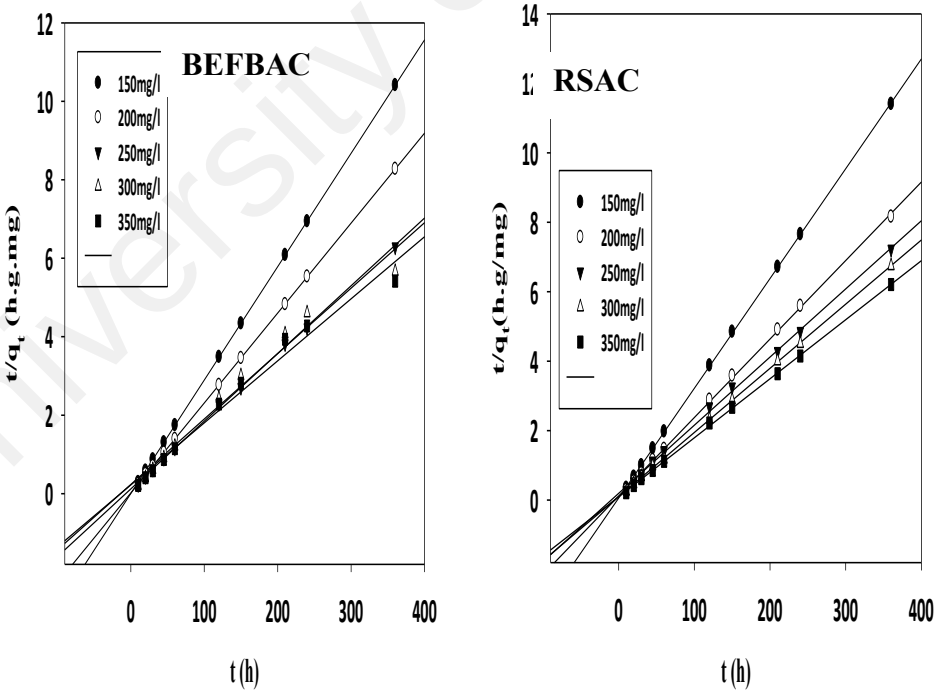

Figure 5.16: Linearized plots of pseud-second-order kinetic model for Zn(II) adsorption on BEFBAC and RSAC at 30ºC

Table 5.3: Pseudo-first-order and pseudo-second-order model constants, correlation coefficients and normalized standard deviation values for Adsorption of Pb (II) on BEFBAC and RSAC at 30°C

	Pseudo First Order							Pseudo Second Order				
Adsorbent	**Lead Initial Concentration Co (mg/L)**	**Removal %**	**Uptake capacity q_e,exp (mg/g)**	**Theoretical uptake capacity q_e,cal (mg/g)**	**1st order rate constant K_1 (1/h)**	**Correlation coefficient R^2**	**Δq_t (%)**	**Uptake capacity q_e,exp (mg/g)**	**Theoretical uptake capacity q_e,cal (mg/g)**	**2nd order rate constant K_2 (g/mg h)**	**Correlation coefficient R^2**	**Δq_t (%)**
BEFBAC	150	98.87	37.04	1.14	0.014	0.865	96.93	37.04	37.17	0.035	1	0.37
	200	96.20	48.08	1.31	0.008	0.912	97.27	48.08	48.54	0.018	1	0.96
	250	94.88	59.30	1.53	0.004	0.092	97.43	59.30	57.47	0.020	0.990	3.08
	300	87.47	65.53	2.54	0.008	0.704	96.13	65.53	68.97	0.003	0.999	4.98
	350	82.86	72.43	4.39	0.016	0.803	93.95	72.43	72.46	0.006	0.992	0.05
RSAC	150	93.20	34.86	0.43	0.012	0.818	98.77	34.86	34.84	0.064	1	0.06
	200	89.60	44.78	1.77	0.016	0.759	96.05	44.78	45.05	0.013	1	0.59
	250	84.96	52.99	2.82	0.010	0.939	94.68	52.99	54.35	0.001	0.971	2.49
	300	86.27	64.60	3.70	0.015	0.944	94.28	64.60	66.67	0.002	0.999	3.10
	350	86.71	75.72	4.75	0.014	0.937	93.73	75.72	81.97	0.001	0.997	7.62

Table 5.4: Pseudo-first-order and pseudo-second-order model constants, correlation coefficients and normalized standard deviation values for Adsorption of Zn (II) on BEFBAC and RSAC at 30°C

	Pseudo First Order							Pseudo Second Order				
Adsorbent	**Lead Initial Concentration Co (mg/L)**	**Removal %**	**Uptake capacity q_e,exp (mg/g)**	**Theoretical uptake capacity q_e,cal (mg/g)**	**1st order rate constant K_1 (1/h)**	**Correlation coefficient R^2**	**Δq_t (%)**	**Uptake capacity q_e,exp (mg/g)**	**Theoretical uptake capacity q_e,cal (mg/g)**	**2nd order rate constant K_2 (g/mg h)**	**Correlation coefficient R^2**	**Δq_t (%)**
BEFBAC	150	92.33	34.57	1.77	0.01	0.796	94.88	34.57	34.60	0.15	1	0.09
	200	87.05	43.44	1.11	0.02	0.661	97.44	43.44	43.67	0.03	1	0.53
	250	88.72	55.34	3.20	119.76	0.891	94.22	55.34	59.88	0.001	0.977	7.58
	300	66.70	49.93	3.24	0.001	0.842	93.50	49.93	59.88	0.001	0.977	16.63
	350	61.03	53.32	2.54	0.01	0.694	95.24	53.32	56.50	0.004	0.999	5.62
RSAC	150	82.67	30.97	1.40	0.01	0.969	95.50	30.97	31.65	0.017	1	2.14
	200	84	41.92	2.37	0.01	0.926	94.36	41.92	44.25	0.004	0.999	5.27
	250	70.64	44.11	3.11	0.006	0.890	92.94	44.11	47.85	0.002	0.998	7.82
	300	69.43	52.00	3.02	0.004	0.598	94.18	52.00	56.18	0.002	0.994	7.45
	350	64.26	56.11	3.65	0.017	0.842	93.50	56.11	59.17	0.002	0.998	5.17

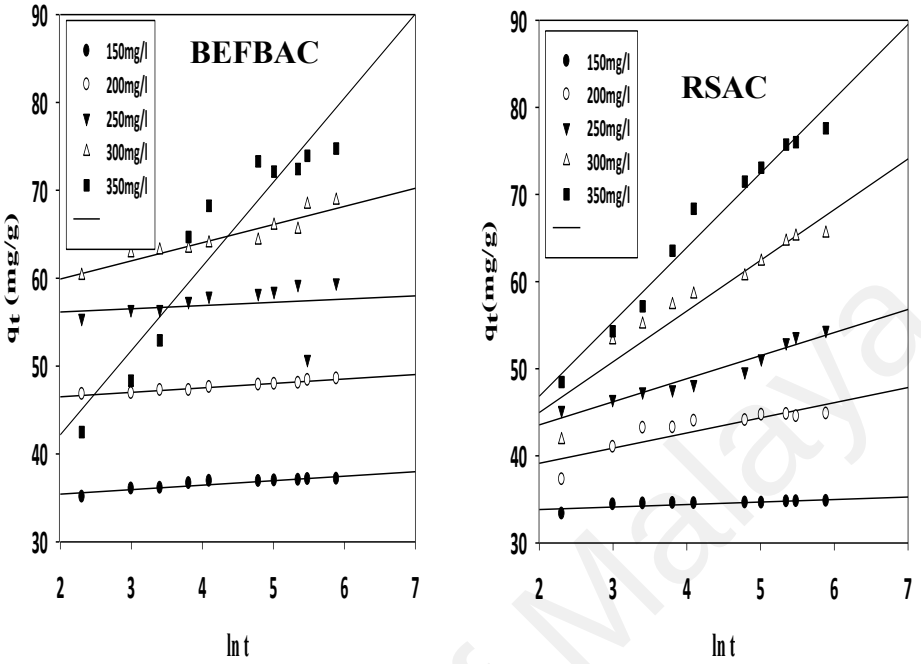

Figure 5.17: Linearized plots of Elovich Equation model for Pb(II) adsorption on BEFBAC and RSAC at 30ºC.

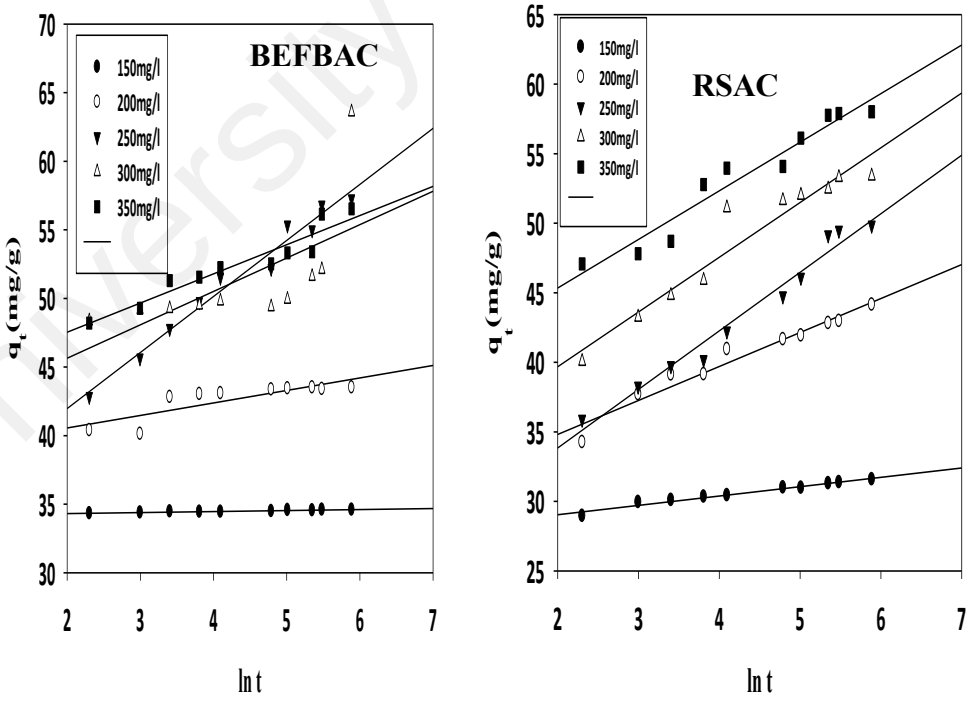

Figure 5.18: Linearized plots of Elovich Equation model for Zn(II) adsorption on BEFBAC and RSAC at 30ºC.

Table 5.5: Elovich equation constants, correlation coefficients and normalized standard deviation values for adsorption of Pb (II) on BEFBAC and RSAC at 30°C

Adsorbent	Initial Concentration C_o (mg/L)	Removal (%)	Uptake capacity q_eExp (mg/g)	Theoretical uptake capacity q_e Cal (mg/g)	(1/b)lnab (mg/g)	1/b (mg/g)	R^2	Δqt (%)
BEFBAC	150	98.87	37.04	34.96	34.40	0.51	0.850	5.61
	200	96.20	48.08	46.97	45.49	0.51	0.966	2.29
	250	94.88	59.30	57.17	55.41	0.37	0.029	3.59
	300	87.47	65.53	60.90	55.78	0.06	0.883	7.07
	350	82.86	72.43	70.10	23.03	9.58	0.894	3.21
RSAC	150	93.20	34.86	33.41	33.27	0.29	0.635	3.87
	200	89.60	44.78	40.58	35.68	1.74	0.753	9.37
	250	84.96	52.99	50.38	38.24	2.65	0.941	4.53
	300	86.27	64.60	60.17	33.32	5.82	0.906	6.86
	350	86.71	75.72	80.07	2.18	14.03	0.833	5.43

Table 5.6: Intra-particle diffusion model constants and correlation Coefficients for adsorption of Pb (II) on BEFBAC and RSAC at 30°C

Adsorbent	Initial Concentration (mg/L)	Removal (%)	Reaction rate constant Kp1	Layer effect C1	R^2
BEFBAC	150	98.87	0.10	35.59	0.674
	200	96.2	0.11	46.54	0.964
	250	94.88	0.06	56.37	0.690
	300	87.47	0.47	60.03	0.899
	350	82.86	1.95	44.89	0.739
RSAC	150	93.2	0.05	33.95	0.468
	200	89.6	0.33	39.84	0.557
	250	84.96	0.60	43.65	0.979
	300	86.27	1.20	46.48	0.766
	350	86.71	2.78	34.96	0.653

Table 5.7: Elovich equation constants, correlation coefficients and normalized standard deviation values for adsorption of Zn (II) on BEFBAC and RSAC at 30°C

Adsorbent	Initial Concentr C_o (mg/L)	Removal (%)	Uptake capacity q_eExp (mg/g)	Theoretical uptake capacity q_e Cal (mg/g)	(1/b) lnab (mg/g)	1b (mg/g)	R^2	Δqt (%)
BEFBAC	150	92.33	34.57	33.95	34.17	0.70	0.915	1.44
	200	87.05	43.44	34.10	38.72	0.92	0.695	5.39
	250	88.72	55.34	50.24	33.80	4.09	0.976	9.21
	300	66.70	49.93	45.41	40.77	2.44	0.413	9.04
	350	61.03	53.32	50.47	43.29	2.13	0.909	5.34
RSAC	150	82.67	30.97	31.49	24.70	0.67	0.969	1.65
	200	84	41.92	40.41	29.92	2.44	0.950	3.60
	250	70.64	44.11	40.24	22.51	4.17	0.967	8.77
	300	69.43	52.00	50.24	30.95	4.16	0.886	3.38
	350	64.26	56.11	50.28	36.65	3.55	0.803	10.39

Table 5.8: **Intra-particle diffusion model constants and correlation Coefficients for adsorption of Zn (II) on BEFBAC and RSAC at 30°C.**

Adsorbent	Initial Concentration (mg/L)	Removal (%)	Reaction rate constant Kp1	Layer effect C1	R^2
BEFBAC	150	98.87	0.10	35.59	0.674
	200	96.2	0.11	46.54	0.964
	250	94.88	0.06	56.37	0.690
	300	87.47	0.47	60.03	0.899
	350	82.86	1.95	44.89	0.739
RSAC	150	82.67	0.14	29.17	0.875
	200	84	0.51	35.33	0.841
	250	70.64	0.92	31.30	0.943
	300	69.43	0.90	39.94	0.823
	350	64.26	0.83	43.67	0.878

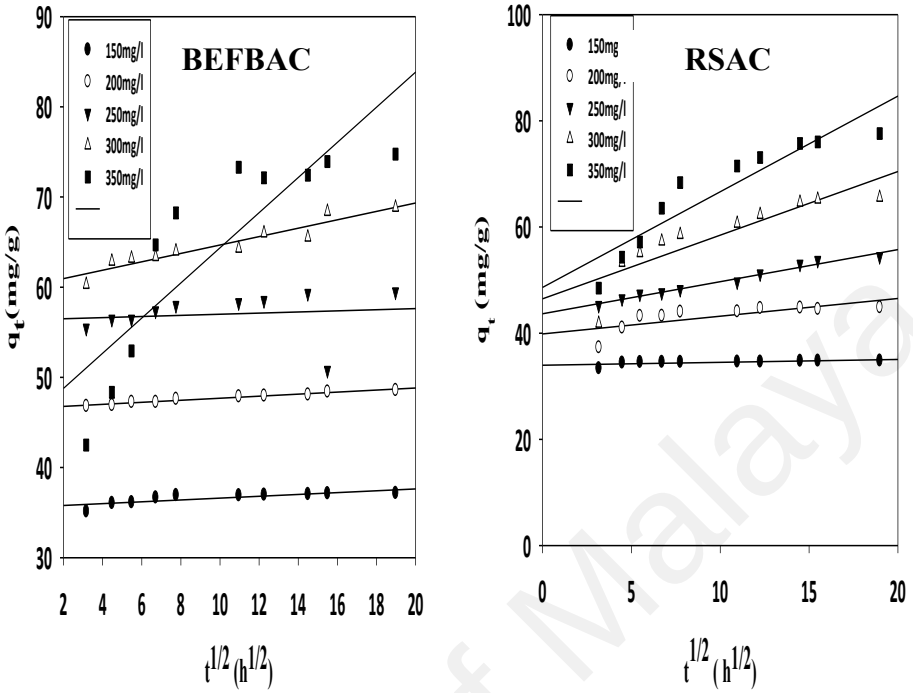

Figure 5.19: Plots of Intraparticle Diffusion model for Pb (II) adsorption on BEFBAC and RSAC at 30ºC

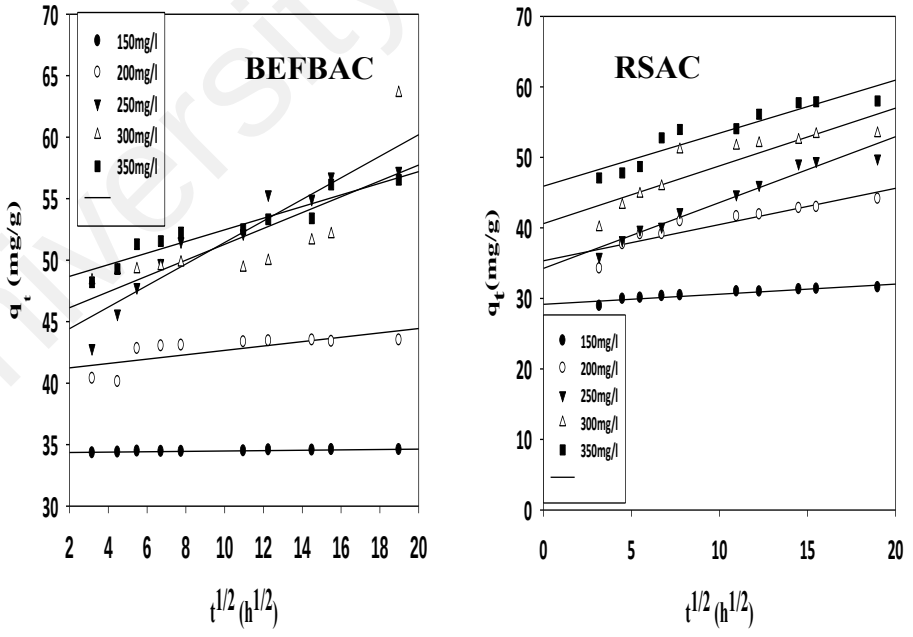

Figure 5.20: Plots of Intraparticle Diffusion model for Zn (II) adsorption on BEFBAC and RSAC at 30ºC

5.4 Adsorption Thermodynamic Study

In the thermodynamic study, parameters such as the enthalpy change (ΔH^o), entropy change (ΔS^o) and change in Gibbs free energy (ΔG^o) were evaluated. The parameters are related to the coefficient of distribution of the solute between the adsorbent (solid phase) and the adsorbate (liquid phase) during the process of adsorption. The thermodynamic parameters were obtained from the plots of ln K_L versus 1/T where K_L is the Langmuir constant obtained at temperatures 303K, 333K and 353K and T is the absolute temperature in Kelvin. By applying the following equation, the thermodynamic values were obtained:

$$\ln K = \frac{\Delta S}{R} - \frac{\Delta H}{RT} \quad 5.8$$

where $\frac{\Delta S}{R}$ = intercept of the curve.

Therefore, ΔS = R x Intercept

$\frac{\Delta H}{R}$ = Slope of the curve

$$\Delta H = R \times \text{Slope} \quad 5.9$$

R = 8.314 (gas constant).

After subjecting the experimental data to thermodynamic evaluation, the results obtained showed that standard enthalpy change (ΔH^o) and the standard entropy change (ΔS^o) values obtained for BEFBAC and RSAC were 0.1106 KJmol^{-1} and 0.3459 KJmol^{-1}: 0.1297 KJmol^{-1} and 0.5738 KJmol^{-1} for lead; and 0.1347 KJmol^{-1} and 0.7092 KJmol^{-1} ; 0.123 KJmol^{-1} and 2.7644 KJmol^{-1} for zinc respectively. These positive values indicate the endothermic nature of the adsorption process. This is an indication that the

heat generated during the adsorption process is absorbed within the system as it involves breaking of bonds between molecules during the process of adsorption thereby leading to absorption of heat from the sorroundings (Zhao et al., 2008). Moreover, the adsorption of lead and zinc increases with increase in temperature.

The positive values of entropy change (ΔS^o) is an indication of the good affinity of the metal ions towards the adsorbent and the increasing randomness at the solid-solution interface during the adsorption process. The negative values obtained for standard free energy is an indication that the process of adsorption is spontaneous (Cui, Jang, Cho, & Khim, 2010).

5.5 Desorption Study

Regeneration of spent activated carbon can be achieved by using either thermal or chemical regeneration technique. The use of thermal regeneration usually requires high energy which will equally lead to loss of adsorbent (M. M. Rao, Ramesh, Rao, & Seshaiah, 2006). In this study, chemical regeneration method was adopted using 1M each of acetic acid, hydrochloric acid, sulphuric acid, nitric acid and deionized water. This was done to determine the suitability of the solutions for the regeneration of the spent activated carbons. The result as shown in tables 5.11 and 5.12 above indicated that nitric acid has the highest recovery efficiency for both lead and zinc, suggesting that 1M nitric acid is most suitable for the regeneration of both BEFBAC and RSAC used for adsorption of lead and zinc. The result also indicated that BEFBAC with Pb(II) was more recovered than with Zn(II) whereas it was the opposite in case of RSAC.

Table 5.9: Thermodynamic Parameters of Pb (II) adsorption onto BEFBAC and RSAC.

	Temp. (K)	ΔG^o $KJmol^{-1}$	ΔH^o $KJmol^{-1}$	ΔS^o $kJmol^{-1}$	R^2
BEFBAC	303	-6.497			
	333	-4.433	0.1347	0.7092	0.999
	353	-4.355			
RSAC	303	-8.996			
	333	-8.357	0.123	2.7644	0.999
	353	-9.302			

Table 5.10: Thermodynamic Parameters of Zn (II) adsorption onto BEFBAC and RSAC.

	Temp. (K)	ΔG^o $Kjmol^{-1}$	ΔH^o $Kjmol^{-1}$	ΔS^o $Kjmol^{-1}$	R^2
BEFBAC	303	-3.029			
	333	-3.062	0.1106	0.3459	0.997
	353	-3.316			
RSAC	303	-7.963			
	333	-3.696	0.1297	0.5138	0.997
	353	-3.771			

Table 5.11: Regeneration of BEFBAC and RSAC for Pb (II)

Adsorbent	Removal Efficiency %	Recovery Efficiency (%)				
		1M CH_3COOH	1M HCl	1M H_2SO_4	1M HNO_3	Deionized water
BEFBAC	61.03	32.97	53.20	55.53	62.12	48.50
RSAC	64.26	24.09	69.98	39.89	92.88	25.88

Table 5.12: Regeneration of BEFBAC and RSAC for Zn(II)

Adsorbent	Removal Efficiency %	Recovery Efficiency (%)				
		1M CH_3COOH	1M HCl	1M H_2SO_4	1M HNO_3	Deionized water
BEFBAC	82.86	38.52	64.80	40.65	68.1	35.50
RSAC	86.71	21.33	64.77	32.54	86.87	15.89

CHAPTER 6: BINARY ADSORPTION STUDY

In the following chapter, the results obtained from adsorption onto granular activated carbon prepared from longan fruit shell (LFS) of Pb(II) and Zn(II) cations both in a single solute and binary systems are presented. It is made up of two main sections. While section one presents the results of batch adsorption in single solute system, section two discusses the result of adsorption in binary system.

6.1 Adsorption Study in single solute system

6.1.1 Effect of Contact Time and Initial Concentration of Adsorbate

To carry out the batch equilibrium adsorption study, 50mls of the adsorbate [(Pb(II) and Zn(II)] solutions of varying initial concentrations of between 150 to 350 mg/L having equivalent mass of 0.2g of the adsorbent (LFSAC) were used. Figure 6.1 below demonstrates the equilibrium uptake of Pb(II) and Zn(II) cations versus contact time (min) at various initial concentrations of 150 – 350 mg/L onto LFSAC.

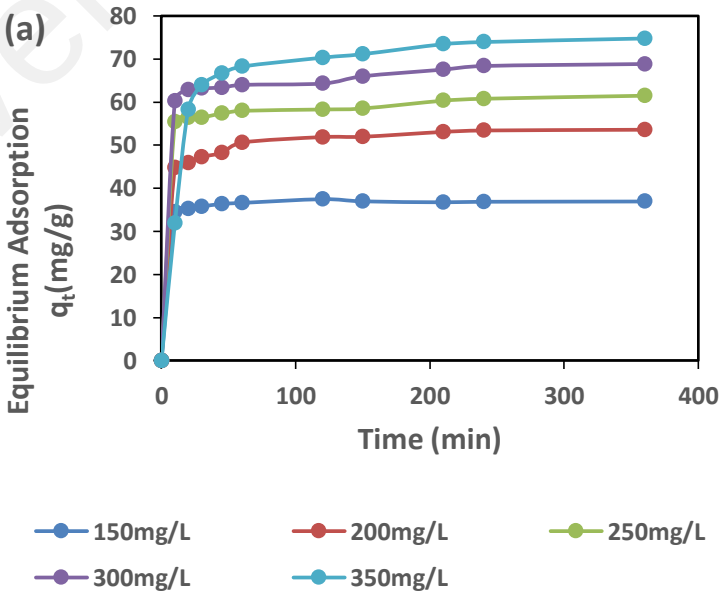

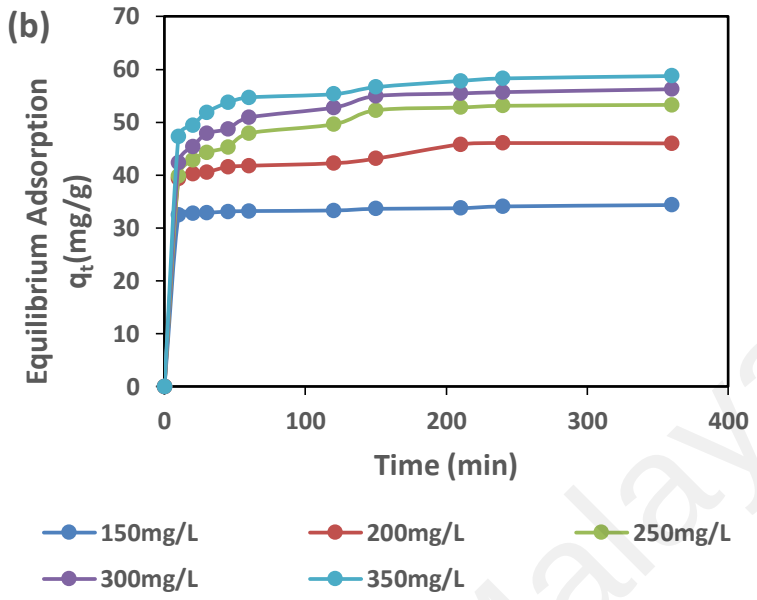

Figure 6.1: **Adsorption of (a) Pb (II) and (b) Zn (II) versus adsorption time at various initial concentrations at 30°C on LFSAC respectively.**

The influence which the contact time exerted on the sorption process at equilibrium for the adsorbent (LFSAC) is as presented in figure 6.1. From the figure, it could be seen that the sorption level of the adsorbent increased with initial increase in sorption time up to 220 min but remained relatively constant afterwards. The above trend suggested that at about a little above three and half hours, all the active sites must have been saturated with the adsorbate (Pb (II) and Zn (II) ions as the case may be). A similar trend has been observed by (Khezami et al., 2012) and (Z. Z. Chowdhury, Zain, Khan, Rafique, *et al*., 2012). The point of the observed saturation corresponds to the maximum sorption limit of the adsorbent.

6.1.2 Adsorption Isotherm

The adsorption isotherm provides an insight into the distribution pattern of the adsorbate species between the adsorbate phase and the adsorbent phase over the surface of the adsorbent at equilibrium position. To be able to do this perfectly, the experimental data obtained are fitted to different types of isotherm models, so as to be able to determine which correlation will be most appropriate for the isotherm curves (Z. Chowdhury, Zain, & Rashid, 2011) (Z Chowdhury et al., 2011). In this study, the isotherm experiment for the adsorption process was done by using three isotherm models namely Langmuir, Freundlich and Temkin isotherm models.

From the Table 6.1 below, it could be observed that the equilibrium data fitted satisfactorily into Langmuir isotherm model than the Freundlich and Temkin models. The separation factor R_L obtained from Langmuir equation and 1/n values obtained from the Freundlich model both fell below the value of one, an indication that the two cations were duly and favourably adsorbed by LFSAC.

6.1.3 Adsorption Kinetics

In table 6.2 below, the experimental and calculated values are presented. Equally, the coefficients of correlation (R^2) are presented for both the first order and second order kinetics and tabulated in the table. As can be observed from the table 6.2, there exists a wide gap between the values obtained experimentally and the values obtained by calculation, thereby leading to a very high values of Δq_t (>90%) for all the initial concentrations for the two cations in the case of first order kinetic model. However, as could be observed for the second order kinetic model values, the experimental values

and the calculated values are very close for all the initial concentrations for the two cations. This has led to low values of $\Delta q_t\%$. The implication of this is that the experimental values obtained for both cations satisfactorily fit into pseudo second order kinetic model. This implication is further supported by the correlation coefficient, R^2 values obtained for pseudo second order kinetics model which are very close to value of one for all the initial concentrations, since the closer the value of R^2 to unity (one), the more the adsorption process satisfactorilyfits into the model (Z. Z. Chowdhury, Zain, Khan, Rafique, et al., 2012).

The Elovich equation, presented in table 6.3 above is a model that is frequently used for describing chemisorption process and usually expressed by equation below (Z. Z. Chowdhury, Zain, Khan, Rafique, et al., 2012).

$$h_2 = k_2 q_e^2 \qquad 6.1$$

while the value (1/b) indicates the number of sites that are available for sorption, the value of (1/b)ln (ab) on the other hand signifies the adsorption quantity when ln t value equals zero. These values are summarized in table 6.3 below. In the table, the values of experimental uptake capacity are close to the theoretical uptake capacity, thereby leading to low values of $\Delta q_t\%$ ranging from 3.40 – 11.17 for all the initial concentrations, an indication that chemisorption has taken place in adsorption process for both Pb(II) and Zn(II) cations. To study the mechanism of adsorption, the experimental data obtained were subjected to intra particle diffusion model analysis. This model had earlier been expressed by equation 6.2 (Z Chowdhury et al., 2011).

$$\Delta q\ (\%) = 100\sqrt{\frac{\sum[(q_{t,exp} - q_{t\,cal})/q_{t,exp}]^2}{(N-1)}} \qquad 6.2$$

The intra particle diffusion model constants (K and C) together with the correlation constants for the two cations are presented in table 6.4 below. From the table, it is evident that the values of intra particle diffusion constant C increased as the initial concentration increased for both metals. This is an expected phenomenon in view of greater driving force of the adsorbates at higher concentrations (Z. Z. Chowdhury et al., 2013).

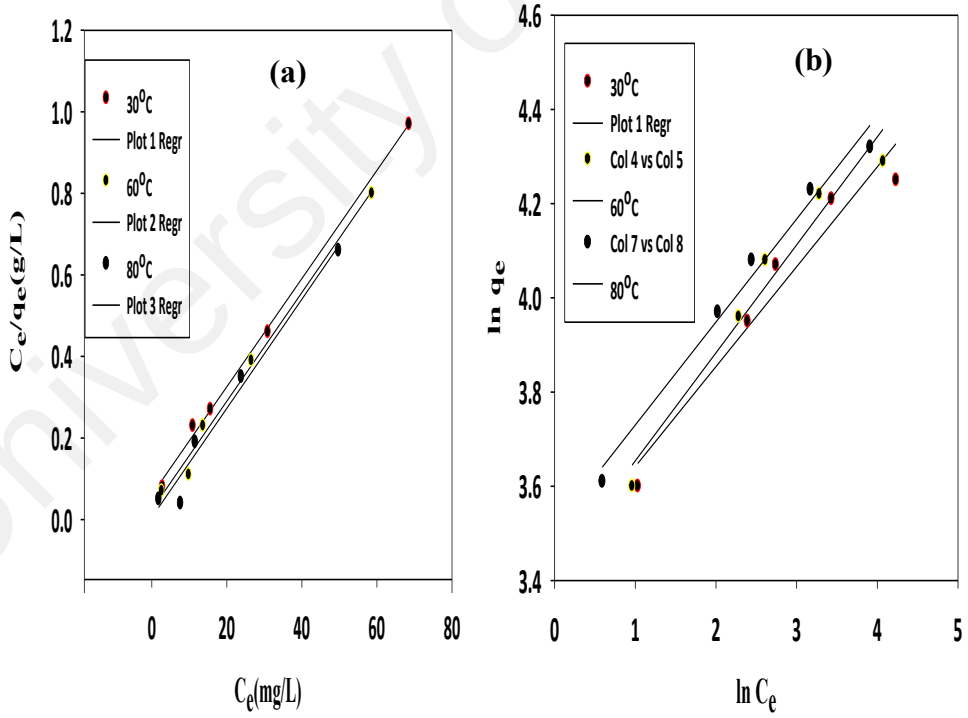

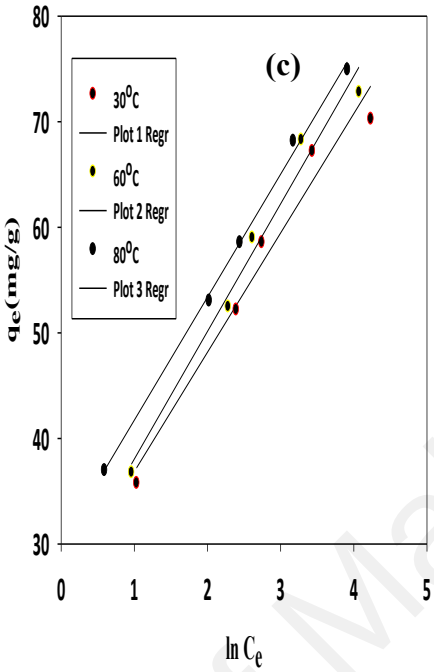

Figure 6.2: Plots of (a) Langmuir (b) Freundlich and (c) Temkin Isotherms for Pb(II) adsorption on LFSAC at 30, 60 and 80°C.

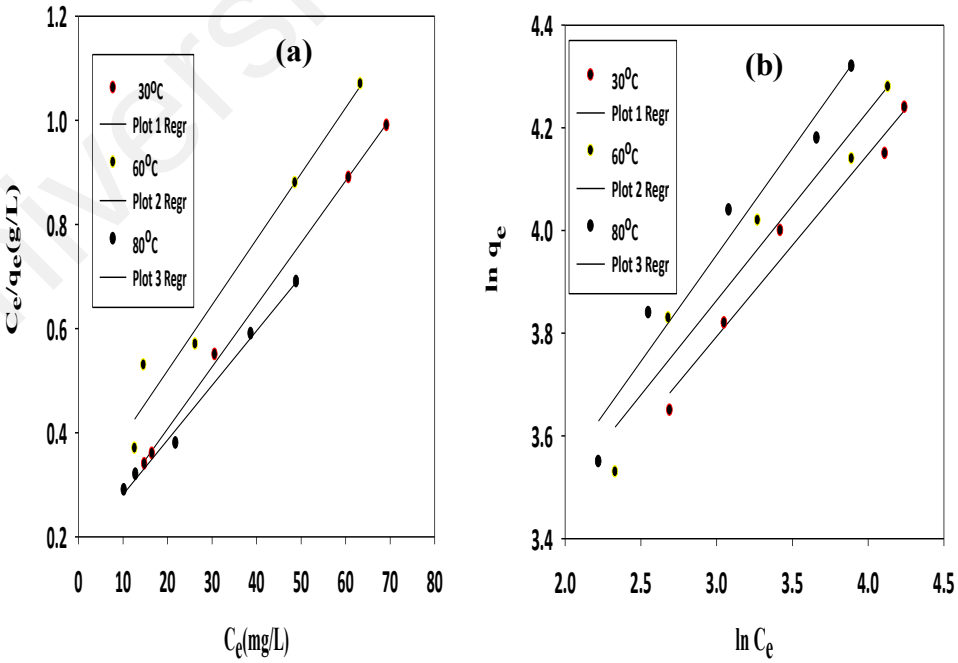

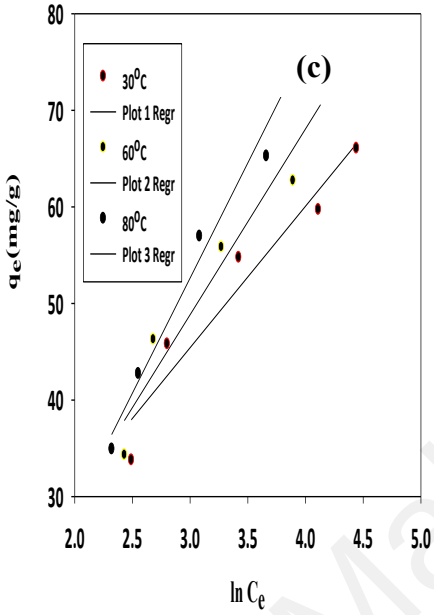

Figure 6.3: Plots of (a) Langmuir (b) Freundlich and (c) Temkin Isotherms for Zn(II) adsorption on LFSAC at 30, 60 and 80°C.

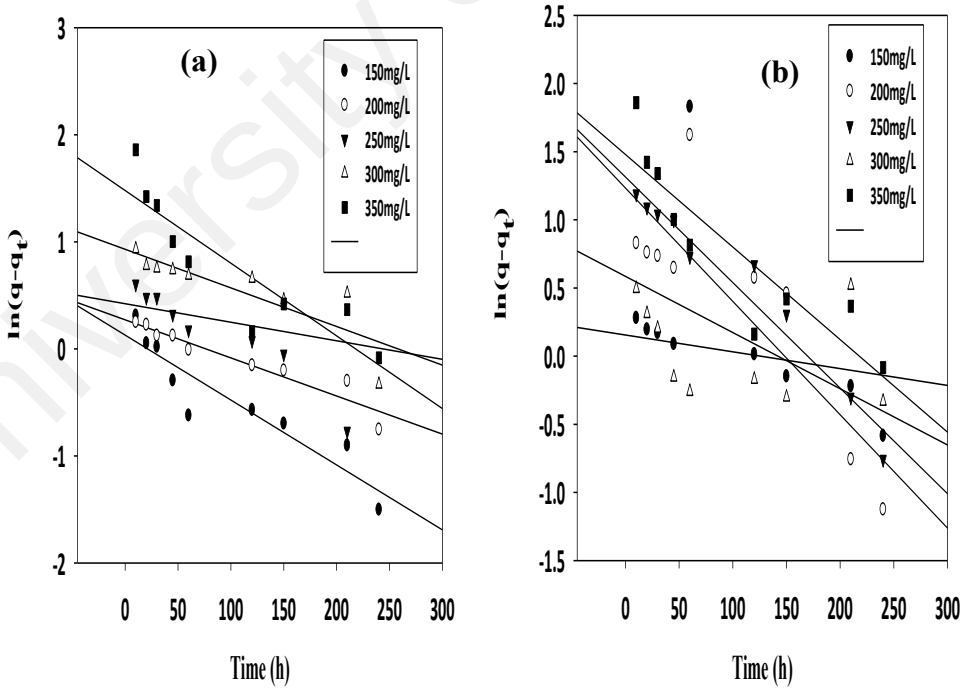

Figure 6.4: Linearized plots of pseudo-first-order kinetic model for (a) Pb(II) and (b) Zn(II) adsorption on LFSAC at 30°C.

Table 6.1: Langmuir, Freundlich and Temkin isotherm model parameters and correlation coefficients for adsorption of Pb (II) and Zn (II) on LFSAC at 30°C for Single Solute Adsorption

Pollutant	Isotherm									
	Langmuir Isotherm				Freundlich Isotherm			Temkin Isotherm		
	Maximum monolayer adsorption capacity q_{max} (mg/g)	Langmuir constant K_L (L/mg)	Correlation coefficient R^2	Separation factor R_L(mg/g) $(L/mg)^{(1/n)}$	Affinity factor K_F	Freundlich exponent 1/n	Correlation coefficient R^2	Binding constant K_T (L/mg)	Temkin constant B	Correlation coefficient R^2
Pb(II)	74.63	0.23	0.997	0.012	29.86	0.22	0.937	8.83	11.33	0.940
Zn(II)	50.25	0.34	0.987	0.008	33.01	0.09	0.251	11.19	13.61	0.231

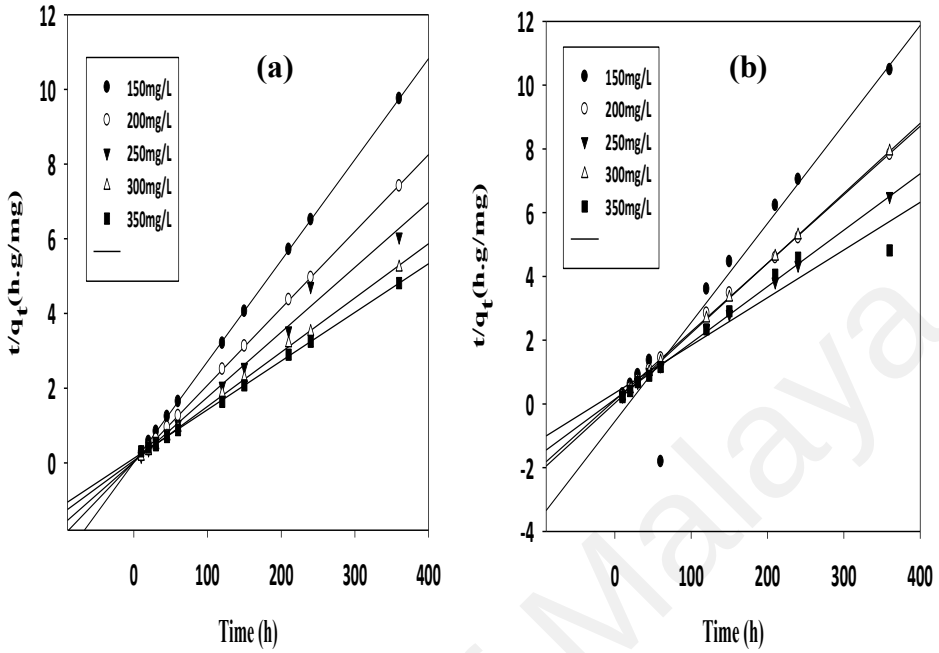

Figure 6.5: Linearized plots of pseud-second-order kinetic model for(a) Pb(II) and (b) Zn(II) adsorption on LFSAC at 30ºC.

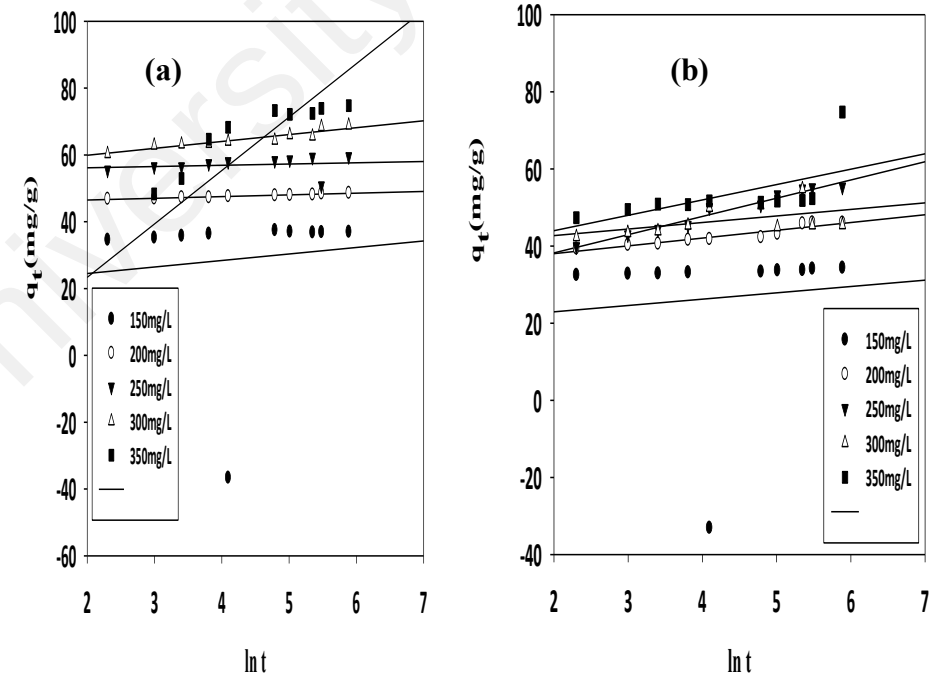

Figure 6.6: Linearized plots of Elovich Equation model for(a) Pb(II) and (b) Zn(II) adsorption on LFSAC at 30 ºC

Table 6.2: Pseudo-first-order and pseudo-second-order model constants, correlation coefficients and normalized standard deviation values for Adsorption of Pb(II) and Zn(II) on LFSAC at 30ºC

Adsorbate	Pseudo-First-Order						Pseudo-Second-Order				
	Initial concentration C_o (mg/L)	Uptake capacity q_e,exp (mg/g)	Theoretical uptake capacity q_e,cal (mg/g)	1st order rate constant K_1	Correlation coefficient R^2	Δq_t (%)	Uptake capacity q_e,exp (mg/g)	Theoretical uptake capacity q_e,cal (mg/g)	2nd order rate constant K_2(g/mg h)	Correlation coefficient R^2	Δq_t (%)
Pb(II)	150	36.76	1.14	0.014	0.865	96.91	36.76	37.17	0.046	1	1.11
	200	47.25	1.31	0.008	0.912	97.23	47.25	48.54	0.018	1	2.66
	250	58.60	1.53	0.004	0.094	97.40	58.60	57.47	0.018	0.989	1.93
	300	67.21	2.54	0.008	0.704	96.23	67.21	68.97	0.003	0.999	2.55
	350	70.30	4.38	0.016	0.803	93.76	70.30	72.46	0.002	0.9995	2.98
Zn(II)	150	33.75	1.79	0.009	0.275	94.68	33.75	32.15	0.002	0.911	4.73
	200	45.78	3.43	0.019	0.714	92.51	45.78	49.26	0.017	0.876	7.06
	250	54.74	3.72	0.018	0.953	93.21	54.74	56.50	0.002	0.999	3.11
	300	45.41	1.17	0.003	0.092	97.43	45.41	45.66	0.019	1	0.55
	350	51.	4.38	0.016	0.803	91.54	51.80	66.67	0.0007	0.934	22.30

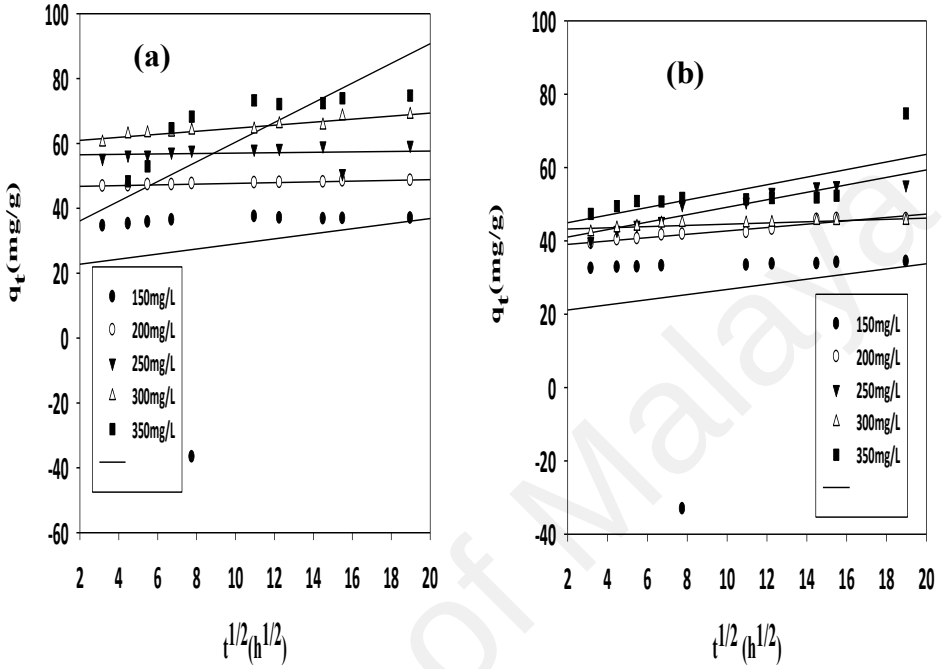

Figure 6.7: Plots of Intraparticle Diffusion model for(a) Pb(II) and (b) Zn(II) adsorption on LFSAC at 30 ºC

6.1.4 Adsorption Thermodynamic Study

The table 6.5 below shows the thermodynamic parameters of adsorption of Pb(II) and Zn(II) onto LFSAC. The results showed that ΔS^o were o.6805 $KJmol^{-1}$ and 0.7554 $KJmol^{-1}$ for Pb(II) and Zn(II) respectively, positive values, indicating that the adsorption process is endothermic. However, the negative values obtained for ΔG^o is an indication that the process is highly spontaneous (Cui et al., 2010).

Table 6.3: Elovich equation constants, correlation coefficients and normalizedstandard deviation values for adsorption of Pb(II) and Zn (II) on LFSAC at 30 ºC

Pollutant	Initial Concentration C_o (mg/L)	Removal (%)	Uptake capacity q_{eExp} (mg/g)	Theoretical uptake capacity q_{eCal} (mg/g)	(1/b) lnab (mg/g)	1/b (mg/g)	Δqt (%)
Pb(II)	150	98.13	36.76	35.51	20.63	1.95	3.40
	200	94.55	47.25	41.97	45.49	0.51	11.17
	250	93.76	58.60	52.71	55.41	0.37	10.04
	300	89.70	67.21	70.48	55.78	0.06	4.65
	350	80.43	70.30	65.06	8.61	15.99	7.46
Zn(II)	150	90.13	33.75	30.61	19.66	1.64	9.30
	200	91.75	45.78	41.60	35.65	0.62	9.13
	250	87.76	54.74	50.21	28.76	4.73	8.27
	300	60.67	45.41	40.59	39.30	1.70	10.61
	350	59.29	51.80	50.25	36.03	3.98	2.98

Table 6.4: Intra-particle diffusion model constants and correlation Coefficients for adsorption of Pb(II) and Zn(II) on LFSAC at 30 ºC.

Pollutant	Initial Concentration (mg/L)	Removal (%)	Reaction rate constant Kp1	Layer effect C1	Correlation coefficient R^2
Pb(II)	150	98.87	0.78	21.21	0.032
	200	96.20	0.11	46.54	0.964
	250	94.88	0.06	56.37	0.690
	300	87.47	0.47	60.03	0.899
	350	82.86	3.04	65.05	0.516
Zn(II)	150	90.13	0.70	19.74	0.309
	200	91.75	0.11	32.45	0.621
	250	87.76	0.02	38.98	0.898
	300	60.67	0.16	42.89	0.715
	350	59.29	1.04	45.85	0.504

Table 6.5: Thermodynamic Parameters of Pb(II) and Zn (II) adsorption onto LFSAC.

Pollutant	Temp. (k)	ΔG^o $KJmol^{-1}$	ΔH^o $KJmol^{-1}$	ΔS^o $kJmol^{-1}$	R^2
Pb(II)	303	-5.623			
	333	-5.895	0.1264	0.6805	0.996
	353	-6.266			
Zn(II)	303	-8.963			
	333	-9.157	0.1375	0.7554	0.997
	353	-9.685			

6.1.5 Binary Adsorption Study

It is always a very difficult task to describe heavy metals adsorption from waste waters containing more than one heavy metal at a time. Such occurrence usually leads to interference and adsorption competition between the components for available sorption sites (Abdullah, Jamari, & Choong, 2010). The adsorption of Pb(II) and Zn(II) ions simultaneously from binary solute system was investigated. Figures 6.8 and 6.9 below represent the non-linear adsorption isotherms of Pb(II) and Zn(II) with increasing concentrations of Zn(II) and Pb(II) ions respectively (150mg/l – 350mg/l) while figure 6.10 shows the Langmuir non-linear isotherms of Pb(II) and Zn(II) in both the single solute system and binary solute system. It could be observed from figure 6.10 that the adsorption of Pb(II) ion was interfered by the presence of Zn(II) cation and vice-versa. Moreover, Table 6.6 presents the adsorption isotherms parameters for binary adsorption system. The effect exerted by competing ions in a binary system could be described by the ratio of the maximum adsorption capacity in equilibrium in the binary system to the maximum adsorption capacity in equilibrium in a single solute system, that is, the ratio of q_{max} (binary) to q_{max} (single) (D Mohan & Chander, 2001). This relationship can be represented by the following equations and deductions made there from:

$$\frac{q_{max}\ (\text{binary})}{q_{max}(\text{single})} > 1\ (\text{there is positive interference} - \text{synergestic effect}) \quad 6.3$$

$$\frac{q_{max}(\text{binary})}{q_{max}(\text{single})} = 1\ (\text{no observable interference}) \quad 6.4$$

$$\frac{q_{max}(\text{binary})}{q_{max}(\text{single})} < 1\ (\text{there is negative interference} - \text{antagonistic effect}) \quad 6.5$$

From tables 6.1 above and 6.6 below, the above ratio gives 0.45 and 0.58 for Pb(II) and Zn(II) respectively. This is an indication that the presence of one particular ion significantly suppressed the adsorption of the other in the binary system since the values are less than one in both cases.

Furthermore, appendix E shows the individual adsorption capacity (%) and the competitive adsorption capacity for Pb(II) and Zn(II) cations onto the adsorbent at 30ºC at varying initial concentrations (150 – 350mg/L). From the table, it could be observed that the equilibrium uptake of Zn(II) ions decreases with increase in the initial concentration of Pb(II) ions while the adsorption of the cations from the binary mixture was usually lower than that for the single component system. For instance, the maximum adsorption capacity obtained for Pb(II) and Zn(II) cations at the equilibrium conditions are 75.49% and 59.2% respectively, whereas they are 62.77% and 41.86% for the same cations respectively in the binary mixture system containing the highest concentrations (350mg/L each of the cations) at equilibrium adsorption conditions. This clearly indicates that there was strong competitive adsorption of these divalent metals on the surface of the adsorbent (LFSAC). This is in agreement with what was obtained for the bisorption of binary mixture of heavy metals by Medikago sativa (Al-Qahtani, 2012).

The result equally shows that the adsorption capacity of a primary metal usually decreases with increase in the concentration of the other metal present in the system. This is an indication that such adsorption competition is antagonistic innature (Al-Qahtani, 2012).

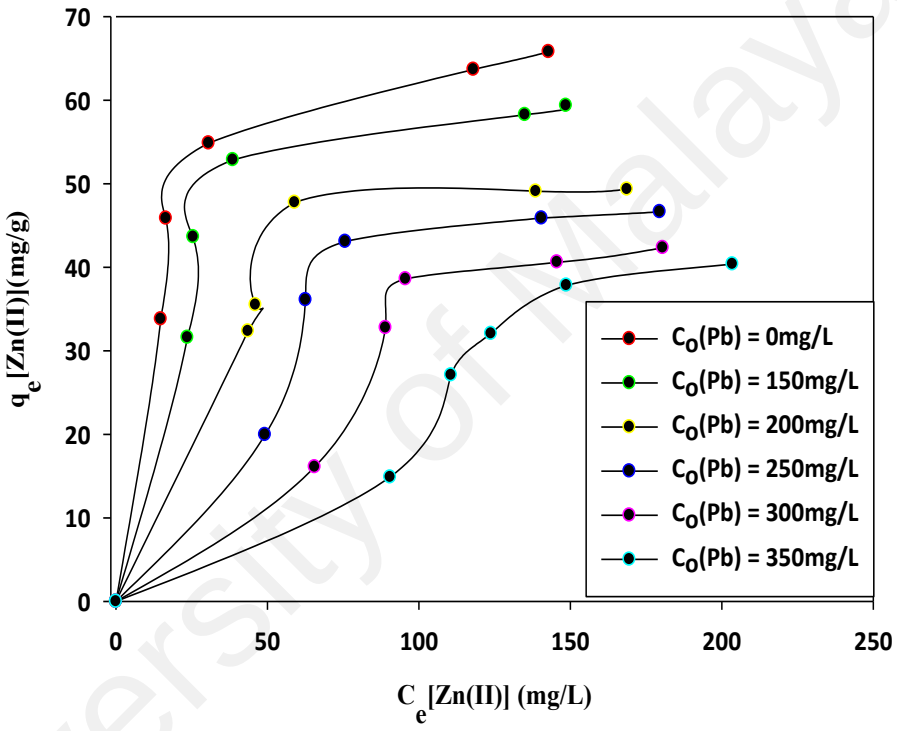

Figure 6.8: Comparison of non-linearized adsorption of Pb(II) ion in the presence of increasing concentration of Zn(II) ion, pH 5.5, T= 30ºC, t=210min, Co{Zn(II)} = 150-350mg/l, LFSAC dosage = 4g/L, Pb(II) = 350mg/L.

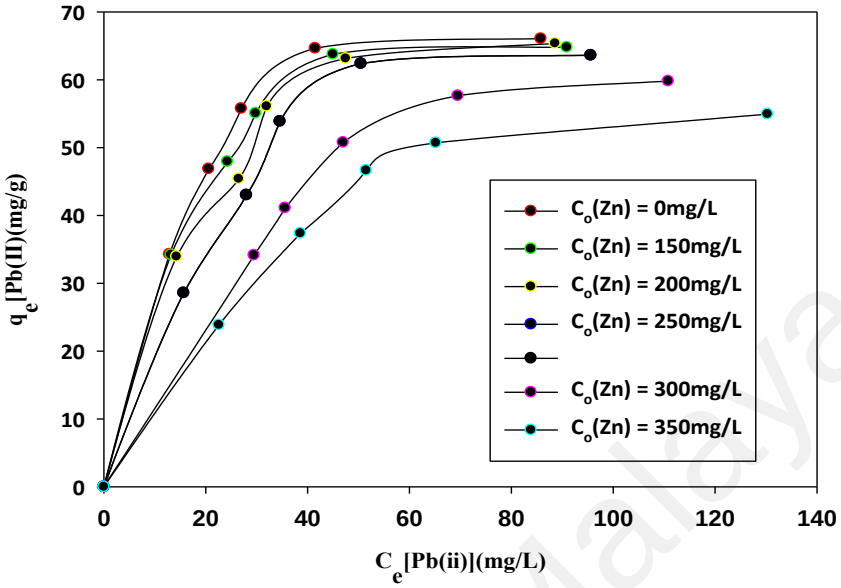

Figure 6.9: Comparison of non-linearized adsorption of Zn(II) ion in the presence of increasing concentration of Pb(II) ion, pH 5.5, T= 30°C, t=210min, Co{Pb(II)} = 150-350mg/l, LFSAC dosage = 4g/L, Zn(II) = 350mg/L.

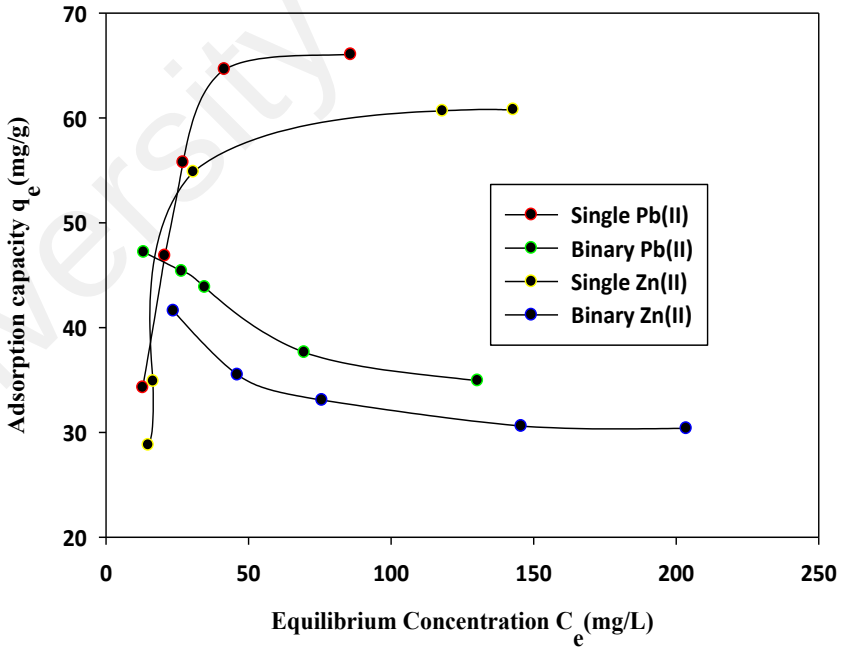

Figure 6.10: Langmuir non-linear isotherms of Pb(II) and Zn(II) adsorption in single solute and binary mixture systems at initial pH 5.5, T= 30°C, t=210min, Co{Pb(II) and Zn(II)} = 150-350mg/l, LFSAC dosage = 4g/L

Table 6.6: Langmuir, Freundlich and Temkin isotherm model parameters and correlation coefficients for adsorption of Pb (II) and Zn (II) on LFSAC at 30ºC for Binary System Adsorption

Pollutant	Isotherm									
	Langmuir Isotherm				Freundlich Isotherm			Temkin Isotherm		
	Maximum monolayer adsorption capacity q_{max}(mg/g)	Langmuir constant K_L(L/mg)	Correlation coefficient R^2	Separation factor R_L(mg/g) $(L/mg)^{(1/n)}$	Affinity factor K_F	Freundlich exponent 1/n	Correlation coefficient R^2	Binding constant K_T(L/mg)	Temkin constant B	Correlation coefficient R^2
Pb(II)	33.44	-.0.16	0.999	0.019	70.44	-0.14	0.95	10.88	-5.83	0.96
Zn(II)	29.15	-0.13	1	0.023	63.66	-0.15	0.94	11.02	-5.12	0.92

CHAPTER 7: CONCLUSIONS AND RECOMMENDATIONS

7.1 Conclusions

The preparation, adsorption kinetics, isotherms and thermodynamic studies of Pb (II) and Zn (II) cations onto activated carbons prepared from banana empty fruit bunch (BEFB) and rattan sawdust (RS) have been carried out. Based on the results obtained from the research, the following conclusions can be drawn.

- The work has shown that adsorbent prepared from these agricultural wastes could effectively be used for the adsorption of Pb (II) and Zn (II) ions from aqueous solutions (BEFBAC – 82.86% and 61.03% for Pb (II) and Zn (II) respectively; RSAC – 86.71% and 64.26% for Pb (II) and Zn (II) respectively).
- The two-step preparation technique (hydrothermal pre-treatment and chemical activation/carbonization) used greatly enhanced the solid carbon yield and the surface characteristics of the activated carbons thereby leading to improved adsorption capacity.
- The optimization of the preparation conditions of carbonization temperature, holding time and concentration of impregnating agent highly influenced the development of activated carbons with high yield and enhanced adsorption capacity.
- RSAC showed higher adsorption capacity for both Pb (II) and Zn (II) (86.71% and 64.26% respectively) than BEFBAC (82.86% and 61.03% respectively) at the optimum adsorption conditions (temp = 30oC, time = 210min and pH = 5.5) with Pb (II) ions being more adsorbed than Zn (II) ions by both adsorbents.

- While the mode of adsorption of the metal ions onto the adsorbent followed the pseudo-second-order kinetic model, the experimental data fitted satisfactorily into the Langmuir isotherm model than all of the other evaluated models. The experimental data equally fits satisfactorily into Elovich equation model thereby signifying that chemisorption has taken place in the adsorption processes.
- The thermodynamic study revealed a positive change in the standard enthalpy thereby suggesting the adsorption process for the metal ions is endothermic in nature. Moreover, the negative value obtained for the adsorption standard free energy supports the fact that the reaction is spontaneous and feasible under the investigated temperatures.

* The regeneration experiment carried out revealed that the spent activated carbons can be significantly recovered after use, using chemical regeneration method with 1M HNO3. BEFBAC with Pb (II) and with Zn (II) can be recovered up to 68.10% and 62.12% respectively while RSAC with Pb (II) and Zn (II) can be recovered up to 86.87% and 92.88% respectively. This indicated that the activated carbons can be used repeatedly without any fear of being lost during the process.

* The work further demonstrated the adsorption of Pb(II) and Zn(II) cations both in a single solute and binary mixture systems using granular activated carbon prepared from longan fruit shell (LFSAC). The result obtained showed that there was strong adsorption competition by the competing components (cations) to occupy the available sorption sites on the surface of the adsorbent, with the adsorption competition being antagonistic in nature.

7.2 Recommendations

Based on the outcome of this research, a few recommendations that will enhance future development on the study are hereby made;

- Since this study has confirmed the suitability and feasibility of using H_3PO_4 as an effective activating agent to enhance the adsorption capacity of the chosen precursors, further studies are required to use other activating agents to also evaluate their effectiveness on the precursors.
- This study involves the removal of Pb(II) and Zn(II) cations in a single solute and binary mixture systems respectively, further studies should be extended to other metal ions, such as Fe(II), Mn(II), Hg(II) and Cd(II) and even to include organic pollutants, as activated carbons require different modifications for different applications.
- Suggestion is hereby made to evaluate the actual adsorption performance in this study in removal of the metal ions [Pb(II) and Zn(II)] from actual industrial effluents as there could be interference from other pollutants that may be present in the effluents.
- Since many other biomass (agricultural wastes) which are both renewable and abundantly available at little or no cost both in Malaysia and Nigeria, it is hereby suggested to convert these wastes to activated carbon, a added-value product.

REFERENCES

Abdel-Halim, S., Shehata, A., & El-Shahat, M. (2003). Removal of lead ions from industrial waste water by different types of natural materials. *Water Research, 37*(7), 1678-1683.

Abdullah, L. C., Jamari, S. S., & Choong, T. S. Y. (2010). Modelling of Single and Binary Adsorptions of Heavy metals onto Activated carbon-Equilibrium studies. *Pertanika Journal of Science & Technology, 18*(1), 83-93.

Abioye, A. M., & Ani, F. N. (2015). Recent development in the production of activated carbon electrodes from agricultural waste biomass for supercapacitors: A review. *Renewable and Sustainable Energy Reviews, 52*, 1282-1293.

Acharya, J., Sahu, J., Sahoo, B., Mohanty, C., & Meikap, B. (2009). Removal of chromium (VI) from wastewater by activated carbon developed from Tamarind wood activated with zinc chloride. *Chemical Engineering Journal, 150*(1), 25-39.

Adeniyi, F., & Anetor, J. (1998). Lead-poisoning in two distant states of Nigeria: an indication of the real size of the problem. *African journal of medicine and medical sciences, 28*(1-2), 107-112.

Aharoni, C., & Tompkins, F. (1970). Kinetics of adsorption and desorption and the Elovich equation. *Advances in catalysis and related subjects, 21*, 1-49.

Ahluwalia, S. S., & Goyal, D. (2007). Microbial and plant derived biomass for removal of heavy metals from wastewater. *Bioresource Technology, 98*(12), 2243-2257.

Ahmad, A., Hameed, B., & Ahmad, A. (2008). Equilibrium And Kinetics Of Disperse Dye Adsorption On Activated Carbon Prepared From Rattan Sawdust By Chemical Activation.

Ahmad, A., Hameed, B., & Ahmad, A. (2009). Removal of disperse dye from aqueous solution using waste-derived activated carbon: Optimization study. *Journal of Hazardous Materials, 170*(2), 612-619.

Ahmad, F., Daud, W. M. A. W., Ahmad, M. A., & Radzi, R. (2013). The effects of acid leaching on porosity and surface functional groups of cocoa (Theobroma cacao)-shell based activated carbon. *Chemical Engineering Research and Design, 91*(6), 1028-1038.

Ahmadpour, A., & Do, D. (1997). The preparation of activated carbon from macadamia nutshell by chemical activation. *carbon, 35*(12), 1723-1732.

Al-Khaldi, F. A., Abusharkh, B., Khaled, M., Atieh, M. A., Nasser, M., Saleh, T. A., . . . Gupta, V. K. (2015). Adsorptive removal of cadmium (II) ions from liquid phase using acid modified carbon-based adsorbents. *Journal of Molecular Liquids, 204*, 255-263.

Al-Qahtani, K. M. (2012). Biosorption of Binary Mixtures of Heavy Metals by Medicago Sativa. *World Applied Sciences Journal, 16*(3), 465-473.

Alaba, P. A., Sani, Y. M., & Daud, W. M. A. W. (2015). Kaolinite properties and advances for solid acid and basic catalyst synthesis. *RSC Advances, 5*(122), 101127-101147.

Alcaniz-Monge, J., De La Casa-Lillo, M., Cazorla-Amorós, D., & Linares-Solano, A. (1997). Methane storage in activated carbon fibres. *carbon, 35*(2), 291-297.

AlOthman, Z., Habila, M., & Ali, R. (2011). Preparation of activated carbon using the copyrolysis of agricultural and municipal solid wastes at a low carbonization temperature. *carbon, 20*, 21.

Alslaibi, T. M., Abustan, I., Ahmad, M. A., & Foul, A. A. (2013). A review: production of activated carbon from agricultural byproducts via conventional and microwave heating. *Journal of Chemical Technology and Biotechnology, 88*(7), 1183-1190.

Amaya, A., Medero, N., Tancredi, N., Silva, H., & Deiana, C. (2007). Activated carbon briquettes from biomass materials. *Bioresource Technology, 98*(8), 1635-1641.

Ampthill, B. (2010). Sapindaceous fruits: botany and horticulture. *Horticultural reviews, 16*, 143.

Amuda, O., Giwa, A., & Bello, I. (2007). Removal of heavy metal from industrial wastewater using modified activated coconut shell carbon. *Biochemical Engineering Journal, 36*(2), 174-181.

Amuda, O., & Ibrahim, A. (2006). Industrial wastewater treatment using natural material as adsorbent. *African Journal of Biotechnology, 5*(16).

An, H., Park, B., & Kim, D. (2001). Crab shell for the removal of heavy metals from aqueous solution. *Water research, 35*(15), 3551-3556.

Anderson, M. J., & Whitcomb, P. J. (2000). *Design of experiments*: Wiley Online Library.

Arami-Niya, A., Abnisa, F., Sahfeeyan, M. S., Daud, W. W., & Sahu, J. N. (2011). Optimization of synthesis and characterization of palm shell-based bio-char as a by-product of bio-oil production process. *BioResources, 7*(1), 0246-0264.

Aworn, A., Thiravetyan, P., & Nakbanpote, W. (2008). Preparation and characteristics of agricultural waste activated carbon by physical activation having micro-and mesopores. *Journal of Analytical and Applied Pyrolysis, 82*(2), 279-285.

Ayala, J., Blanco, F., Garcìa, P., Rodriguez, P., & Sancho, J. (1998). Asturian fly ash as a heavy metals removal material. *Fuel, 77*(11), 1147-1154.

Babel, S., & Kurniawan, T. A. (2003). Low-cost adsorbents for heavy metals uptake from contaminated water: a review. *Journal of Hazardous Materials, 97*(1), 219-243.

Babel, S., & Kurniawan, T. A. (2004). Cr (VI) removal from synthetic wastewater using coconut shell charcoal and commercial activated carbon modified with oxidizing agents and/or chitosan. *Chemosphere, 54*(7), 951-967.

Baccar, R., Bouzid, J., Feki, M., & Montiel, A. (2009). Preparation of activated carbon from Tunisian olive-waste cakes and its application for adsorption of heavy metal ions. *Journal of Hazardous Materials, 162*(2), 1522-1529.

Bansal, O. (1998). Heavy metal pollution of soils and plants due to sewage irrigation. *Indian Journal of Environmental Health, 40*(1), 51-57.

Bhattacharya, A., Mandal, S., & Das, S. (2006). Adsorption of Zn (II) from aqueous solution by using different adsorbents. *Chemical Engineering Journal, 123*(1), 43-51.

Bigham, J., Schwertmann, U., Traina, S., Winland, R., & Wolf, M. (1996). Schwertmannite and the chemical modeling of iron in acid sulfate waters. *Geochimica et Cosmochimica Acta, 60*(12), 2111-2121.

Bilgiç, C. (2005). Investigation of the factors affecting organic cation adsorption on some silicate minerals. *Journal of colloid and interface science, 281*(1), 33-38.

Biškup, B., & Subotić, B. (2005). Removal of heavy metal ions from solutions using zeolites. III. Influence of sodium ion concentration in the liquid phase on the kinetics of exchange processes between cadmium ions from solution and sodium ions from zeolite A. *Separation science and technology, 39*(4), 925-940.

Bouchelta, C., Medjram, M. S., Bertrand, O., & Bellat, J.-P. (2008). Preparation and characterization of activated carbon from date stones by physical activation with steam. *Journal of Analytical and Applied Pyrolysis, 82*(1), 70-77.

Brown, P., Jefcoat, I. A., Parrish, D., Gill, S., & Graham, E. (2000). Evaluation of the adsorptive capacity of peanut hull pellets for heavy metals in solution. *Advances in Environmental Research, 4*(1), 19-29.

Cao, Q., Xie, K.-C., Lv, Y.-K., & Bao, W.-R. (2006). Process effects on activated carbon with large specific surface area from corn cob. *Bioresource Technology, 97*(1), 110-115.

Cassini, A., Tessaro, I., Marczak, L., & Pertile, C. (2010). Ultrafiltration of wastewater from isolated soy protein production: a comparison of three UF membranes. *Journal of Cleaner Production, 18*(3), 260-265.

Castro-Muñiz, A., Suárez-García, F., Martínez-Alonso, A., & Tascón, J. M. (2011). Activated carbon fibers with a high content of surface functional groups by phosphoric acid activation of PPTA. *Journal of Colloid and Interface Science, 361*(1), 307-315.

Ceyhan, A. A., Şahin, Ö., Saka, C., & Yalçın, A. (2013). A novel thermal process for activated carbon production from the vetch biomass with air at low temperature by two-stage procedure. *Journal of Analytical and Applied Pyrolysis, 104*, 170-175.

Chary, N. S., Kamala, C., & Raj, D. S. S. (2008). Assessing risk of heavy metals from consuming food grown on sewage irrigated soils and food chain transfer. *Ecotoxicology and environmental safety, 69*(3), 513-524.

Chauhan, G., & Chauhan, U. Human health risk assessment of heavy metals via dietary intake of vegetables grown in wastewater irrigated area of Rewa, India.

Cheremisinoff, N. P. (2001). *Handbook of water and wastewater treatment technologies*: Butterworth-Heinemann.

Chigondo, F., Nyamunda, B., Sithole, S., & Gwatidzo, L. (2013). Removal of lead (II) and copper (II) ions from aqueous solution by baobab (Adononsia digitata) fruit shells biomass. *IOSRJ. Appl. Chem, 5*(1), 43-50.

Chowdhury, Z., Zain, S., Khan, R., Ahmad, A., Islam, M., & Arami-Niya, A. (2011). Application of central composite design for preparation of Kenaf fiber based activated carbon for adsorption of manganese (II) ion. *International Journal of Physical Sciences, 6*(31), 7191-7202.

Chowdhury, Z., Zain, S. M., & Rashid, A. (2011). Equilibrium isotherm modeling, kinetics and thermodynamics study for removal of lead from waste water. *Journal of Chemistry, 8*(1), 333-339.

Chowdhury, Z. Z., Hamid, S. B. A., Das, R., Hasan, M. R., Zain, S. M., Khalid, K., & Uddin, M. N. (2013). Preparation of carbonaceous adsorbents from lignocellulosic biomass and their use in removal of contaminants from aqueous solution. *BioResources, 8*(4), 6523-6555.

Chowdhury, Z. Z., Zain, S. M., Khan, R. A., Arami-Niya, A., & Khalid, K. (2012). Process variables optimization for preparation and characterization of novel adsorbent from lignocellulosic waste. *BioResources, 7*(3), 3732-3754.

Chowdhury, Z. Z., Zain, S. M., Khan, R. A., Rafique, R. F., & Khalid, K. (2012). Batch and fixed bed adsorption studies of lead (II) cations from aqueous solutions onto granular activated carbon derived from Mangostana garcinia shell. *BioResources, 7*(3), 2895-2915.

Choy, K. K., Porter, J. F., & McKay, G. (2000). Langmuir isotherm models applied to the multicomponent sorption of acid dyes from effluent onto activated carbon. *Journal of Chemical & Engineering Data, 45*(4), 575-584.

Chu, W. (1999). Lead metal removal by recycled alum sludge. *Water research, 33*(13), 3019-3025.

Chung, B., Song, C., Park, B., & Cho, J. (2011). Heavy metals in brown rice (Oryza sativa L.) and soil after long-term irrigation of wastewater discharged from domestic sewage treatment plants. *Pedosphere, 21*(5), 621-627.

Ciardelli, G., Corsi, L., & Marcucci, M. (2001). Membrane separation for wastewater reuse in the textile industry. *Resources, Conservation and Recycling, 31*(2), 189-197.

Cruz, G., Pirilä, M., Huuhtanen, M., Carrión, L., Alvarenga, E., & Keiski, R. (2012). Production of activated carbon from cocoa (Theobroma cacao) pod husk. *J Civil Environment Engg, 2*(109), 2.

Cui, M., Jang, M., Cho, S. H., & Khim, J. (2010). Kinetic and thermodynamic studies of the adsorption of heavy metals on to a new adsorbent: coal mine drainage sludge. *Environmental technology, 31*(11), 1203-1211.

Dahl, J., Liu, S., & Carlson, R. (2003). Isolation and structure of higher diamondoids, nanometer-sized diamond molecules. *science, 299*(5603), 96-99.

Demirbas, E., Kobya, M., Senturk, E., & Ozkan, T. (2004). Adsorption kinetics for the removal of chromium (VI) from aqueous solutions on the activated carbons prepared from agricultural wastes. *Water Sa, 30*(4), p. 533-539.

Deng, H., Li, G., Yang, H., Tang, J., & Tang, J. (2010). Preparation of activated carbons from cotton stalk by microwave assisted KOH and K 2 CO 3 activation. *Chemical Engineering Journal, 163*(3), 373-381.

Deng, H., Yang, L., Tao, G., & Dai, J. (2009). Preparation and characterization of activated carbon from cotton stalk by microwave assisted chemical activation—application in methylene blue adsorption from aqueous solution. *Journal of Hazardous Materials, 166*(2), 1514-1521.

Deng, H., Zhang, G., Xu, X., Tao, G., & Dai, J. (2010). Optimization of preparation of activated carbon from cotton stalk by microwave assisted phosphoric acid-chemical activation. *Journal of Hazardous Materials, 182*(1), 217-224.

Depci, T., Kul, A. R., & Önal, Y. (2012). Competitive adsorption of lead and zinc from aqueous solution on activated carbon prepared from Van apple pulp: study in single-and multi-solute systems. *Chemical Engineering Journal, 200*, 224-236.

Devkota, B., & Schmidt, G. (2000). Accumulation of heavy metals in food plants and grasshoppers from the Taigetos Mountains, Greece. *Agriculture, ecosystems & environment, 78*(1), 85-91.

Di Natale, F., Erto, A., Lancia, A., & Musmarra, D. (2011). Mercury adsorption on granular activated carbon in aqueous solutions containing nitrates and chlorides. *Journal of Hazardous Materials, 192*(3), 1842-1850.

Diniz, C. V., Doyle, F. M., & Ciminelli, V. S. (2002). Effect of pH on the adsorption of selected heavy metal ions from concentrated chloride solutions by the chelating resin Dowex M-4195. *Separation science and technology, 37*(14), 3169-3185.

Donati, C., Drikas, M., Hayes, R., & Newcombe, G. (1994). Microcystin-LR adsorption by powdered activated carbon. *Water Research, 28*(8), 1735-1742.

Dooyema, C. A., Neri, A., Lo, Y.-C., Durant, J., Dargan, P. I., Swarthout, T., . . . Sani-Gwarzo, N. (2011). Outbreak of fatal childhood lead poisoning related to artisanal gold mining in northwestern Nigeria, 2010. *Environ Health Perspect*.

Dorez, G., Ferry, L., Sonnier, R., Taguet, A., & Lopez-Cuesta, J.-M. (2014). Effect of cellulose, hemicellulose and lignin contents on pyrolysis and combustion of natural fibers. *Journal of Analytical and Applied Pyrolysis, 107*, 323-331.

Dransfield, J. (1992). Traditional uses of rattan. *A guide to the cultivation of rattan. Forest research institute: forest record*(35), 59-64.

Durán-Valle, C. J., Gómez-Corzo, M., Pastor-Villegas, J., & Gómez-Serrano, V. (2005). Study of cherry stones as raw material in preparation of carbonaceous adsorbents. *Journal of Analytical and Applied Pyrolysis, 73*(1), 59-67.

Egila, J., Dauda, B., Iyaka, Y., & Jimoh, T. (2011). Agricultural waste as a low cost adsorbent for heavy metal removal from wastewater. *Int. J. Phys. Sci, 6*(8), 2152-2157.

Ekmekyapar, F., Aslan, A., Bayhan, Y. K., & Cakici, A. (2006). Biosorption of copper (II) by nonliving lichen biomass of Cladonia rangiformis hoffm. *Journal of Hazardous Materials, 137*(1), 293-298.

El-Hendawy, A.-N. A. (2005). Surface and adsorptive properties of carbons prepared from biomass. *Applied surface science, 252*(2), 287-295.

El-Hendawy, A.-N. A., Alexander, A. J., Andrews, R. J., & Forrest, G. (2008). Effects of activation schemes on porous, surface and thermal properties of activated carbons prepared from cotton stalks. *Journal of Analytical and Applied Pyrolysis, 82*(2), 272-278.

El Nemr, A., Abdelwahab, O., El-Sikaily, A., & Khaled, A. (2009). Removal of direct blue-86 from aqueous solution by new activated carbon developed from orange peel. *Journal of Hazardous Materials, 161*(1), 102-110.

Elaigwu, S., Usman, L., Awolola, G., Adebayo, G., & Ajayi, R. (2010). Adsorption of Pb (II) from aqueous solution by activated carbon prepared from Cow Dung. *Environmental Research Journal, 4*(4), 257-260.

Elaigwu, S. E., Rocher, V., Kyriakou, G., & Greenway, G. M. (2014). Removal of Pb 2+ and Cd 2+ from aqueous solution using chars from pyrolysis and microwave-assisted hydrothermal carbonization of Prosopis africana shell. *Journal of Industrial and Engineering Chemistry, 20*(5), 3467-3473.

Elmouwahidi, A., Zapata-Benabithe, Z., Carrasco-Marín, F., & Moreno-Castilla, C. (2012). Activated carbons from KOH-activation of argan (Argania spinosa) seed shells as supercapacitor electrodes. *Bioresource technology, 111*, 185-190.

Erdem, M., Ucar, S., Karagöz, S., & Tay, T. (2013). Removal of lead (II) ions from aqueous solutions onto activated carbon derived from waste biomass. *The Scientific World Journal, 2013*.

Fan, T., Liu, Y., Feng, B., Zeng, G., Yang, C., Zhou, M., . . . Wang, X. (2008). Biosorption of cadmium (II), zinc (II) and lead (II) by Penicillium simplicissimum: Isotherms, kinetics and thermodynamics. *Journal of Hazardous Materials, 160*(2), 655-661.

Farma, R., Deraman, M., Awitdrus, A., Talib, I., Taer, E., Basri, N., . . . Hashmi, S. (2013). Preparation of highly porous binderless activated carbon electrodes from fibres of oil palm empty fruit bunches for application in supercapacitors. *Bioresource technology, 132*, 254-261.

Ferreira, S. C., Bruns, R., Ferreira, H., Matos, G., David, J., Brandao, G., . . . Souza, A. (2007). Box-Behnken design: an alternative for the optimization of analytical methods. *Analytica chimica acta, 597*(2), 179-186.

Fiol, N., Villaescusa, I., Martínez, M., Miralles, N., Poch, J., & Serarols, J. (2006). Sorption of Pb (II), Ni (II), Cu (II) and Cd (II) from aqueous solution by olive stone waste. *Separation and Purification Technology, 50*(1), 132-140.

Foo, K., & Hameed, B. (2009). An overview of landfill leachate treatment via activated carbon adsorption process. *Journal of Hazardous Materials, 171*(1), 54-60.

Foo, K., & Hameed, B. (2011a). Preparation and characterization of activated carbon from pistachio nut shells via microwave-induced chemical activation. *biomass and bioenergy, 35*(7), 3257-3261.

Foo, K., & Hameed, B. (2011b). Preparation and characterization of activated carbon from sunflower seed oil residue via microwave assisted K 2 CO 3 activation. *Bioresource Technology, 102*(20), 9794-9799.

Foo, K., & Hameed, B. (2011c). Preparation of activated carbon from date stones by microwave induced chemical activation: application for methylene blue adsorption. *Chemical Engineering Journal, 170*(1), 338-341.

Foo, K., & Hameed, B. (2011d). Preparation of oil palm (Elaeis) empty fruit bunch activated carbon by microwave-assisted KOH activation for the adsorption of methylene blue. *Desalination, 275*(1), 302-305.

Foo, K., & Hameed, B. (2011e). Utilization of rice husks as a feedstock for preparation of activated carbon by microwave induced KOH and K 2 CO 3 activation. *Bioresource technology, 102*(20), 9814-9817.

Foo, K., & Hameed, B. (2012a). Adsorption characteristics of industrial solid waste derived activated carbon prepared by microwave heating for methylene blue. *Fuel Processing Technology, 99*, 103-109.

Foo, K., & Hameed, B. (2012b). Mesoporous activated carbon from wood sawdust by K 2 CO 3 activation using microwave heating. *Bioresource technology, 111*, 425-432.

Foo, K., & Hameed, B. (2012c). Preparation of activated carbon by microwave heating of langsat (Lansium domesticum) empty fruit bunch waste. *Bioresource technology, 116*, 522-525.

Foo, K., & Hameed, B. (2013). Utilization of oil palm biodiesel solid residue as renewable sources for preparation of granular activated carbon by microwave induced KOH activation. *Bioresource technology, 130*, 696-702.

Fu, F., & Wang, Q. (2011). Removal of heavy metal ions from wastewaters: a review. *Journal of Environmental Management, 92*(3), 407-418.

Gao, Y., Wang, X.-H., Yang, H.-P., & Chen, H.-P. (2012). Characterization of products from hydrothermal treatments of cellulose. *Energy, 42*(1), 457-465.

Ghrefat, H., & Yusuf, N. (2006). Assessing Mn, Fe, Cu, Zn, and Cd pollution in bottom sediments of Wadi Al-Arab Dam, Jordan. *Chemosphere, 65*(11), 2114-2121.

González-García, P., Centeno, T., Urones-Garrote, E., Ávila-Brande, D., & Otero-Díaz, L. (2013). Microstructure and surface properties of lignocellulosic-based activated carbons. *Applied Surface Science, 265*, 731-737.

Gottipati, R. (2012). *Preparation and Characterization of Microporous Activated Carbon from Biomass and its Application in the Removal of Chromium (VI) from Aqueous Phase.* National Institute of Technology Rourkela.

Goyal, M., Bhagat, M., & Dhawan, R. (2009). Removal of mercury from water by fixed bed activated carbon columns. *Journal of Hazardous Materials, 171*(1), 1009-1015.

Gratuito, M. K. B., Panyathanmaporn, T., Chumnanklang, R.-A., Sirinuntawittaya, N., & Dutta, A. (2008). Production of activated carbon from coconut shell: Optimization using response surface methodology. *Bioresource Technology, 99*(11), 4887-4895.

Grierson, D. S., & Carpick, R. W. (2007). Nanotribology of carbon-based materials. *Nano Today, 2*(5), 12-21.

Gunaraj, V., & Murugan, N. (1999). Application of response surface methodology for predicting weld bead quality in submerged arc welding of pipes. *Journal of Materials Processing Technology, 88*(1), 266-275.

Hameed, B., Ahmad, A., & Latiff, K. (2007). Adsorption of basic dye (methylene blue) onto activated carbon prepared from rattan sawdust. *Dyes and Pigments, 75*(1), 143-149.

Hameed, B., Tan, I., & Ahmad, A. (2009). Preparation of oil palm empty fruit bunch-based activated carbon for removal of 2, 4, 6-trichlorophenol: Optimization using response surface methodology. *Journal of Hazardous Materials, 164*(2), 1316-1324.

Hao, W., Björkman, E., Lilliestråle, M., & Hedin, N. (2014). Activated carbons for water treatment prepared by phosphoric acid activation of hydrothermally treated beer waste. *Industrial & engineering chemistry research, 53*(40), 15389-15397.

Harrison, R. M. (2001). *Pollution: causes, effects and control*: Royal Society of Chemistry.

Hassan, N. M. (2005). Nematodes in banana in Malaysia. *Towards management of Musa nematodes in Asia and the Pacific*, 47-50.

Hawari, A., Rawajfih, Z., & Nsour, N. (2009). Equilibrium and thermodynamic analysis of zinc ions adsorption by olive oil mill solid residues. *Journal of Hazardous Materials, 168*(2), 1284-1289.

Hawari, A. H., & Mulligan, C. N. (2006). Biosorption of lead (II), cadmium (II), copper (II) and nickel (II) by anaerobic granular biomass. *Bioresource technology, 97*(4), 692-700.

He, X., Ling, P., Qiu, J., Yu, M., Zhang, X., Yu, C., & Zheng, M. (2013). Efficient preparation of biomass-based mesoporous carbons for supercapacitors with both high energy density and high power density. *Journal of Power Sources, 240*, 109-113.

Herrera, G. M. D., Anaguano, A. H., & Suarez, D. G. (2013). Structural characterization of the husks from modified rice as an alternative absorbant and effective for the removal of Cr (VI) in solution/Caracterización estructural de la cascarilla de arroz modificada como adsorbente alternativo y eficiente para la remoción de Cr (VI) en solución/Caracterizacao estrutural de cascas de arroz modificados como adsorvente alternativo e eficiente para a remocao do Cr (VI) em solucao. *Revista de Investigacion Agraria y Ambiental, 4*(1), 21-30.

Hidayu, A., Mohamad, N., Matali, S., & Sharifah, A. (2013). Characterization of activated carbon prepared from oil palm empty fruit bunch using BET and FT-IR techniques. *Procedia Engineering, 68*, 379-384.

Hidayu, A., & Muda, N. (2016). Preparation and Characterization of Impregnated Activated Carbon from Palm Kernel Shell and Coconut Shell for CO 2 Capture. *Procedia Engineering, 148*, 106-113.

Hijnen, W., Suylen, G., Bahlman, J., Brouwer-Hanzens, A., & Medema, G. (2010). GAC adsorption filters as barriers for viruses, bacteria and protozoan (oo) cysts in water treatment. *Water Research, 44*(4), 1224-1234.

Ho, Y., & McKay, G. (1999). The sorption of lead (II) ions on peat. *Water research, 33*(2), 578-584.

Huang, M., Zhou, S., Sun, B., & Zhao, Q. (2008). Heavy metals in wheat grain: assessment of potential health risk for inhabitants in Kunshan, China. *Science of the Total Environment, 405*(1), 54-61.

Ihsanullah, Al-Khaldi, F. A., Abu-Sharkh, B., Abulkibash, A. M., Qureshi, M. I., Laoui, T., & Atieh, M. A. (2015). Effect of acid modification on adsorption of hexavalent chromium (Cr (VI)) from aqueous solution by activated carbon and carbon nanotubes. *Desalination and Water Treatment*(ahead-of-print), 1-13.

Ioannidou, O., & Zabaniotou, A. (2007). Agricultural residues as precursors for activated carbon production—a review. *Renewable and Sustainable Energy Reviews, 11*(9), 1966-2005.

Ismanto, A. E., Wang, S., Soetaredjo, F. E., & Ismadji, S. (2010). Preparation of capacitor's electrode from cassava peel waste. *Bioresource technology, 101*(10), 3534-3540.

Jain, C., & Ram, D. (1997). Adsorption of lead and zinc on bed sediments of the river Kali. *Water Research, 31*(1), 154-162.

Järup, L. (2003). Hazards of heavy metal contamination. *British medical bulletin, 68*(1), 167-182.

Jessop, P. G., & Leitner, W. Chemical Synthesis Using Supercritical Fluids: Wiley Online Library.

Jin, H., Wang, X., Gu, Z., & Polin, J. (2013). Carbon materials from high ash biochar for supercapacitor and improvement of capacitance with HNO 3 surface oxidation. *Journal of Power Sources, 236*, 285-292.

Justi, K. C., Fávere, V. T., Laranjeira, M. C., Neves, A., & Peralta, R. A. (2005). Kinetics and equilibrium adsorption of Cu (II), Cd (II), and Ni (II) ions by chitosan functionalized with 2 [-bis-(pyridylmethyl) aminomethyl]-4-methyl-6-formylphenol. *Journal of colloid and interface science, 291*(2), 369-374.

Kadirvelu, K., Faur-Brasquet, C., & Cloirec, P. L. (2000). Removal of Cu (II), Pb (II), and Ni (II) by adsorption onto activated carbon cloths. *Langmuir, 16*(22), 8404-8409.

Kadirvelu, K., Kavipriya, M., Karthika, C., Radhika, M., Vennilamani, N., & Pattabhi, S. (2003). Utilization of various agricultural wastes for activated carbon preparation and application for the removal of dyes and metal ions from aqueous solutions. *Bioresource Technology, 87*(1), 129-132.

Kadirvelu, K., Thamaraiselvi, K., & Namasivayam, C. (2001). Removal of heavy metals from industrial wastewaters by adsorption onto activated carbon prepared from an agricultural solid waste. *Bioresource Technology, 76*(1), 63-65.

Kalderis, D., Bethanis, S., Paraskeva, P., & Diamadopoulos, E. (2008). Production of activated carbon from bagasse and rice husk by a single-stage chemical activation method at low retention times. *Bioresource technology, 99*(15), 6809-6816.

Kalmykova, Y., Strömvall, A.-M., & Steenari, B.-M. (2008). Adsorption of Cd, Cu, Ni, Pb and Zn on Sphagnum peat from solutions with low metal concentrations. *Journal of Hazardous Materials, 152*(2), 885-891.

Kannan, N., & Sundaram, M. M. (2001). Kinetics and mechanism of removal of methylene blue by adsorption on various carbons—a comparative study. *Dyes and Pigments, 51*(1), 25-40.

Karacan, F., Ozden, U., & Karacan, S. (2007). Optimization of manufacturing conditions for activated carbon from Turkish lignite by chemical activation using response surface methodology. *Applied Thermal Engineering, 27*(7), 1212-1218.

Katsigiannis, A., Noutsopoulos, C., Mantziaras, J., & Gioldasi, M. (2015). Removal of emerging pollutants through Granular Activated Carbon. *Chemical Engineering Journal, 280*, 49-57.

Kennedy, L. J., Vijaya, J. J., Kayalvizhi, K., & Sekaran, G. (2007). Adsorption of phenol from aqueous solutions using mesoporous carbon prepared by two-stage process. *Chemical Engineering Journal, 132*(1), 279-287.

Khalili, N. R., Campbell, M., Sandi, G., & Golaś, J. (2000). Production of micro-and mesoporous activated carbon from paper mill sludge: I. Effect of zinc chloride activation. *carbon, 38*(14), 1905-1915.

Khan, S., Cao, Q., Zheng, Y., Huang, Y., & Zhu, Y. (2008). Health risks of heavy metals in contaminated soils and food crops irrigated with wastewater in Beijing, China. *Environmental pollution, 152*(3), 686-692.

Khandanlou, R., Ahmad, M. B., Masoumi, H. R. F., Shameli, K., Basri, M., & Kalantari, K. (2015). Rapid Adsorption of Copper (II) and Lead (II) by Rice Straw/Fe 3 O 4 Nanocomposite: Optimization, Equilibrium Isotherms, and Adsorption Kinetics Study. *PloS one, 10*(3), e0120264.

Khezami, L., Bessadok-Jemai, A., Al-Dauij, O., & Amami, E. (2012). Individual and competitive adsorption of Lead (II) and Nickel (II) ions by chemically activated carbons. *IJPS, 7*, 6075-6081.

Kim, E.-J., Lee, C.-S., Chang, Y.-Y., & Chang, Y.-S. (2013). Hierarchically structured manganese oxide-coated magnetic nanocomposites for the efficient removal of heavy metal ions from aqueous systems. *ACS applied materials & interfaces, 5*(19), 9628-9634.

Körbahti, B. K., Artut, K., Geçgel, C., & Özer, A. (2011). Electrochemical decolorization of textile dyes and removal of metal ions from textile dye and metal ion binary mixtures. *Chemical Engineering Journal, 173*(3), 677-688.

Lăcătuşu, R., & Lăcătuşu, A.-R. (2008). Vegetable and fruits quality within heavy metals polluted areas in Romania. *Carpth J of Earth and Environmental Science, 3*, 115-129.

Latif, A., Mohd, A., & Husain, H. (1990). *Rattan processing industry in Peninsular Malaysia: its status, problems and prospects.* Paper presented at the IUFRO XIXTH World Congress, Montreal, Canada.

Lee, T., Ooi, C.-H., Othman, R., & Yeoh, F.-Y. (2014). Activated carbon fiber-the hybrid of carbon fiber and activated carbon. *Reviews on Advanced Materials Science, 36*(2), 118-136.

Lee, T., Zubir, Z. A., Jamil, F. M., Matsumoto, A., & Yeoh, F.-Y. (2014). Combustion and pyrolysis of activated carbon fibre from oil palm empty fruit bunch fibre assisted through chemical activation with acid treatment. *Journal of Analytical and Applied Pyrolysis, 110*, 408-418.

Li, Q., Wu, S., Liu, G., Liao, X., Deng, X., Sun, D., . . . Huang, Y. (2004). Simultaneous biosorption of cadmium (II) and lead (II) ions by pretreated biomass of Phanerochaete chrysosporium. *Separation and Purification Technology, 34*(1), 135-142.

Li, W., Zhang, L.-b., Peng, J.-h., Li, N., & Zhu, X.-y. (2008). Preparation of high surface area activated carbons from tobacco stems with K 2 CO 3 activation using microwave radiation. *Industrial crops and products, 27*(3), 341-347.

Li, X., Xing, W., Zhuo, S., Zhou, J., Li, F., Qiao, S.-Z., & Lu, G.-Q. (2011). Preparation of capacitor's electrode from sunflower seed shell. *Bioresource technology, 102*(2), 1118-1123.

Lifshitz, Y. (1999). Diamond-like carbon—present status. *Diamond and Related materials, 8*(8), 1659-1676.

Liu, C., Bai, R., & San Ly, Q. (2008). Selective removal of copper and lead ions by diethylenetriamine-functionalized adsorbent: Behaviors and mechanisms. *Water research, 42*(6), 1511-1522.

Liu, F., & Guo, M. (2015). Comparison of the characteristics of hydrothermal carbons derived from holocellulose and crude biomass. *Journal of Materials Science, 50*(4), 1624-1631.

Liu, Q.-S., Zheng, T., Wang, P., & Guo, L. (2010). Preparation and characterization of activated carbon from bamboo by microwave-induced phosphoric acid activation. *Industrial crops and products, 31*(2), 233-238.

Luo, X., Zhang, Z., Zhou, P., Liu, Y., Ma, G., & Lei, Z. (2015). Synergic adsorption of acid blue 80 and heavy metal ions (Cu 2+/Ni 2+) onto activated carbon and its mechanisms. *Journal of Industrial and Engineering Chemistry*.

Mapanda, F., Mangwayana, E., Nyamangara, J., & Giller, K. (2005). The effect of long-term irrigation using wastewater on heavy metal contents of soils under vegetables in Harare, Zimbabwe. *Agriculture, ecosystems & environment, 107*(2), 151-165.

Marr, R., & Gamse, T. (2000). Use of supercritical fluids for different processes including new developments—a review. *Chemical Engineering and Processing: Process Intensification, 39*(1), 19-28.

Martinez, M., Torres, M., Guzman, C., & Maestri, D. (2006). Preparation and characteristics of activated carbon from olive stones and walnut shells. *Industrial Crops and Products, 23*(1), 23-28.

Meena, A. K., Mishra, G., Rai, P., Rajagopal, C., & Nagar, P. (2005). Removal of heavy metal ions from aqueous solutions using carbon aerogel as an adsorbent. *Journal of Hazardous Materials, 122*(1), 161-170.

Mishra, P., & Patel, R. (2009). Removal of lead and zinc ions from water by low cost adsorbents. *Journal of Hazardous Materials, 168*(1), 319-325.

Mobasherpour, I., Salahi, E., & Ebrahimi, M. (2012). Removal of divalent nickel cations from aqueous solution by multi-walled carbon nano tubes: equilibrium and kinetic processes. *Research on Chemical Intermediates, 38*(9), 2205-2222.

Modak, D., Singh, K., Chandra, H., & Ray, P. (1992). Mobile and bound forms of trace metals in sediments of the lower Ganges. *Water Research, 26*(11), 1541-1548.

Mohan, D., & Chander, S. (2001). Single component and multi-component adsorption of metal ions by activated carbons. *Colloids and Surfaces A: Physicochemical and Engineering Aspects, 177*(2), 183-196.

Mohan, D., & Singh, K. P. (2002). Single-and multi-component adsorption of cadmium and zinc using activated carbon derived from bagasse—an agricultural waste. *Water Research, 36*(9), 2304-2318.

Mohan, D., Singh, K. P., & Singh, V. K. (2008). Wastewater treatment using low cost activated carbons derived from agricultural byproducts—a case study. *Journal of Hazardous Materials, 152*(3), 1045-1053.

Mohanty, K., Jha, M., Meikap, B., & Biswas, M. (2005). Removal of chromium (VI) from dilute aqueous solutions by activated carbon developed from Terminalia arjuna nuts activated with zinc chloride. *Chemical Engineering Science, 60*(11), 3049-3059.

Monser, L., & Adhoum, N. (2002). Modified activated carbon for the removal of copper, zinc, chromium and cyanide from wastewater. *Separation and Purification Technology, 26*(2), 137-146.

Moreno-Barbosa, J. J., López-Velandia, C., del Pilar Maldonado, A., Giraldo, L., & Moreno-Piraján, J. C. (2013). Removal of lead (II) and zinc (II) ions from aqueous solutions by adsorption onto activated carbon synthesized from watermelon shell and walnut shell. *Adsorption, 19*(2-4), 675-685.

Nabais, J. M. V., Nunes, P., Carrott, P. J., Carrott, M. M. L. R., García, A. M., & Díaz-Díez, M. (2008). Production of activated carbons from coffee endocarp by CO 2 and steam activation. *Fuel Processing Technology, 89*(3), 262-268.

Nabais, J. V., Carrott, P., Carrott, M. R., Luz, V., & Ortiz, A. L. (2008). Influence of preparation conditions in the textural and chemical properties of activated carbons from a novel biomass precursor: The coffee endocarp. *Bioresource technology, 99*(15), 7224-7231.

Nabais, J. V., Teixeira, J. G., & Almeida, I. (2011). Development of easy made low cost bindless monolithic electrodes from biomass with controlled properties to be used as electrochemical capacitors. *Bioresource technology, 102*(3), 2781-2787.

Nahil, M. A., & Williams, P. T. (2012). Pore characteristics of activated carbons from the phosphoric acid chemical activation of cotton stalks. *Biomass and Bioenergy, 37*, 142-149.

Narayanan, N. V., & Ganesan, M. (2009). Use of adsorption using granular activated carbon (GAC) for the enhancement of removal of chromium from synthetic wastewater by electrocoagulation. *Journal of Hazardous Materials, 161*(1), 575-580.

Nguyen, T., Ngo, H., Guo, W., Zhang, J., Liang, S., Yue, Q., . . . Nguyen, T. (2013). Applicability of agricultural waste and by-products for adsorptive removal of heavy metals from wastewater. *Bioresource technology, 148*, 574-585.

Novoselov, K. S., Geim, A. K., Morozov, S., Jiang, D., Zhang, Y., Dubonos, S. a., . . . Firsov, A. (2004). Electric field effect in atomically thin carbon films. *science, 306*(5696), 666-669.

Nriagu, J., Oleru, N. T., Cudjoe, C., & Chine, A. (1997). Lead poisoning of children in Africa, III. Kaduna, Nigeria. *Science of the Total Environment, 197*(1), 13-19.

Obute, G. C., & Ekiye, E. (2008). Ethnobotanical Applications of Some Floral Species in Bayelsa State, Nigeria. *Ethnobotanical Leaflets, 2008*(1), 96.

Onundi, Y. B., Mamun, A., Al Khatib, M., & Ahmed, Y. M. (2010). Adsorption of copper, nickel and lead ions from synthetic semiconductor industrial wastewater by palm shell activated carbon. *International Journal of Environmental Science & Technology, 7*(4), 751-758.

Ormad, M., Miguel, N., Claver, A., Matesanz, J., & Ovelleiro, J. (2008). Pesticides removal in the process of drinking water production. *Chemosphere, 71*(1), 97-106.

Pan, S.-C., Lin, C.-C., & Tseng, D.-H. (2003). Reusing sewage sludge ash as adsorbent for copper removal from wastewater. *Resources, Conservation and Recycling, 39*(1), 79-90.

Panswad, T., & Wongchaisuwan, S. (1986). Mechanisms of dye wastewater colour removal by magnesium carbonate-hydrated basic. *Water Science & Technology, 18*(3), 139-144.

Rafatullah, M., Sulaiman, O., Hashim, R., & Ahmad, A. (2010). Adsorption of methylene blue on low-cost adsorbents: a review. *Journal of Hazardous Materials, 177*(1), 70-80.

Rahim, Y. A., Aqmar, S. N., & Dewi, D. R. (2010). ESR study of electron trapped on activated carbon by KOH and ZnCl2 activation. *Journal of Materials Science and Engineering, 4*(3), 28.

Rao, G. P., Lu, C., & Su, F. (2007). Sorption of divalent metal ions from aqueous solution by carbon nanotubes: a review. *Separation and Purification Technology, 58*(1), 224-231.

Rao, M., Parwate, A., & Bhole, A. (2002). Removal of Cr 6+ and Ni 2+ from aqueous solution using bagasse and fly ash. *Waste management, 22*(7), 821-830.

Rao, M. M., Ramesh, A., Rao, G. P. C., & Seshaiah, K. (2006). Removal of copper and cadmium from the aqueous solutions by activated carbon derived from Ceiba pentandra hulls. *Journal of Hazardous Materials, 129*(1), 123-129.

Rao, M. M., Rao, G. C., Seshaiah, K., Choudary, N., & Wang, M. (2008). Activated carbon from Ceiba pentandra hulls, an agricultural waste, as an adsorbent in the removal of lead and zinc from aqueous solutions. *Waste Management, 28*(5), 849-858.

Reddad, Z., Gerente, C., Andres, Y., & Le Cloirec, P. (2002). Adsorption of several metal ions onto a low-cost biosorbent: kinetic and equilibrium studies. *Environmental science & technology, 36*(9), 2067-2073.

Robertson, J. (1998). *Deposition and properties of diamond-like carbons.* Paper presented at the MRS Proceedings.

Robertson, J. (2002). Diamond-like amorphous carbon. *Materials Science and Engineering: R: Reports, 37*(4), 129-281.

Roman, S., Nabais, J. V., Ledesma, B., González, J., Laginhas, C., & Titirici, M. (2013). Production of low-cost adsorbents with tunable surface chemistry by conjunction of hydrothermal carbonization and activation processes. *Microporous and mesoporous materials, 165*, 127-133.

Rouquerol, J., Rouquerol, F., Llewellyn, P., Maurin, G., & Sing, K. S. (2013). *Adsorption by powders and porous solids: principles, methodology and applications*: Academic press.

Roy, A., Adhikari, B., & Majumder, S. (2013). Equilibrium, kinetic, and thermodynamic studies of azo dye adsorption from aqueous solution by chemically modified lignocellulosic jute fiber. *Industrial & Engineering Chemistry Research, 52*(19), 6502-6512.

Rufford, T. E., Hulicova-Jurcakova, D., Khosla, K., Zhu, Z., & Lu, G. Q. (2010). Microstructure and electrochemical double-layer capacitance of carbon electrodes prepared by zinc chloride activation of sugar cane bagasse. *Journal of Power Sources, 195*(3), 912-918.

Rufford, T. E., Hulicova-Jurcakova, D., Zhu, Z., & Lu, G. Q. (2008). Nanoporous carbon electrode from waste coffee beans for high performance supercapacitors. *Electrochemistry Communications, 10*(10), 1594-1597.

Şahin, Ö., Saka, C., Ceyhan, A. A., & Baytar, O. (2015). Preparation of High Surface Area Activated Carbon from Elaeagnus angustifolia Seeds by Chemical Activation with ZnCl2 in One-Step Treatment and its Iodine Adsorption. *Separation Science and Technology, 50*(6), 886-891.

Saidur, R., Abdelaziz, E., Demirbas, A., Hossain, M., & Mekhilef, S. (2011). A review on biomass as a fuel for boilers. *Renewable and Sustainable Energy Reviews, 15*(5), 2262-2289.

Sanchez-Silva, L., López-González, D., Garcia-Minguillan, A., & Valverde, J. (2013). Pyrolysis, combustion and gasification characteristics of Nannochloropsis gaditana microalgae. *Bioresource technology, 130*, 321-331.

Satyawali, Y., & Balakrishnan, M. (2009). Effect of PAC addition on sludge properties in an MBR treating high strength wastewater. *Water Research, 43*(6), 1577-1588.

SE, A., Gimba, C., Uzairu, A., & Dallatu, Y. (2013). Preparation and characterization of activated carbon from Palm Kernel shell by chemical activation. *Research Journal of Chemical Sciences ISSN, 2231*, 606X.

Selvi, K., Pattabhi, S., & Kadirvelu, K. (2001). Removal of Cr (VI) from aqueous solution by adsorption onto activated carbon. *Bioresource Technology, 80*(1), 87-89.

Sevilla, M., & Fuertes, A. B. (2009). The production of carbon materials by hydrothermal carbonization of cellulose. *Carbon, 47*(9), 2281-2289.

ShamsiJazeyi, H., & Kaghazchi, T. (2010). Investigation of nitric acid treatment of activated carbon for enhanced aqueous mercury removal. *Journal of Industrial and Engineering Chemistry, 16*(5), 852-858.

Sharma, R. K., Agrawal, M., & Marshall, F. (2007). Heavy metal contamination of soil and vegetables in suburban areas of Varanasi, India. *Ecotoxicology and environmental safety, 66*(2), 258-266.

Shrestha, S., Son, G., Lee, S. H., & Lee, T. G. (2013). Isotherm and thermodynamic studies of Zn (II) adsorption on lignite and coconut shell-based activated carbon fiber. *Chemosphere, 92*(8), 1053-1061.

SI, W.-J., WU, X.-Z., XING, W., ZHOU, J., & Zhuo, S.-P. (2011). Bagasse-based nanoporous carbon for supercapacitor application. *无机材料学报, 26*(1).

Silva, R. V., Casilli, A., Sampaio, A. L., Ávila, B. M., Veloso, M. C., Azevedo, D. A., & Romeiro, G. A. (2014). The analytical characterization of castor seed cake pyrolysis bio-oils by using comprehensive GC coupled to time of flight mass spectrometry. *Journal of Analytical and Applied Pyrolysis, 106*, 152-159.

Singh, S. K., Townsend, T. G., Mazyck, D., & Boyer, T. H. (2012). Equilibrium and intra-particle diffusion of stabilized landfill leachate onto micro-and meso-porous activated carbon. *Water research, 46*(2), 491-499.

Sivakumar, S., Senthilkumar, P., & Subburam, V. (2001). Carbon from cassava peel, an agricultural waste, as an adsorbent in the removal of dyes and metal ions from aqueous solution. *Bioresource Technology, 80*(3), 233-235.

Skubiszewska-Zięba, J. (2010). VPO catalysts synthesized on substrates with modified activated carbons. *Applied surface science, 256*(17), 5520-5527.

Sobukola, O., Adeniran, O., Odedairo, A., & Kajihausa, O. (2010). Heavy metal levels of some fruits and leafy vegetables from selected markets in Lagos, Nigeria. *African Journal of food science, 4*(2), 389-393.

Sudaryanto, Y., Hartono, S., Irawaty, W., Hindarso, H., & Ismadji, S. (2006). High surface area activated carbon prepared from cassava peel by chemical activation. *Bioresource Technology, 97*(5), 734-739.

Sumathi, S., Bhatia, S., Lee, K., & Mohamed, A. (2009). Optimization of microporous palm shell activated carbon production for flue gas desulphurization: Experimental and statistical studies. *Bioresource Technology, 100*(4), 1614-1621.

Suzuki, M. (1994). Activated carbon fiber: fundamentals and applications. *carbon, 32*(4), 577-586.

Taer, E., Deraman, M., Talib, I., Awitdrus, A., Hashmi, S., & Umar, A. (2011). Preparation of a highly porous binderless activated carbon monolith from rubber wood sawdust by a multi-step activation process for application in supercapacitors. *Int. J. Electrochem. Sci, 6*(8), 3301-3315.

Tan, I., Ahmad, A., & Hameed, B. (2008). Optimization of preparation conditions for activated carbons from coconut husk using response surface methodology. *Chemical Engineering Journal, 137*(3), 462-470.

Tay, T., Ucar, S., & Karagöz, S. (2009). Preparation and characterization of activated carbon from waste biomass. *Journal of Hazardous Materials, 165*(1), 481-485.

Theydan, S. K., & Ahmed, M. J. (2012). Optimization of preparation conditions for activated carbons from date stones using response surface methodology. *Powder Technology, 224*, 101-108.

Titirici, M. M., Thomas, A., Yu, S.-H., Müller, J.-O., & Antonietti, M. (2007). A direct synthesis of mesoporous carbons with bicontinuous pore morphology from crude plant material by hydrothermal carbonization. *Chemistry of Materials, 19*(17), 4205-4212.

Tong, X.-j., Li, J.-y., Yuan, J.-h., & Xu, R.-k. (2011). Adsorption of Cu (II) by biochars generated from three crop straws. *Chemical Engineering Journal, 172*(2), 828-834.

Tongpoothorn, W., Sriuttha, M., Homchan, P., Chanthai, S., & Ruangviriyachai, C. (2011). Preparation of activated carbon derived from Jatropha curcas fruit shell by simple thermo-chemical activation and characterization of their physico-chemical properties. *Chemical Engineering Research and Design, 89*(3), 335-340.

Triantafyllou, A. (2001). PM10 pollution episodes as a function of synoptic climatology in a mountainous industrial area. *Environmental pollution, 112*(3), 491-500.

Tseng, H.-H., & Wey, M.-Y. (2006). Effects of acid treatments of activated carbon on its physiochemical structure as a support for copper oxide in DeSO 2 reaction catalysts. *Chemosphere, 62*(5), 756-766.

Valix, M., Cheung, W., & Zhang, K. (2006). Role of heteroatoms in activated carbon for removal of hexavalent chromium from wastewaters. *Journal of Hazardous Materials, 135*(1), 395-405.

Venkateshwarulu, V., & Kumar, S. PT, 1982. *Chemical and biological assessment of pollution in the River Musi, Hyderabad. Indian Biol. Bull, 4*, 23-30.

Vernersson, T., Bonelli, P., Cerrella, E., & Cukierman, A. (2002). Arundo donax cane as a precursor for activated carbons preparation by phosphoric acid activation. *Bioresource Technology, 83*(2), 95-104.

Wang, J.-P., Chen, Y.-Z., Wang, Y., Yuan, S.-J., & Yu, H.-Q. (2011). Optimization of the coagulation-flocculation process for pulp mill wastewater treatment using a combination of uniform design and response surface methodology. *Water Research, 45*(17), 5633-5640.

Wang, J. (2005). Carbon-nanotube based electrochemical biosensors: A review. *Electroanalysis, 17*(1), 7-14.

Wang, S., Soudi, M., Li, L., & Zhu, Z. (2006). Coal ash conversion into effective adsorbents for removal of heavy metals and dyes from wastewater. *Journal of Hazardous Materials, 133*(1), 243-251.

Wang, T., Tan, S., & Liang, C. (2009). Preparation and characterization of activated carbon from wood via microwave-induced ZnCl 2 activation. *Carbon, 47*(7), 1880-1883.

Wang, X.-s., & Qin, Y. (2005). Equilibrium sorption isotherms for of Cu 2+ on rice bran. *Process Biochemistry, 40*(2), 677-680.

Wang, Y., Qiao, M., Liu, Y., & Zhu, Y. (2012). Health risk assessment of heavy metals in soils and vegetables from wastewater irrigated area, Beijing-Tianjin city cluster, China. *Journal of Environmental Sciences, 24*(4), 690-698.

Weber, W. J., & Morris, J. C. (1963). Kinetics of adsorption on carbon from solution. *Journal of the Sanitary Engineering Division, 89*(2), 31-60.

Weng, C.-H., & Huang, C. (2004). Adsorption characteristics of Zn (II) from dilute aqueous solution by fly ash. *Colloids and Surfaces A: Physicochemical and Engineering Aspects, 247*(1), 137-143.

Wilson, K., Yang, H., Seo, C. W., & Marshall, W. E. (2006). Select metal adsorption by activated carbon made from peanut shells. *Bioresource Technology, 97*(18), 2266-2270.

Wong, C., Kiew, R., Loh, J. P., Gan, L. H., Set, O., Lee, S. K., . . . Gan, Y. Y. (2001). Genetic diversity of the wild banana Musa acuminata Colla in Malaysia as evidenced by AFLP. *Annals of Botany, 88*(6), 1017-1025.

Wu, F.-C., Tseng, R.-L., & Juang, R.-S. (1999). Pore structure and adsorption performance of the activated carbons prepared from plum kernels. *Journal of Hazardous Materials, 69*(3), 287-302.

Xin-Hui, D., Srinivasakannan, C., Jin-Hui, P., Li-Bo, Z., & Zheng-Yong, Z. (2011a). Comparison of activated carbon prepared from Jatropha hull by conventional heating and microwave heating. *Biomass and Bioenergy, 35*(9), 3920-3926.

Xin-Hui, D., Srinivasakannan, C., Jin-Hui, P., Li-Bo, Z., & Zheng-Yong, Z. (2011b). Preparation of activated carbon from Jatropha hull with microwave heating: optimization using response surface methodology. *Fuel Processing Technology, 92*(3), 394-400.

Xiu, S., Shahbazi, A., Shirley, V., & Cheng, D. (2010). Hydrothermal pyrolysis of swine manure to bio-oil: effects of operating parameters on products yield and characterization of bio-oil. *Journal of Analytical and Applied Pyrolysis, 88*(1), 73-79.

Xu, B., Chen, Y., Wei, G., Cao, G., Zhang, H., & Yang, Y. (2010). Activated carbon with high capacitance prepared by NaOH activation for supercapacitors. *Materials Chemistry and Physics, 124*(1), 504-509.

Yagmur, E., Ozmak, M., & Aktas, Z. (2008). A novel method for production of activated carbon from waste tea by chemical activation with microwave energy. *Fuel, 87*(15), 3278-3285.

Yang, K., Peng, J., Srinivasakannan, C., Zhang, L., Xia, H., & Duan, X. (2010). Preparation of high surface area activated carbon from coconut shells using microwave heating. *Bioresource technology, 101*(15), 6163-6169.

Yang, S., Li, J., Shao, D., Hu, J., & Wang, X. (2009). Adsorption of Ni (II) on oxidized multi-walled carbon nanotubes: effect of contact time, pH, foreign ions and PAA. *Journal of Hazardous Materials, 166*(1), 109-116.

Yang, T., & Lua, A. C. (2006). Textural and chemical properties of zinc chloride activated carbons prepared from pistachio-nut shells. *Materials chemistry and physics, 100*(2), 438-444.

Yavuz, Ö., Altunkaynak, Y., & Güzel, F. (2003). Removal of copper, nickel, cobalt and manganese from aqueous solution by kaolinite. *Water research, 37*(4), 948-952.

Yin, C. Y., Aroua, M. K., & Daud, W. M. A. W. (2007). Review of modifications of activated carbon for enhancing contaminant uptakes from aqueous solutions. *Separation and Purification Technology, 52*(3), 403-415.

Zahangir, A., Suleyman, A., & Noraini, K. (2008). *Production of activated carbon from oil palm empty fruit Bunch for Zn removal.* Paper presented at the Bul. conference proceedings 12th int. water Tech conf. IWTC12 Egypt.

Zhang, J., Gong, L., Sun, K., Jiang, J., & Zhang, X. (2012). Preparation of activated carbon from waste Camellia oleifera shell for supercapacitor application. *Journal of Solid State Electrochemistry, 16*(6), 2179-2186.

Zhang, K., Cheung, W., & Valix, M. (2005). Roles of physical and chemical properties of activated carbon in the adsorption of lead ions. *Chemosphere, 60*(8), 1129-1140.

Zhao, D., Feng, S., Chen, C., Chen, S., Xu, D., & Wang, X. (2008). Adsorption of thorium (IV) on MX-80 bentonite: Effect of pH, ionic strength and temperature. *Applied Clay Science, 41*(1), 17-23.

LIST OF PUBLICATIONS AND PAPERS PRESENTED

PUBLICATIONS

Ganiyu Abimbola Adebisi, Zaira Zaman Chowdhury, Sharifah Bee Abd Hamid, Md. Eaqub Ali (2016).”Hydrothermally-Treated Banana Empty Fruit Bunch Fiber Activated Carbon for Pb(II) and Zn(II) removal”. *Bioresources,* 11(3), 9686-9709. (Q1)

Ganiyu Abimbola Adebisi, Zaira Zaman Chowdhury, Sharifah Bee Abd Hamid, Md. Eaqub Ali. “Equilibrium Isotherm, Kinetics and Thermodynamics studies of Divalent Cations onto *Calamus gracilis* Sawdust Based Activated Carbon’’. *Bioresources*, 12(2), 2872-2898. (Q1).

Ganiyu Abimbola Adebisi, Zaira Zaman Chowdhury, Md. Eaqub Ali. ”Single and Binary Solute Equilibrium Studies using Longan Fruit Shell Based Carbon (LFSGAC)” (RSC Advances – under review) (Q1)

BOOK CHAPTER

Chowdhury Zaira Zaman, Kaushik Pal , Wageeh A. Yehye, Suresh Sagadevan, Syed Tawab Shah, Ganiyu Abimbola Adebisi, Emy Marliana, Rahman Faijur Rafique (2017). ‘Pyrolysis: A Sustainable Way to Generate Energy from Waste’. DOI: 10.5772/intechopen.69036.

Chowdhury Z. Z. , Kaushik Pal, Suresh Sagadevan, Rafie Bin Johan, Syed Tawab Shah, Ganiyu Abimbola Adebisi, Md. Sakinul Islam, and Rafique R. F. (2017). ‘Electrochemically Active Carbon Nanotube (CNTs) Membrane Filter for Desalination and Purification of water’. Elsivier-Publisher, NY,10010, United State.

CONFERENCE PAPER

Ganiyu Abimbola Adebisi. A Novel Route for Synthesis of Carbonaceous Adsorbent Materials for Equilibrium Kinetics, Isotherm and Thermodynamics for Cu (II) Ions in Single Solute System. A paper presented at the 2nd International Conference on Purity, Utility Reaction and Environmental Research – PURE2015 held at Golden Horses Hotel, Kuala Lumpur, 9th – 11th November, 2015.

APPENDIX

APPENDIX A: PSEUDO-FIRST-ORDER KINETIC MODEL CONSTANTS, CORRELATION COEFFICIENTS AND NORMALIZED STANDARD VALUES FOR ADSORPTION OF Pb(II) AND Zn(II) ON BEFBAC AND RSAC AT 60 AND 80°C RESPECTIVELY.

Table A1: Pseudo-first-order kinetic model constants, correlation coefficients and normalized standard values for adsorption of Pb(II) on BEFBAC and RSAC at 60°C

Activated Carbon	Lead Initial Concentration C_o (mg/L)	Lead Final Concentration C_e (mg/L)	Removal %	q_e, exp (mg/g)	q_e, cal (mg/g)	K1 (1/h)	R^2	Δqt (%)
BEFBAC	150	1.4	99.07	37.11	1.08	0.015	0.909	97.09
	200	7.5	96.25	48.10	1.24	0.006	0.966	97.42
	250	12.6	94.96	59.35	1.76	0.007	0.852	97.04
	300	33.9	88.7	66.46	2.76	0.013	0.662	95.85
	350	59.7	82.94	72.50	2.66	0.009	0.781	96.33
RSAC	150	1.1	93.2	37.13	2.63	0.0005	0.893	92.93
	200	5.7	97.15	48.55	1.49	0.006	0.983	96.92
	250	26.6	89.36	55.74	1.65	0.007	0.951	97.04
	300	42.5	85.83	64.28	1.89	0.005	0.913	97.06
	350	44.8	87.2	76.15	2.28	0.003	0.921	97.01

Table A2: Pseudo-first-order kinetic model constants, correlation coefficients and normalized standard values for adsorption of Pb(II) on BEFBAC and RSAC at 80°C

Activated Carbon	Lead Initial Concentration C_o (mg/L)	Lead Final Concentration C_e (mg/L)	Removal %	q_e, exp (mg/g)	Q_e, cal (mg/g)	Kl (1/h)	R^2	Δqt (%)
BEFBAC	150	1.4	99.07	37.11	1.04	0.01	0.840	97.19
	200	7.5	96.25	48.10	1.46	0.003	0.835	96.96
	250	10.3	95.88	59.93	2.07	0.004	0.912	96.54
	300	33.4	88.87	66.58	2.26	0.006	0.926	96.61
	350	51.7	85.23	74.50	2.75	0.01	0.819	96.31
RSAC	150	1.1	93.2	37.13	2.47	0.008	0.846	93.35
	200	9.6	95.2	47.58	1.81	0.003	0.857	96.20
	250	9.2	96.32	60.08	1.58	0.003	0.808	97.36
	300	30.5	89.83	67.27	2.46	0.008	0.934	96.35
	350	45.7	86.94	75.92	1.54	0.002	0.910	97.97

Table A3: Pseudo-first-order kinetic model constants, correlation coefficients and normalized standard values for adsorption of Zn(II) on BEFBAC and RSAC at 60°C

Activated Carbon	Zinc Initial Concentration C_o (mg/L)	Zinc Final Concentration C_e (mg/L)	Removal %	q_e,exp (mg/g)	q_e, cal (mg/g)	K2 (1/h)	R^2	Δqt (%)
BEFBAC	150	7.9	94.73	35.47	1.08	0.01	0.989	96.95
	200	18.6	90.7	45.26	2.31	0.003	0.493	94.91
	250	27.8	88.88	55.44	3.61	0.006	0.967	93.49
	300	70.8	76.4	57.19	2.24	0.012	0.961	96.07
	350	124.7	64.37	56.24	4.06	0.001	0.965	92.77
RSAC	150	2.1	98.6	36.94	1.71	0.014	0.741	95.36
	200	26.5	86.75	43.29	2.79	0.003	0.865	93.55
	250	68.5	72.6	45.33	4.05	0.003	0.835	91.07
	300	84.1	71.97	53.89	3.68	0.018	0.890	93.17
	350	116.3	66.77	58.31	4.19	0.002	0.961	92.82

Table A4: Pseudo-first-order kinetic model constants, correlation coefficients and normalized standard values for adsorption of Zn(II) on BEFBAC and RSAC at 80°C

Activated Carbon	Zinc Initial Concentration C_o (mg/L)	Zinc Final Concentration C_e (mg/L)	Removal %	q_e,exp (mg/g)	q_e, cal (mg/g)	Kl (1/h)	R^2	Δqt (%)
BEFBAC	150	18	88	32.95	1.09	0.01	0.857	96.69
	200	34.6	82.7	41.27	2.23	0.002	0.647	94.59
	250	63.5	74.6	46.53	3.37	0.005	0.993	92.76
	300	76.3	74.57	55.81	2.23	0.01	0.835	96.00
	350	118	66.29	57.91	3.77	0.0009	0.879	93.48
RSAC	150	7.3	95.13	35.64	1.57	0.019	0.960	95.60
	200	17.7	91.15	45.48	2.63	0.0005	0.630	94.21
	250	26.6	89.36	55.79	4.09	0.003	0.925	92.67
	300	52.6	82.47	61.76	3.82	0.02	0.960	93.81
	350	108.6	68.97	60.23	3.93	0.002	0.978	93.48

APPENDIX B: PSEUDO-SECOND-ORDER KINETIC MODEL CONSTANTS, CORRELATION COEFFICIENTS AND NORMALIZED STANDARD VALUES FOR ADSORPTION OF Pb(II) AND Zn(II) ON BEFBAC AND RSAC AT 60 AND 80°C RESPECTIVELY.

Table B1: Pseudo-second-order kinetic model constants, correlation coefficients and normalized standard values for adsorption of Pb(II) on BEFBAC and RSAC at 60°C

Activated Carbon	Lead Initial Concentration C_o (mg/L)	Lead Final Concentration C_e (mg/L)	Removal %	q_e,exp (mg/g)	q_e, cal (mg/g)	K2 (g/mg h)	R^2	Δqt (%)
BEFBAC	150	1.4	99.07	37.11	37.31	0.04	1	0.54
	200	7.5	96.25	48.10	48.54	0.02	1	0.92
	250	12.6	94.96	59.35	60.24	0.008	0.9999	1.48
	300	33.9	88.7	66.46	68.97	0.004	0.9995	3.77
	350	59.7	82.94	72.50	75.19	0.003	0.9997	3.70
RSAC	150	1.1	93.2	37.13	37.31	0.21	1	0.49
	200	5.7	97.15	48.55	47.85	0.01	0.9999	1.45
	250	26.6	89.36	55.74	61.73	0.01	0.9999	9.70
	300	42.5	85.83	64.28	65.79	0.006	0.9998	2.30
	350	44.8	87.2	76.15	75.19	0.003	0.9989	1.26

Table B2: Pseudo-second-order kinetic model constants, correlation coefficients and normalized standard values for adsorption of Pb(II) on BEFBAC and RSAC at 80°C

Activated Carbon	Lead Initial Concentration C_o (mg/L)	Lead Final Concentration C_e (mg/L)	Removal %	q_e, exp (mg/g)	q_e, cal (mg/g)	K2 (g/mg h)	R^2	Δqt (%)
BEFBAC	150	1.4	99.07	37.11	37.31	0.041	1	0.54
	200	7.5	96.25	48.10	49.50	0.009	0.9996	2.92
	250	10.3	95.88	59.93	61.73	0.004	0.9993	2.92
	300	33.4	88.87	66.58	68.49	0.004	0.9996	2.87
	350	51.7	85.23	74.50	76.34	0.003	0.9997	2.46
RSAC	150	1.1	93.2	37.13	37.31	0.287	1	0.49
	200	9.6	95.2	47.58	49.26	0.006	0.9993	3.54
	250	9.2	96.32	60.08	61.35	0.008	0.9997	2.11
	300	30.5	89.83	67.27	68.97	0.004	0.9995	2.51
	350	45.7	86.94	75.92	75.76	0.005	0.9995	0.22

Table B3: Pseudo-second-order kinetic model constants, correlation coefficients and normalized standard values for adsorption of Zn(II) on BEFBAC and RSAC at 60°C

Activated Carbon	Zinc Initial Concentration C_o (mg/L)	Zinc Final Concentration C_e (mg/L)	Removal %	q_e,exp (mg/g)	q_e, cal (mg/g)	K2 (g/mg h)	R^2	Δqt (%)
BEFBAC	150	7.9	94.73	35.47	35.71	0.033	1	0.68
	200	18.6	90.7	45.26	48.78	0.003	0.9663	7.78
	250	27.8	88.88	55.44	59.88	0.001	0.9773	8.01
	300	70.8	76.4	57.19	57.80	0.006	0.9999	1.08
	350	124.7	64.37	56.24	60.61	0.0009	9849	7.76
RSAC	150	2.1	98.6	36.94	35.84	0.011	0.9999	2.97
	200	26.5	86.75	43.29	43.48	0.004	0.9932	0.44
	250	68.5	72.6	45.33	49.02	0.001	0.9623	8.14
	300	84.1	71.97	53.89	56.18	0.002	0.9996	4.24
	350	116.3	66.77	58.31	58.82	0.002	0.9977	0.88

Table B4: Pseudo-first-order kinetic model constants, correlation coefficients and normalized standard values for adsorption of Zn(II) on BEFBAC and RSAC at 80°C

Activated Carbon	Zinc Initial Concentration C_o (mg/L)	Zinc Final Concentration C_e (mg/L)	Removal %	q_e,exp (mg/g)	q_e, cal (mg/g)	K2 (g/mg h)	R^2	Δqt (%)
BEFBAC	150	18	88	32.95	35.84	0.026	1	8.78
	200	34.6	82.7	41.27	48.78	0.004	0.9966	18.21
	250	63.5	74.6	46.53	61.35	0.001	0.9948	31.84
	300	76.3	74.57	55.81	62.5	0.005	0.9998	11.98
	350	118	66.29	57.91	69.93	0.001	0.9646	20.75
RSAC	150	7.3	95.13	35.64	33.22	0.020	1	6.78
	200	17.7	91.15	45.48	47.17	0.002	0.9831	3.71
	250	26.6	89.36	55.79	58.48	0.0007	0.9645	4.81
	300	52.6	82.47	61.76	57.47	0.002	0.9995	6.94
	350	108.6	68.97	60.23	62.89	0.0009	0.972	4.42

APPENDIX C: ELOVICH EQUATION CONSTANTS, CORRELATION COEFFICIENTS AND NORMALIZED STANDARD VALUES FOR ADSORPTION OF Pb(II) AND Zn(II) ON BEFBAC AND RSAC AT 60 AND 80ºC RESPECTIVELY.

Table C1: Elovich equation constants, correlation coefficients and normalized standard values for adsorption of Pb(II) on BEFBAC and RSAC at 60ºC

Activated Carbon	Lead Initial Concentration C_o (mg/L)	Lead Final Concentration C_e (mg/L)	Removal %	q_e, exp (mg/g)	q_e, cal (mg/g)	(1/b)lnab (mg/g)	1/b (mg/g)	R^2	Δqt (%)
BEFBAC	150	1.4	99.07	37.11	36.27	34.67	0.474	0.86	2.26
	200	7.5	96.25	48.10	47.44	45.89	0.438	0.92	1.38
	250	12.6	94.96	59.35	56.16	52.78	1.217	0.96	6.01
	300	33.9	88.7	66.46	63.97	55.92	2.086	0.92	3.74
	350	59.7	82.94	72.50	78.85	56.73	3.096	0.94	8.04
RSAC	150	1.1	99.27	37.13	37.92	36.84	0.076	0.76	2.07
	200	5.7	97.15	48.55	47.45	45.53	0.653	0.93	2.2
	250	26.6	89.36	55.74	58.71	56.11	0.957	0.98	5.06
	300	42.5	85.83	64.28	61.64	58.26	1.218	0.93	4.11
	350	44.8	87.2	76.15	69.31	64.51	1.569	0.81	8.98

Table C2 Elovich equation constants, correlation coefficients and normalized standard values for adsorption of Pb(II) on BEFBAC and RSAC at 80ºC

Activated Carbon	Lead Initial Concentration C_o (mg/L)	Lead Final Concentration C_e (mg/L)	Removal %	q_e, exp (mg/g)	q_e, cal (mg/g)	(1/b)lnab (mg/g)	1/b (mg/g)	R^2	Δqt (%)
BEFBAC	150	1.4	99.07	37.11	36.25	34.633	0.484	0.85	4.47
	200	7.5	96.25	48.10	47.56	45.906	0.501	0.68	3.47
	250	10.3	95.88	59.93	56.59	52.965	1.287	0.82	6.40
	300	33.4	88.87	66.58	63.54	59.976	1.882	0.96	5.61
	350	51.7	85.23	74.50	74.23	76.442	2.878	0.96	2.90
RSAC	150	1.1	99.27	37.13	38.04	36.999	0.043	0.92	2.39
	200	9.6	95.2	47.58	45.53	42.743	1.024	0.88	4.31
	250	9.2	96.32	60.08	58.86	56.835	0.705	0.81	2.06
	300	30.5	89.83	67.27	63.56	56.352	1.975	0.90	5.52
	350	45.7	86.94	75.92	71.49	67.341	1.423	0.79	5.84

Table C3 Elovich equation constants, correlation coefficients and normalized standard values for adsorption of Zn(II) on BEFBAC and RSAC at 60°C

Activated Carbon	Zinc Initial Concentration C_o (mg/L)	Zinc Final Concentration C_e (mg/L)	Removal %	q_e, exp (mg/g)	q_e, cal (mg/g)	(1/b)lnab (mg/g)	1/b (mg/g)	R^2	Δqt (%)
BEFBAC	150	7.9	94.73	35.47	35.11	33.727	0.326	0.96	1.01
	200	18.6	90.7	45.26	43.39	36.414	1.943	0.97	4.12
	250	27.8	88.88	55.44	58.31	39.992	2.908	0.98	31.42
	300	70.8	76.4	57.19	53.28	48.099	1.644	0.93	6.84
	350	124.7	64.37	56.24	63.57	37.204	3.272	0.95	11.53
RSAC	150	2.1	98.6	36.94	33.85	27.782	1.803	0.95	8.37
	200	26.5	86.75	43.29	47.39	31.201	0.623	0.83	8.65
	250	68.5	72.6	45.33	46.30	28.644	2.871	0.97	2.09
	300	84.1	71.97	53.89	56.52	31.007	3.239	0.96	4.64
	350	116.3	66.77	58.31	58.36	21.695	3.602	0.98	0.08

Table C4 Elovich equation constants, correlation coefficients and normalized standard values for adsorption of Zn(II) on BEFBAC and RSAC at 80°C

Activated Carbon	Zinc Initial Concentration C_o (mg/L)	Zinc Final Concentration C_e (mg/L)	Removal %	q_e, exp (mg/g)	q_e, cal (mg/g)	(1/b)lnab (mg/g)	1/b (mg/g)	R^2	Δqt (%)
BEFBAC	150	18	88	32.95	35.44	34.137	0.266	0.83	7.03
	200	34.6	82.7	41.27	41.22	35.578	1.730	0.91	0.12
	250	63.5	74.6	46.53	45.82	34.699	2.408	0.96	1.54
	300	76.3	74.57	55.81	58.02	51.079	1.938	0.95	3.80
	350	118	66.29	57.91	55.82	43.042	2.548	0.93	3.61
RSAC	150	7.3	95.13	35.64	34.91	28.213	1.902	0.92	2.05
	200	17.7	91.15	45.48	42.61	35.583	1.949	0.96	6.33
	250	26.6	89.36	55.79	55.83	18.354	3.624	0.89	0.06
	300	52.6	82.47	61.76	60.18	31.693	3.350	0.96	2.55
	350	108.6	68.97	60.23	58.61	38.74	2.989	0.89	2.68

APPENDIX D: INTRAPARTICLE DIFFUSION KINETIC MODEL CONSTANTS AND CORRELATION COEFFICIENTS FOR ADSORPTION OF Pb(II) AND Zn(II) ON BEFBAC AND RSAC AT 60 AND 80ºC RESPECTIVELY.

Table D1 Intraparticle diffusion kinetic model constants and correlation coefficients for adsorption of Pb(II) on BEFBAC and RSAC at 60ºC

Activated Carbon	Lead Initial Concentration C_o (mg/L)	Lead Final Concentration C_e (mg/L)	Removal %	Kp1	C1	R^2
BEFBAC	150	1.4	99.07	0.09	35.77	0.6883
	200	7.5	96.25	0.10	46.77	0.9787
	250	12.6	94.96	0.27	55.37	0.9312
	300	33.9	88.7	0.45	60.23	0.9361
	350	59.7	82.94	0.66	63.45	0.8735
RSAC	150	1.1	93.2	0.02	37.01	0.6042
	200	5.7	97.15	0.15	46.84	0.9901
	250	26.6	89.36	0.21	58.15	0.9402
	300	42.5	85.83	0.27	60.77	0.9504
	350	44.8	87.2	0.37	67.59	0.9012

Table D2 Intraparticle diffusion kinetic model constants and correlation coefficients for adsorption of Pb(II) on BEFBAC and RSAC at 80ºC

Activated Carbon	Lead Initial Concentration C_o (mg/L)	Lead Final Concentration C_e (mg/L)	Removal %	Kp1	C1	R^2
BEFBAC	150	1.4	98.87	0.10	35.76	0.6737
	200	7.5	96.2	0.12	46.84	0.8223
	250	10.3	94.88	0.30	55.49	0.9178
	300	33.4	87.47	0.42	60.93	0.9458
	350	51.7	82.86	0.73	63.73	0.8973
RSAC	150	1.1	93.2	0.01	37.09	0.8329
	200	9.6	89.6	0.23	44.84	0.9114
	250	9.2	84.96	0.16	58.24	0.8734
	300	30.5	86.27	0.45	60.24	0.9714
	350	45.7	86.71	0.29	70.59	0.654

Table D3 Intraparticle diffusion kinetic model constants and correlation coefficients for adsorption of Zn(II) on BEFBAC and RSAC at 60°C

Activated Carbon	Zinc Initial Concentration C_o (mg/L)	Zinc Final Concentration C_e (mg/L)	Removal %	Kp1	C1	R^2
BEFBAC	150	7.9	94.73	0.07	34.41	0.9484
	200	18.6	90.7	0.42	40.57	0.7406
	250	27.8	88.88	1.15	39.69	0.9745
	300	70.8	76.4	0.37	51.55	0.9243
	350	124.7	64.37	1.12	44.44	0.6326
RSAC	150	2.1	98.6	0.17	29.52	0.8865
	200	26.5	86.75	0.61	36.45	0.8992
	250	68.5	72.6	1.37	30.25	0.8626
	300	84.1	71.97	0.93	40.03	0.9289
	350	116.3	66.77	1.37	42.15	0.8192

Table D4 Intraparticle diffusion kinetic model constants and correlation coefficients for adsorption of Zn(II) on BEFBAC and RSAC at 80°C

Activated Carbon	Zinc Initial Concentration C_o (mg/L)	Zinc Final Concentration C_e (mg/L)	Removal %	Kp1	C1	R^2
BEFBAC	150	18	88	0.06	34.66	0.9314
	200	34.6	82.7	0.38	41.26	0.6965
	250	63.5	74.6	0.95	42.48	0.9729
	300	76.3	74.57	0.43	55.19	0.9158
	350	118	66.29	0.93	49.11	0.5896
RSAC	150	7.3	95.13	0.18	30.26	0.7737
	200	17.7	91.15	0.38	38.03	0.5018
	250	26.6	89.36	1.40	29.88	0.897
	300	52.6	82.47	0.96	40.92	0.929
	350	108.6	68.97	1.13	46.83	0.7565

APPENDIX E: Binary Adsorption of Pb (II) and Zn (II) onto LFSAC at 30ºC, pH 5.5 and at varying initial concentrations

C_o Pb	C_o Zn	C_e Pb	C_e Zn	q_e Pb	q_e Zn	Ads Pb (%)	Ads Zn (%)	AdTot%
0	0	0	0	0	0	0	0	0
150	0	12.9	0	34.28	0	91.4	0	91.4
200	0	20.6	0	46.85	0	89.7	0	89.7
250	0	27	0	55.75	0	89.2	0	89.2
300	0	41.5	0	64.63	0	86.17	0	86.17
350	0	85.8	0	66.05	0	75.49	0	75.49
0	150	0	14.8	0	28.8	0	90.13	90.13
150	150	13.2	23.6	47.2	41.6	91.2	84.27	87.73
200	150	24.3	43.6	47.93	32.35	87.85	70.93	79.39
250	150	29.8	49.2	55.05	19.95	88.08	67.2	77.64
300	150	45	65.6	63.75	16.1	85	56.27	70.63
350	150	90.9	90.5	64.78	14.88	74.03	39.67	56.85
0	200	0	16.5	0	34.88	0	91.75	91.75
150	200	14.3	25.5	33.93	43.63	90.47	87.25	88.86
200	200	26.5	46.07	45.38	35.5	86.75	76.965	81.86
250	200	32	62.6	56.07	36.1	87.2	68.7	77.95
300	200	47.5	89	63.13	32.75	84.17	55.5	69.83
350	200	88.6	110.6	65.35	27.1	74.69	44.7	59.69
0	250	0	30.6	0	54.85	0	87.76	87.76
150	250	15.7	38.6	28.58	52.85	89.53	84.56	87.05
200	250	28	59	43	47.75	86	76.4	81.2
250	250	34.6	75.7	43.85	33.08	86.16	69.72	77.94
300	250	50.5	95.6	62.38	38.6	83.17	61.76	72.46
350	250	95.6	123.8	63.6	32.05	72.69	50.48	61.58
0	300	0	118	0	60.67	0	60.67	60.67
150	300	29.5	135	34.13	58.25	80.33	55	67.67
200	300	35.6	138.6	41.1	49.1	82.2	53.8	68
250	300	47	140.5	50.75	45.88	81.2	83.08	82.14
300	300	69.5	145.6	47.63	30.6	76.83	51.47	64.15
350	300	110.8	148.7	59.8	37.83	68.34	50.43	59.39
0	350	0	142.8	0	60.8	0	59.2	59.2
150	350	22.6	148.6	23.85	59.35	84.93	57.54	71.24
200	350	38.6	168.7	37.35	49.33	80.7	51.8	66.25
250	350	51.5	179.5	46.63	46.63	79.4	48.71	64.06
300	350	65.2	180.5	50.7	42.33	78.27	48.43	63.35
350	350	130.3	203.5	34.93	30.38	62.77	41.86	52.31

APPENDIX F: Adsorption Isotherms

F1 Langmuir isotherm

Langmuir Adsorption Isotherm shows the variation between the quantities absorbed with respect to pressure. It depicts the relationship between pressure and the amount of active site of the adsorbent. With respect to the adsorption energy, Langmuir model assumes homogeneous surface where there is no interaction between the whole active sites and the adsorbed molecules due to the weak force of attraction between the same types of molecules (Choy, Porter, & McKay, 2000). However, Langmuir Isotherm is only applicable at low. Langmuir adsorption model is described by

$$\frac{C_e}{q_e} = \frac{1}{k_f q_m} + \frac{C_e}{q_m} \qquad \text{F.1}$$

Where, q_e denotes the quantity of adsorbed solute at equilibrium in mmol g^{-1}, Ce stands for the equilibrium concentration of the adsorbate in aqueous solution (mmol L^{-1}), q_m (mmol g^{-1}) is the maximum monolayer adsorption capacity, K_f is the Langmuir adsorption constant L $mmol^{-1}$, which indicates the energy of adsorption.

F2 Freundlich isotherm

Freundlich isotherm represents a special form of Langmuir model. It is an empirical model that presents interactions between the adsorbed molecules in a heterogeneous systems. The model can be applied to non-ideal adsorption having heterogeneous surfaces with multilayer adsorption (X.-s. Wang & Qin, 2005), and is given by

$$ln\ q_e = ln\ k_f + \frac{1}{n}\ ln\ C_e \qquad \text{F.2}$$

where q_e stands for the equilibrium concentration of the absorbed solute on adsorbent (mmol g^{-1}), C_e is the concentration of the solute at equilibrium position (mmol L^{-1}), K_f

defines the Freundlich constant, which is an indication of the adsorption extent in $mmol^{1-1/n}\ L^{1/n}\ g^{-1}$, and n is the heterogeneity factor, which indicates the effectiveness of adsorption.

F3 Temkin Isotherm

Temkin isotherm is applicable to the inhomogeneous electrolyte interface. Temkin adsorption isotherm is simply obtainable from the Frumkin adsorption isotherm defined below (Aharoni & Tompkins, 1970)

$$\left(\frac{\boldsymbol{\theta}}{\mathbf{1-\boldsymbol{\theta}}}\right) \boldsymbol{e^{(g\theta)}} = \boldsymbol{K_0 C_H^+\, e^{(-EF/RT)}} \qquad \text{F.3}$$

where K_0 represents the equilibrium constant for OPD H at g = 0, g is the Frumkin adsorption isotherm interaction parameter, r is the rate of change of the standard free energy of OPD H with $\boldsymbol{\theta}$, i.e., $0 \leq \boldsymbol{\theta} \leq 1$, and K is the equilibrium constant for OPD H.

The typical form of the Temkin adsorption isotherm for an electrochemical system ($\boldsymbol{\theta}$ vs. E) of OPD H is simply represented as follows:

$$\boldsymbol{e^{(g\theta)} = K_0 C_H^+\, e^{(-EF/RT)}} \qquad \text{F.4}$$

The isotherm relates to the Frumkin or the Langmuir adsorption isotherm, and this can be efficiently converted by means of constant conversion factors ($\boldsymbol{\theta}$/(1- $\boldsymbol{\theta}$)). This factors can be excellently used as a new electrochemical technique for determination of the adsorption isotherms (Frumkin, Langmuir, Temkin) of H suitable for the cathodic HER in an electrochemical systems.

APPENDIX G: Adsorption Kinetics

G1 Pseudo-first-order kinetic model

Pseudo-first-order kinetic model is described by

$$\frac{1}{q_t} = \frac{k_1}{q_e t} + \frac{1}{q_e} \quad \text{G.1}$$

Where, q_e represents the equilibrium uptake, k_1 (min^{-1}) denotes the pseudo-first-order adsorption rate constant, and q_t symbolizes the quantity absorbed at time t (min), both in mmol g^{-1}.

G2 Pseudo-second-order kinetic model

The pseudo-second-order kinetic model is given by

$$\frac{t}{q_t} = \frac{1}{k_1 q_e^2 t} + \frac{1}{q_e} t \quad \text{G.2}$$

Where, k_2 is the pseudo-second-order adsorption rate constant in g $mmol^{-1}$ min^{-1}, q_t and q_e are the quantity of each heavy metal ion adsorbed at time t (min) and equilibrium, respectively, both in mmol g^{-1}. The rate of adsorption concentration h in mmol g^{-1} min^{-1} is given by

$$h = k_2 q_e^2 \quad \text{G.3}$$

G3 Elovich equation

Elovich model is used to describe gas adsorption on the s surface of an adsorbent without product desorption. The rate of adsorption herein decreases with time because of the coverage of the active sites (Aharoni & Tompkins, 1970) . Elovich model is given by

$$\frac{dq_t}{dt} = a \exp(-bq_t) \quad \text{G.4}$$

where a and b are the experimental constants and a is the initial rate as dq_t /dt approaches a and q_t approaches 0.

Given that $q_t = q_t$ at t = t and $q_t = 0$ at t = 0, the integrated form of the above equation is

$$q_t = \left(\frac{1}{b}\right) \ln(t + t_0) - \left(\frac{1}{b}\right) \ln t_0 \quad \text{G.5}$$

Where, $t_0 = 1/ab$. If $t \gg t_0$, the equation can be further simplified as

$$q_t = \left(\frac{1}{b}\right) \ln(ab) + \left(\frac{1}{b}\right) \ln t \quad \text{G.6}$$

The validity of $t \gg t_0$ assumption for the above equation is verifiable by the linear plot of q_t vs. ln t. For an adsorption system, the longest time for the adsorption process be let t_{ref} and q_{ref} be the concentration of the solid phase at time $t = t_{ref}$.

Therefore, the above equation is rewritten as

$$q_{ref} = \left(\frac{1}{b}\right) \ln(ab) + \left(\frac{1}{b}\right) \ln t_{ref} \quad \text{G.7}$$

Subtracting the two previous equation from each other, we have:

$$q_t - q_{ref} = \left(\frac{1}{b}\right) \ln\left(\frac{t}{t_{ref}}\right) \quad \text{G.8}$$

Dividing both sides of the equations by q_{ref} yields:

$$\left(\frac{q_t}{q_{ref}}\right) = \left(\frac{1}{q_{ref} b}\right) \ln\left(\frac{t}{t_{ref}}\right) + 1 \quad \text{G.9}$$

The above equation is referred to as dimensionless Elovich equation. Let RE = 1/(q_{ref} b), which is the Elovich towards factor equilibrium; therefore the Equation becomes

$$\left(\frac{q_t}{q_{ref}}\right) = R_E \ln\left(\frac{t}{t_{ref}}\right) + 1 \qquad \text{G.1}$$

G4 Intra-particle diffusion

Analysis of intra-particle diffusion is of vital importance in sorption of adsorbate unto adsorbent such as AC due to their properties. The control of sorption process is achievable by the following steps in sequence (Singh, Townsend, Mazyck, & Boyer, 2012):

I. The bulk solution diffusion, which involves transportation of the adsorbate from the solution to the boundary layer of solution surrounding the AC particles;
II. film diffusion, which involves transportation of the adsorbate through the liquid film surrounding the particles of the adsorbent; and
III. pore diffusion and adsorption, which involves transportation of the adsorbate to the pores of adsorbent to the available active sites.

A time dependent intra-particle diffusion kinetic model was developed by Weber and Morris (Weber & Morris, 1963). The model shows that the process is diffusion controlled if the sorption rate depends on the rate of diffusion of the adsorbent and the adsorbate to one another. The model is given by

$$q_t = k_{id} t^{1/2} + C \qquad \text{G.11}$$

where q_t (mg g^{-1}) stands for the amount of adsorbate adsorbed on the adsorbent (solid phase) at time t, k_{id} (mg g^{-1} $min^{1/2}$) denotes the rate constant for the intra-particle diffusion, and C (mg g^{-1}) is the constant, which is proportional to the boundary layer thickness; that

is, the value of C increases by increasing the thickness of the boundary layer (McKay et al., 1980).

The diffusion controlled sorption process is presented by the straight line graph of q_t versus $t^{1/2}$. Sorption process with multiple linear plots is controlled by more than one factor.